

30803

NATIONAL LIBRARY
OTTAWA



BIBLIOTHÈQUE NATIONALE
OTTAWA

NAME OF AUTHOR..... *Jeffrey Reece*

TITLE OF THESIS..... *The debate XY model*

.....

UNIVERSITY..... *Albela*

DEGREE FOR WHICH THESIS WAS PRESENTED..... *Ph.D.*

YEAR THIS DEGREE GRANTED..... *1976*

Permission is hereby granted to THE NATIONAL LIBRARY OF CANADA to microfilm this thesis and to lend or sell copies of the film.

The author reserves other publication rights, and neither the thesis nor extensive extracts from it may be printed or otherwise reproduced without the author's written permission.

(Signed)..... *J. Reece*

PERMANENT ADDRESS:

..... *#6 Carlton Tce*

..... *New Plymouth*

..... *New Zealand*

DATED..... *July 8th* 19 *76*

INFORMATION TO USERS

THIS DISSERTATION HAS BEEN
MICROFILMED EXACTLY AS RECEIVED

This copy was produced from a microfiche copy of the original document. The quality of the copy is heavily dependent upon the quality of the original thesis submitted for microfilming. Every effort has been made to ensure the highest quality of reproduction possible.

PLEASE NOTE: Some pages may have indistinct print. Filmed as received.

Canadian Theses Division
Cataloguing Branch
National Library of Canada
Ottawa, Canada K1A 0N4

AGERS

LA THÈSE A ÉTÉ MICROFILMÉE
TELLE QUE NOUS L'AVONS RECUE

Cette copie a été faite à partir d'une microfiche du document original. La qualité de la copie dépend grandement de la qualité de la thèse soumise pour le microfilmage. Nous avons tout fait pour assurer une qualité supérieure de reproduction.

NOTA BENE: La qualité d'impression de certaines pages peut laisser à désirer. Microfilmée telle que nous l'avons reçue.

Division des thèses canadiennes
Direction du catalogage
Bibliothèque nationale du Canada
Ottawa, Canada K1A 0N4

THE UNIVERSITY OF ALBERTA

THE DILUTE XY MODEL

by



JEFFREY STEPHEN REEVE

A THESIS

SUBMITTED TO THE FACULTY OF GRADUATE STUDIES AND RESEARCH
IN PARTIAL FULFILMENT OF THE REQUIREMENTS FOR THE DEGREE OF
DOCTOR OF PHILOSOPHY

DEPARTMENT OF PHYSICS

EDMONTON, ALBERTA

FALL, 1976

THE UNIVERSITY OF ALBERTA

FACULTY OF GRADUATE STUDIES AND RESEARCH

The undersigned certify that they have read, and recommend to the Faculty of Graduate Studies and Research, for acceptance, a thesis entitled THE DILUTE XY MODEL submitted by JEFFREY STEPHEN REEVE in partial fulfilment of the requirements for the degree of Doctor of Philosophy.

Donald D. Betts
Supervisor

F. H. Keese

Bruce L. Clarke

M. Roy

Bernie S. Hichel
External Examiner

Date *21 May 1976*

To my wife

Monica

ABSTRACT

The critical properties of the quenched and annealed site diluted spin- $\frac{1}{2}$ XY models are investigated, for three cubic lattices, using the finite cluster method. The lines of second order transition points for both models in the temperature-density plane are located. Behavior of the critical exponent γ is found not to agree with the ideas of universality. The annealed site XY model is shown to be equivalent to the Takagi model of He³-He⁴ mixtures. Contours of constant reduced density $n = n_3 + n_4$ in the TX_3 plane are determined and the tricritical point is approximately located for the f.c.c. lattice. The two dimensional quenched and annealed site XY models are analysed for the triangular lattice. The results seem to indicate that a phase transition does occur.

ACKNOWLEDGEMENTS

I would like to take this opportunity to express my sincere thanks to Dr. D. D. Betts, my supervisor, for suggesting the problem studied, for his interest, encouragement and guidance.

I am grateful also to Dr. M. Razavy for acting as my supervisor during a temporary absence of Dr. Betts.

I thank Drs. M. Plischke and J. Rogiers for freely giving their advice and for stimulating useful discussions.

Dr. C. Elliot kindly allowed me use of his computer programs.

The financial support of the University of Alberta is gratefully acknowledged.

Finally, I thank Mrs. Lee Cech for her speed and expertise in typing this thesis.

TABLE OF CONTENTS

Chapter		Page
I	INTRODUCTION	1
II	CRITICAL PHENOMENA	8
	2.1 Introduction	8
	2.2 Critical Exponents	9
	2.3 Scaling Theory	13
	2.4 Fisher Renormalisation	22
	2.5 Universality	24
III	THE XY MODEL AND MAGNETIC DILUTION	28
	3.1 Introduction	28
	3.2 XY Magnetic Insulators	29
	3.3 Quantum Lattice Fluids	31
	3.4 Dilute Models	35
	3.5 Dilution and Critical Phenomena	44
IV	THE FINITE CLUSTER EXPANSION	47
	4.1 Introduction	47
	4.2 Definitions of Graph Theory	48
	4.3 The Finite Cluster Theorem	51
	4.4 Construction of the Expansion	53
	4.5 Perturbation Expansions from the Finite Cluster Theorem	56

Chapter		Page
IV	4.6 Inversion of the Finite Cluster Theorem	65
	4.7 Advantages of the Method	67
V	THE QUENCHED SITE MODEL	69
	5.1 Introduction	69
	5.2 Generation of Series	70
	5.3 Methods of Series Analysis	76
	5.4 Critical Exponent Behavior	78
	5.5 Lattice Dependent Critical Properties	87
	5.6 Discussion and Summary	92
VI	THE ANNEALED SITE PROBLEM	96
	6.1 Introduction	96
	6.2 Generation of Series	97
	6.3 Second Order Transition Lines	99
	6.4 $\text{He}^3\text{-He}^4$ Mixtures	106
	6.5 The Tricritical Point	113
	6.6 Summary and Discussion	118
VII	THE TWO DIMENSIONAL MODELS	120
	7.1 Introduction	120
	7.2 Exact Results and Conjectures	120
	7.3 The Two Dimensional XY Model	122

Chapter		Page
VII	7.4 Analysis of the Density Series	123
	7.5 Summary and Discussion	131
VIII	SUMMARY OF RESULTS AND DISCUSSION	133
	REFERENCES	136
	APPENDIX A EXPECTATION VALUES FOR FINITE CLUSTERS	143
	APPENDIX B LATTICE CONSTANTS AND PERIMETER COUNTS	147

LIST OF TABLES

Table	Page
3.1	Percolation concentrations for various lattices 39
5.1	Coefficients $\bar{c}_2(K)$ in the low density expansion for $Y(p,K)$ for the f.c.c. lattice for various values of K 72
5.2	Coefficients $\bar{c}_2(K)$ in the low density expansion for $Y(p,K)$ for the b.c.c. lattice for various values of K 73
5.3	Coefficients $\bar{c}_2(K)$ in the low density expansion for $Y(p,K)$ for the s.c. lattice for various values of K 74
5.4	Estimates of $\gamma(p)$ from Padé approximants to $d \ln Y(p,K)/dK$ on the f.c.c. lattice" 81
5.5	Estimates of p_c and $\bar{\gamma}(t)$ from ratio plots of the low density expansion of $Y(p,K)$ 84
5.6	Estimates of $\bar{\gamma}(t)$ from Padé approximants to $d \ln Y(p,K)/dp$ on the f.c.c. lattice 85
5.7	Terminal gradients of the phase transition curves for some three dimensional quenched site models 91
6.1	Coefficient $b_2(K)$ for the series in fugacity for $Y(p,K)$ on the f.c.c. lattice for various values of K 98
6.2	Coefficients $a_2(K)$ for the series in density for $Y(n_m, K)$ on the f.c.c. lattice for various values of K 100
6.3	Estimates of $\bar{\gamma}(K)$ from Padé approximants to $dY(K, n_m)/dn_m$ on the f.c.c. lattice for various values of K 102
6.4	Estimates of $\bar{\gamma}(h)$ from Padé approximants to $d \ln Y(n_m, t, h)/dn_m$ on the f.c.c. lattice for various values of h 104

Table	Page
6.5 Estimates of n_m^c from Padé approximants to $[Y(k, n_m, h)]^{3/4m}$ on the f.c.c. lattice for $h = 0.0$	105
6.6 Estimates of $\gamma(k)$ from Padé approximants to $d \ln Y(k, n, z) / dz$ on the f.c.c. lattice for $h = 0.0$	112
6.7 Estimates of $\gamma(k)$ from Padé approximants to series for $d \ln Y(k, z) / dz$ on the f.c.c. lattice near the tricritical point	116
7.1 Estimates of p_c and $\bar{\gamma}$ from Padé approximants to $d \ln Y(p) / dp$ on the triangular lattice	126
7.2 Estimates of \bar{p}_c and $\bar{\gamma}$ from Padé approximants to $d \ln Y(\bar{p}) / d\bar{p}$ on the triangular lattice	128
7.3 Estimates of \bar{p}_c from Padé approximants to $[Y(\bar{p})]^{4/5}$ on the triangular lattice	129

LIST OF FIGURES

Figure		Page
2.1	Schematic phase diagram for He ³ -He ⁴ mixtures showing the tricritical scaling regions	16
3.1	Schematic phase diagram of temperature versus impurity concentration showing the available paths of approach	45
5.1	Ratio plot of coefficients \bar{c}_n/\bar{c}_{n-1} of the low density series for $\chi(p, t=0.9)$ on the f.c.c. lattice	83
5.2	Critical temperature versus density for the three dimensional quenched site models	89
5.3	Critical amplitudes versus temperature for the three dimensional quenched site models	93
6.1	Critical temperature versus density for the three dimensional annealed site models	107
6.2	Critical temperature versus He ³ concentration for various values of h on the f.c.c. lattice	109
6.3	Critical temperature versus fugacity for the f.c.c. lattice with $h=0$	111

CHAPTER I

INTRODUCTION

Many different types of phase transition occur in nature, but it is only in recent years that there has been a concerted effort to understand these phenomena collectively.

Van der Waals formulated in 1873 the law of corresponding states, which asserts that the equation of state for all fluids has the same form. This theory has enjoyed considerable success and it has served to describe a number of liquid gas transitions reasonably well.

Magnetic systems however, could only be explained from a quantum mechanical viewpoint. In simplistic terms the Pauli exclusion principle tends to keep electrons with parallel spins apart and in doing so reduces their Coulomb repulsion. The difference in energy between the parallel and antiparallel configurations is the exchange energy. If the increase in kinetic energy associated with a parallel alignment is less than the decrease in potential energy, then magnetic ordering can occur. The physical mechanisms involved in magnetism are discussed in detail in Mattis (1965).

One of the simplest, yet most successful models of magnetism is the Ising model. The free energy of the Ising ferromagnet on the square lattice was found

analytically by Onsager (1944). As yet no exact results concerning the phase transition for the three dimensional Ising model are known. Because the Ising Hamiltonian in the Pauli representation is diagonal, it is often referred to as a classical model. The XY model, which is a special case of the anisotropic Heisenberg model is "fully" quantum mechanical. The XY model has only been solved exactly in one dimension.

Since exact solutions are out of the question for most realistic models of magnetism a number of approximate methods have been developed. The principle closed form approximations are the methods by Weiss (1907), Bethe (1935), Bragg and Williams (1934) and Kikuchi (1951). Also of importance are the Green's functions techniques. These have been reviewed by Zubarev (1960) and Tyablikov (1967).

By far the most successful method of elucidating the critical properties of direct exchange type models is the method of series expansions. In this method, thermodynamic functions are expanded about the ordered state or about the disordered state in powers of a suitable variable such as temperature or density. The series are then analysed using various methods to reveal any singular behavior which may indicate the occurrence of a continuous (or second order) phase transition. It is this method we exploit here.

Before brief describing the purpose of this thesis though, we mention the very recent development of renormalisation group theory. This is an approximate method, but is enjoying considerable success as an approximation applicable to classical models. For reviews, the reader is referred to Ma (1973), Wilson and Kogut (1974) and Fisher (1974). In its original form renormalisation group calculations are done in a momentum representation, but Niemeyer and Van Leeuwen (1974) have developed the theory in configuration space. This newer formulation appears to be conducive to calculations on quantum systems (Rogiers and Dekeyser (1976) and Betts and Plischke (1976)).

Comprehensive reviews covering most aspects of critical phenomena are contained in the set of volumes edited by Domb and Green (1971) and the articles by Domb (1960) and Fisher (1967). De Jongh and Miedema (1974) have extensively reviewed the experimental situation.

The XY model can be explained from a physical standpoint as follows. Consider the following model of a magnetic crystal. At each lattice site is located an elementary magnet which is allowed to rotate in a pre-determined plane. These magnetic moments can be represented by two dimensional vectors. If the interaction between neighbouring sites is proportional to scalar product of the vectors representing the magnetic moments at those sites,

then the model is called the plane rotator model. Further, if the elementary magnets are allowed to move in three dimensions but are still restricted to interact in two dimensions, then the model becomes the classical or spin infinity XY model.

The spin- $\frac{1}{2}$ XY model is the quantum analogue of the spin infinity XY model. The difference is that the elementary magnets at each site are spins which interact in two dimensions only, while there are still three rotational degrees of freedom available to each spin. It is perhaps more enlightening to regard the spin- $\frac{1}{2}$ XY model as describing a Heisenberg magnet in which the crystal field has the appropriate symmetry and strength so as to prevent interaction between spins in one particular direction in spin space. Several examples of the spin- $\frac{1}{2}$ XY model have been identified experimentally and are listed in Chapter III.

The critical properties of the spin- $\frac{1}{2}$ XY model have been considerably elucidated by Betts (1974) and co-workers and by Dekeyser and Rogiers (1975).

One of the systems studied in this thesis is the quenched site spin- $\frac{1}{2}$ XY model. This is a model for a "dirty" crystalline magnet in which the impurity atoms are frozen, in random distribution, into the lattice. Study of such a system is motivated both from a theoretical and experimental viewpoint.

Theoretically there has been considerable speculation as to the nature of the phase transition of diluted magnets. It has been suggested that phase transitions in random systems may not occur at a well defined temperature but over a small finite range of temperatures. Also there is the question whether or not scaling theory and the universality principle hold for such systems. These questions are expanded on in Chapters III and V, where extensive references can be found.

To date experiments on random systems have been restricted to mixtures of two different types of anti-ferromagnets. However de Jongh (private communication) has begun studies of some randomly diluted XY antiferromagnets and anticipates that he will be able to determine the critical temperature for a number of different impurity concentrations.

Besides being a model for a crystalline magnet the XY model can also be used as a lattice fluid model for the normal fluid to superfluid transition in He^4 . Consider the He^4 fluid as a collection of bosons arranged randomly in space. If we then break up the space into cells large enough only to be occupied by a single particle, then some of these cells will be occupied by He^4 atoms and some will be vacant. The XY model represents such a collection of bosons and allows the He^4 atoms to move to unoccupied neighbouring cells

and in this way accounts for the kinetic energy of the system. Theoretical results for the critical properties of the XY model have been compared with experimental data for the normal fluid to superfluid transition in He^4 with excellent agreement (see Betts (1974)). The lattice fluid picture of the XY model is described in much more detail in Chapter III.

This brings us to the second model studied in this thesis. This is the annealed site spin- $\frac{1}{2}$ XY model which corresponds to He^4 with classical impurities added. Such a model could conceivably be used as a model of $\text{He}^3 - \text{He}^4$ mixtures with the kinetic energy and fermi statistics of the He^3 atoms being disregarded. This approximation is presumably best for temperatures above the tricritical temperature where phase separation first occurs. The annealed site XY model of $\text{He}^3 - \text{He}^4$ mixtures ignores all but the hard core $\text{He}^3 - \text{He}^3$, $\text{He}^3 - \text{He}^4$ and $\text{He}^4 - \text{He}^4$ interactions. However the critical properties of interest to us arise from the kinetic mobility of the He^4 atoms and neglect of the potential tail will not alter the values of the critical exponents. This invariance of critical properties with respect to perturbative effects arises from the universality principle as stated in Chapter II.

The aim then is to find the phase diagram for the spin- $\frac{1}{2}$ XY model in the temperature-density plane and compare this with the experimental result.

The plan of the remainder of this thesis is as follows. In Chapter II some definitions and phenomenological theories of critical phenomena are outlined. The XY model of both magnets and lattice fluids is introduced in Chapter III. Also in Chapter III we define precisely the models studied, namely the quenched and annealed site spin- $\frac{1}{2}$ XY models. The finite cluster method of constructing series expansions is described in Chapter IV. In Chapter V the results of the analysis for the quenched site model in three dimensions are presented, while the results for the annealed site model in three dimensions are given in Chapter VI. The two dimensional quenched and annealed site models are discussed in Chapter VII. Final conclusions are given in Chapter VIII.

CHAPTER II

CRITICAL PHENOMENA

2.1 Introduction

The definitions and general results from the theory of critical phenomena that are referred to in later chapters are outlined in the following sections.

Basic definitions of some thermodynamic functions and their critical amplitudes and exponents are given in Section 2. The theory of tricritical scaling is briefly described in Section 3. Section 4 deals with the Fisher renormalisation of exponents. The concept of universality of critical phenomena is discussed in Section 5.

Throughout this thesis we will use mainly the thermodynamic notation appropriate for magnetic systems. The conversion from magnet to fluid language for any formula is usually easily facilitated by making the substitutions

$$M \rightarrow \rho - \rho_c \tag{2.1.1}$$

$$H \rightarrow \mu - \mu_c$$

where M and H are the magnetisation and the ordering magnetic field respectively. The density and chemical

potential of the fluid system are labelled ρ and μ respectively and have the values ρ_c and μ_c at the critical point. When reference to phase separation in fluid mixtures is desired, the concentration of one of the species is related to the magnetisation and the difference in the chemical potentials of the two species is the ordering field. In particular for $\text{He}^3 - \text{He}^4$ mixtures the order parameter is the He^3 concentration X_3 and the ordering field is $\mu_3 - \mu_4$, the chemical potential difference.

We leave until the next chapter a discussion of just now the dilute XY model can be used to test the phenomenological and thermodynamic theories given below.

2.2 Critical Exponents

The thermodynamic functions usually dealt with when investigating a phase transition are the order parameter and various response and correlation functions. Let $F(T,H)$ be the free energy of a system, where H is the ordering field and irrelevant variables have been suppressed. Then the following functions can be defined:

the magnetisation

$$M(T,H) = (\partial F(T,H)/\partial H)_T \quad (2.2.1)$$

the isothermal susceptibility

$$\bar{\chi}(T,H) = (\partial M(T,H)/\partial H)_T \quad (2.2.2)$$

and the specific heat

$$\bar{C}_H(T,H) = (\partial^2 F(T,H)/\partial T^2)_H \quad (2.2.3)$$

Higher derivatives of the free energy are frequently encountered in the theory of critical phenomena and are usually denoted

$$F^{(\lambda)}(T,H) = (\partial^\lambda F(T,H)/\partial H^\lambda)_T \quad (2.2.4)$$

In addition the spin-spin correlation functions characterise the microscopic behavior of the system. The pair correlation function of greatest interest for the XY model is

$$\Gamma(\underline{r},T,H) = (\langle S_{\underline{0}}^x S_{\underline{r}}^x \rangle - \langle S_{\underline{0}}^x \rangle^2) / S(S+1) \quad (2.2.5)$$

where in (2.2.5) $S_{\underline{r}}^x$ is the x component of the spin at a lattice site a distance \underline{r} from some reference lattice site at $\underline{0}$. The quantity S is the magnitude of the spin at each site. For the XY model $\langle S^x \rangle$ is the order parameter, so for $T > T_c$ (the critical temperature) the self correlation term $\langle S_{\underline{0}}^x \rangle^2$ is zero. In terms of the pair correlation functions the induced susceptibility may be expanded as

$$\chi(T,H) = 1 + \sum_{\underline{r} \neq \underline{0}} \Gamma(\underline{r},T,H) \quad (2.2.6)$$

In general the reduced form of any thermodynamic quantity is formed by dividing that function by the same function for a paramagnet at the same temperature. Thus we have

$$m(T,h) = M(H,T)/M(H \rightarrow \infty, T) \quad (2.2.7a)$$

for the reduced magnetisation and

$$C_H = \bar{C}_H(T, H) / Nk_B T \quad (2.2.7b)$$

is the reduced specific heat. The reduced susceptibility is

$$\chi(T,h) = \bar{\chi}(T, H) / \bar{\chi}(T, H \rightarrow \infty) \quad (2.2.7c)$$

where $h = \mu H / k_B T$ is the reduced ordering field and μ the magnetisation per particle.

The modern theory of critical phenomena is formulated in terms of critical exponents and critical amplitude ratios. Let $t = (T - T_c) / T_c$ be a measure of the distance in temperature from the critical point. Then the critical exponent for $T > T_c$ and $h = 0$ for any thermodynamic quantity $f(t)$ is

$$\lambda \equiv \lim_{t \rightarrow 0^+} \{ \ln f(t) / \ln t \} \quad (2.2.8)$$

with a similar definition for the low temperature critical exponent λ' . If the limit λ exists and is non-zero the

implied asymptotic form for $f(t)$ is

$$f(t) = At^\lambda + \sum_i B_i t^{\mu_i} \quad (2.2.9)$$

where A is called the high temperature amplitude of f and $\mu_i > \lambda$ for all i . The usual notation for the more common exponents and amplitudes is as follows:

$$m(t,0) \approx B(-t)^\beta \quad t < 0 \quad (2.2.10a)$$

$$m(0,h) \approx Dh^{1/\delta} \quad t = 0 \quad (2.2.10b)$$

$$\chi(t,0) \approx \begin{cases} C(-t)^{-\gamma} & t < 0 \\ Ct^{-\gamma} & t > 0 \end{cases} \quad (2.2.10c)$$

$$C_H(t,0) \approx \begin{cases} A(-t)^{-\alpha} & t < 0 \\ At^{-\alpha} & t > 0 \end{cases} \quad (2.2.10d)$$

and

$$F^{(\ell)}(t,0) \approx E^{(\ell)}(-t)^{-\Delta_\ell} F^{(\ell-1)}(t,0) \quad t < 0$$

$$F^{(2\ell)}(t,0) \approx E^{(2\ell)} t^{-2\Delta_{2\ell}} F^{(2\ell)}(t,0) \quad t > 0$$

(2.2.10e)

The correlation function has the form

$$\Gamma(r,t,0) \sim 1/r^{2=d-\eta} \quad t=0 \quad (2.2.11)$$

and the correlation length $\kappa(t)$ has the asymptotic form

$$\kappa(t,0) \approx \begin{cases} K(-t)^{\nu} & t < 0 \\ Kt^{-\nu} & t > 0 \end{cases} \quad (2.2.12)$$

For an extensive list of critical exponents and their values for some experimental situations the reader is referred to Stanley (1971). For the pure spin- $\frac{1}{2}$ XY model the results of Betts (1974) and co-workers and Dekeyser and Rogiers (1975) indicate that $\alpha \approx 0$ (a near logarithmic divergence) and $\gamma = 1.333 \pm 0.002$. Other exponents may be obtained from scaling theory as explained in the next section.

2.3 Scaling Theory

2.3.1 Critical point scaling

Scaling theory is a phenomenological theory of the behavior of thermodynamic functions near a critical point. The theory was originally formulated by Widom (1965a,b) and Domb and Hunter (1965). Kadanoff (1966) has given heuristic arguments in support of the theory. An outline of critical point scaling is given in Stanley (1971) and extensive reviews by Vicentini-Missoni (1972) and Levelt-Sengers (1974) record much of the known experimental evidence in support of scaling.

The static scaling hypothesis asserts that the singular part of the reduced free energy near the critical region is a generalised homogeneous function. This is

usually expressed mathematically as

$$f(\lambda t, \lambda^\Delta h) = \lambda^{\Delta+\beta} f(t, h) \quad (2.3.1)$$

where the exponent Δ is the gap exponent which is equal to Δ_2 for all t .

By taking various derivatives of the free energy equation (2.3.1), every exponent previously defined may be written in terms of the two exponents Δ and β . As a consequence of scaling, Rushbrooke's (1965) thermodynamic inequality

$$\alpha' + 2\beta + \gamma' \geq 2 \quad (2.3.2)$$

and Griffith's (1965a,b) thermodynamic inequality

$$\beta(\delta + 1) \geq 2 - \alpha \quad (2.3.3)$$

are both satisfied as equalities. Scaling theory also predicts that corresponding high and low temperature exponents are equal, for example $\gamma = \gamma'$, $\alpha = \alpha'$. Experimentally the scaling hypothesis can be verified for many substances and for several different types of second order transitions. In particular the scaled magnetisation, $m(t, h)/(-t)^\beta$, has been plotted against the scaled magnetic field, $h/(-t)^{\beta\delta}$, by Kouvel and Comley (1968) for nickel (metallic ferromagnet) and by Ho and Lister

(1969) for CrBr_3 (insulating ferromagnet). Their plots show that all the points for $T = T_c$ fit on one curve and all points for $T > T_c$ fit on another, verifying the predicted temperature independence.

As stated above only two exponents are needed to obtain the complete set of exponents for thermodynamic quantities. For the XY spin- $\frac{1}{2}$ model, assuming $\gamma=4/3$ and $\alpha=0$, scaling theory predicts $\gamma=2/3$, $\Delta=5/3$, $\beta=1/3$ and $\eta=0$.

2.3.2 Tricritical scaling theory

A tricritical point, as defined by Griffiths (1970), is characterised by the existence of two competing order parameters which simultaneously become critical. Examples of tricritical behavior can be found in metamagnets like FeCl_2 (Yelon and Birgeneau (1972)), $\text{Ni}(\text{NO}_3)_2 \cdot 2\text{H}_2\text{O}$ (Schmidt and Friedberg (1970)) and dysprosium aluminium garnet (Landau and Keen (1972)). Some systems which display structural phase transitions such as NH_4Cl (Garland and Weiner (1971)) have tricritical points. Of particular interest to us is the tricritical behavior of He^3 - He^4 mixtures because, as we show later, the annealed site XY model is conceivably a good model for this system.

Figure 2.1 shows the phase diagram for He^3 - He^4 mixtures in the $T\Delta$ plane, where Δ is the chemical potential difference $\mu_3 - \mu_4$.

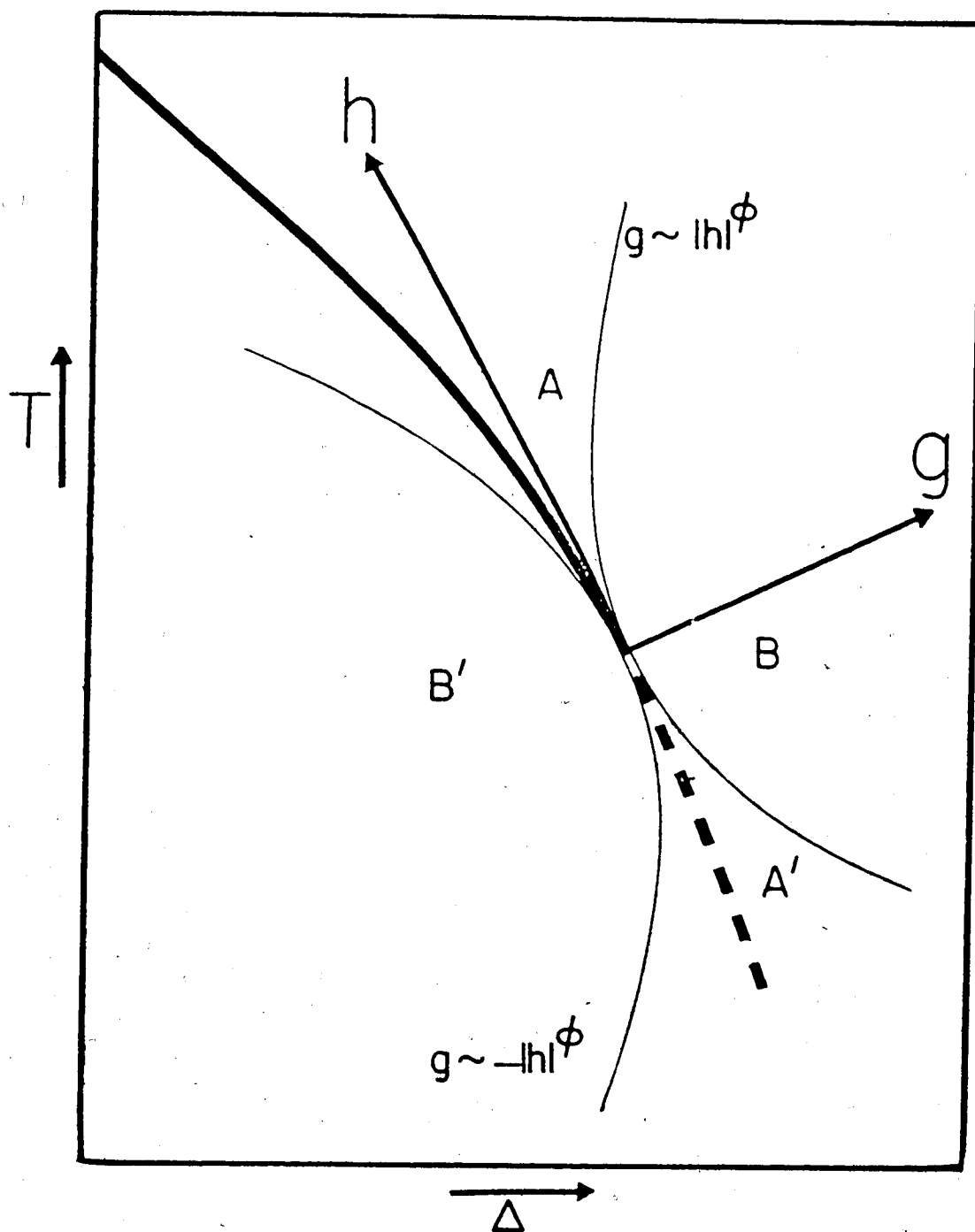


Figure 2.1 Temperature T versus chemical potential difference Δ for He^3 - He^4 mixtures (qualitative). The heavy solid curve represents the second order phase transition line while the dashed curve represents the first order transition line. The scaling axes h and g are plotted and the curve $g = h^\phi$ with $\phi > 1$ divides the plane into regions A and A' (u-like exponents) and B and B' (t-like) exponents.

For constant $\Delta = \Delta_t$ the transition is from the superfluid to the normal fluid state of He^4 . When $\Delta > \Delta_t$ the transition is first order and the line defines the phase boundary of the He^4 -rich and the He^3 -rich phases.

Recently the homogeneity hypothesis has been extended to include tricritical points. Riedel (1972, 1974), Griffiths (1973) and Hankey et al (1972) have developed the theory of tricritical scaling. Let ψ be the superfluid order parameter and ζ the field conjugate to ψ . The field ζ is physically unrealisable. Figure 2.1 is the He^3 - He^4 phase diagram in the $\zeta=0$ plane. In the field space ($T\Delta$ plane) the tangent to the line of critical points singles out a special direction which is used as one of the scaling directions. The co-ordinate along this direction is denoted as h . Another co-ordinate, g , can be chosen so that it makes an arbitrary non-zero angle with the h direction. In figure 2.1 h and g are drawn at right angles. The third scaling variable is ζ .

The tricritical point homogeneity hypothesis can then be written as

$$f(\lambda h, \lambda^\phi g, \lambda^{\phi\Delta_t} \zeta) = \lambda^{\phi(2-\alpha_t)} f(n, g, \zeta) \quad (2.1)$$

where $f(h, g, \zeta)$ is again the most singular part of the reduced free energy. Griffiths (1973) pointed out that the

above assumption results in two sets of tricritical exponents depending on path of approach toward the tricritical point. The two sets are distinguished by subscripting the exponents with a t or u. In (2.3.4) the t subscripted exponents are used and ϕ is called the cross-over exponent, the value of which determines the different scaling regions. Throughout the remainder of this discussion we assume that $\phi > 1$. For $\text{He}^3\text{-He}^4$ mixtures experimental evidence (Godner et al. (1974)) indicates that $\phi \approx 2$.

At this point we make a slight digression to describe some results obtained by Riedel (1974) and co-workers using renormalisation group techniques on the Blume-Emery-Griffiths (BEG) (1971) model. The BEG model is essentially a lattice fluid spin-1 Ising model of $\text{He}^3\text{-He}^4$ mixtures. In this model a He^4 particle, on the i th lattice site, is represented by the $S_i^Z = +1$ state, a He^3 particle by the $S_i^Z = 0$ state and the absence of a particle by the $S_i^Z = -1$ state. The value $\phi = 2$ was obtained by Riedel and Wegner (1972) for the BEG model. Other exponent values they obtained will be presented later in this section.

The role of the cross-over exponent is illustrated below by example. Assuming the ansatz (2.3.4) and using

$$\psi = -(\partial f / \partial \zeta)_{T, \Delta}$$

gives

$$\lambda^{\phi\Delta_t} \psi(\lambda h, \lambda^\phi g, \lambda^{\phi\Delta_t} \zeta) = \lambda^{\phi(2-\alpha_t)} \psi(h, g, \zeta) \quad (2.3.5)$$

Putting $\zeta=0$ and $\lambda = h^{-1}$ in (2.3.5) gives

$$\psi(h, g) = h^{\phi(2-\alpha_t-\Delta_t)} \psi(h/|h|, g/h^\phi) \quad (2.3.6)$$

Equation (2.3.6) is valid when $g < h^\phi$ which we define as the region for the u exponents and $\beta_u = \phi(2-\alpha_t-\Delta_t)$. Now putting $\zeta=0$ and $\lambda=g^{-1/\phi}$ in (2.3.5) gives

$$\psi(h, g) = g^{-\alpha_t+2-\Delta_t} \psi(h/g^{1/\phi}, g/|g|) \quad (2.3.7)$$

Equation (2.3.7) is valid when $g > h^\phi$ which is the region for the t exponents and

$$\beta_t = 2 - \alpha_t - \Delta_t = \beta_u/\phi \quad (2.3.8)$$

In general the t exponents are related to the u exponents by a factor ϕ , except for the specific neat exponents where the relation is

$$\alpha_u = 2 - \phi(2-\alpha_t) \quad (2.3.9)$$

The path $g=h^\phi$ is called the scaling boundary. In figure 2.1 the line $g=h^\phi$ is plotted for $\phi > 1$ and the different scaling regions are identified.

Quantities expected to be singular at the tricritical point only are the concentration χ_3 and the

concentration susceptibility defined by

$$W = (\partial X_3 / \partial \Delta)_{T,p} \quad (2.3.10)$$

where

$$X_3 = (\partial F / \partial \Delta)_{T,p} \quad (2.3.11)$$

If \bar{X}_3 is the value of X_3 at the tricritical point, then using the now standard notation we have

$$X_3 - \bar{X}_3 \sim \begin{cases} t^{\omega_t} & g > h\phi \\ t^{\omega_u} & g < h\phi \end{cases} \quad (2.3.12)$$

and

$$W \sim \begin{cases} t^{-\lambda_t} & g > h\phi \\ t^{-\lambda_u} & g < h\phi \end{cases} \quad (2.3.13)$$

An analogous procedure to that given above gives

$$\omega_u = \phi \omega_t = \phi(1 - \alpha_t)$$

and

$$\lambda_u = \phi \lambda_t = \phi \alpha_t$$

Experimental results for He³-He⁴ mixtures by Goellner et al. (1973) and renormalisation group calculations on the BEG model (Wegner and Riedel (1973)) yield the classical set of tricritical exponents, namely $\phi=2$, $\alpha_t=1/2$, $\gamma_t=1$, $\alpha_u=-1$ and $\gamma_u=2$.

Next we look briefly at cross-over effects.

Cross-over arises from the possibility that there exists a region where both critical and tricritical scaling laws hold.

Consider the susceptibility in the region near both the tricritical point and the line of second order phase transitions. Tricritical scaling predicts that

$$\chi_t(g,h) = \lambda^{\phi\gamma_t} \chi_t(\lambda^\phi g, \lambda h) \quad (2.3.14)$$

and critical scaling asserts that

$$\chi_c(g;h) = \lambda^\gamma \chi_c(\lambda g;h) \quad (2.3.15)$$

where in (2.3.15) h is a parameter and not a scaling variable. When $\lambda = g^{-1}$ we get from (2.3.15) that

$$\chi_c(g;h) = g^{-\gamma} f_c(h) ,$$

where $f_c(h)$ is the amplitude of χ_c . Now $\lambda = g^{-1/\phi}$ implies from (2.3.14) that

$$\chi_t(g,h) \sim g^{-\gamma_t} \chi_t(1, h/g^{1/\phi}) .$$

However near the tricritical region $\chi_t(g,h) = Ag^{-\gamma}$ which means that as $g \rightarrow 0$

$$\chi_t(1, h/g^{1/\phi}) \rightarrow A(h/g^{1/\phi})^{\phi(\gamma-\gamma_t)}$$

The result is that the amplitude of χ_c varies as

$$f_c(h) \sim h^{\phi(\gamma-\gamma_t)} \quad (2.3.16)$$

which diverges or converges as h moves closer to zero, depending on the sign of $\gamma-\gamma_t$. In the cross-over region the observed exponents (say γ for example) will not have either critical or tricritical values, but some effective value

$$\gamma_{\text{eff}} = -d \ln \chi(t,g) / d \ln t$$

which depends on g (Riedel and Wegner (1974)). Wegner and Riedel (1973) have also found that at the tricritical point there may be a logarithmic correction to the simple power law behavior for some thermodynamic functions.

2.4 Fisher Renormalisation

This section deals with the renormalisation of exponents by "hidden" variables.

The results we quote below are for thermally diluted systems, where the impurity concentration is the "hidden" variable. The renormalisation formulae were derived in general by Fisher (1968) and are summarised by the formulae

$$\alpha_x = -\alpha/(1-\alpha)$$

$$\beta_x = \beta/(1-\alpha) \quad (2.4.1)$$

$$\gamma_x = \gamma/(1-\alpha)$$

where γ_x is the exponent γ when the system contains a concentration x of thermal impurities. All exponents are renormalised as γ and β . The pure exponent values are found only when $x=0$. The formulae (2.4.1) are subject to the condition that $\alpha > 0$. In the event that $\alpha < 0$ if the specific heat is discontinuous, but finite (or possibly non-analytic) at T_c , then all exponents γ_x , β_x etc. will be observed to be greater than their values of $x=0$. Only when the specific heat has a logarithmic divergence at T_c is there no change in the observed value of exponents from their "pure" values.

The formulae (2.4.1) have been rigorously shown to hold (Essam and Garelich (1967)) for the Syozi (1965) model, which is transformable to an annealed bond spin- $\frac{1}{2}$ Ising system. In the case of the XY model the specific heat singularity is logarithmic or nearly so. This means that the Fisher renormalisation of exponents will be undetectable even if it is present.

2.5 Universality

The universality hypothesis has been stated by Kadanoff (1971) as follows.

"All phase transition problems can be divided into a small number of different classes depending on the dimensionality of the system and the symmetries of the ordered state. Within each class, all phase transitions have identical behavior in the critical region, only the names of the variables are changed."

The concept of universality is inspired in part by experimental evidence. Most simple fluids have a similar set of exponents for the liquid-gas transition which are very close to the 3-D nearest neighbour spin- $\frac{1}{2}$ Ising exponent, i.e. $\gamma \approx 1.25$, $\alpha \approx 0.125$ and $\beta \approx 0.312$. Many different magnets also have similar exponents. Specific examples can be found in Kadanoff (1971) and Stanley (1971).

In addition to the dimensionality of the system and the symmetry of the ordered state the universality classes are thought to depend on the range of the interaction and possibly for magnetic systems the magnitude of the spin per lattice site. One of the earliest formulations of the universality principle is due to Betts, Guttman and Joyce (1971). Let X and Y be two physical systems, then the most

singular parts of their free energies near their respective transitions satisfy

$$n_x f_x(t_x, h_x) = n_y f_y(t_y, h_y) \quad (2.5.1)$$

with

$$g_x t_x = g_y t_y \quad \text{and} \quad n_x h_x = n_y h_y \quad (2.5.2)$$

where $t = T/T_c - 1$, $h = mH/kT$ and g_x and n_x are critical scale factors. An immediate consequence of (2.5.1) and (2.5.2) is that the critical exponents of X and Y are equal. For the spin-spin correlation function the universality relation is (Ferrer and Wortis (1972))

$$\Gamma_x(\vec{R}_x, t_x, h_x) = \Gamma_y(\vec{R}_y, t_y, h_y) \quad (2.5.3)$$

with

$$R_x / \delta_x \ell_x = R_y / \delta_y \ell_y \quad (2.5.4)$$

where \vec{R}_x is the relative position of the two spins, δ_x is the nearest-neighbour separation and ℓ_x is a third scale factor.

Recently the concept of universality has been refined by two additional postulates. Firstly Stauffer, Ferrer and Wortis (1972) and Ferrer and Wortis (1972) assert that the most singular part of the free energy in a volume with diameter equal to the coherence length is universal. As a consequence of this condition only two independent scale

factors are needed. Secondly Betts and Ritchie (1975) suggest that the most singular part of the energy per bond length is universal. This conjecture necessitates only one scale factor. However the one scale factor universality does not hold for the spherical model of Berlin and Kac (1952) in the same form as for other models.

Some theoretical aspects of universality have been reviewed by Stanley (1974). In general the hypothesis as given above is consistent with a wide range of experimental and theoretical data. However there is considerable doubt as to the applicability to systems having more than two spin interactions. The best example of this is the eight-vertex model, solved exactly by Baxter (1971, 1972). The Hamiltonian for this model contains four-spin interactions and the critical exponents depend on the coupling strength. This phenomenon appears to be a violation of universality, but Kadanoff and Wegner (1971) have shown that the order parameter does have some peculiar symmetries which indicates that the eight-vertex model is in an unusual universality class. However, Suzuki (1974) has proposed an alternative remedy by using a "weak" universality principle. Weak universality requires that all exponents should be defined in terms of the correlation length κ and not t . The result is that the ratio for any two exponents

for systems in the same universality class are equal. More particularly the values $\delta=5$ and $\eta=0$ are universal values for three dimensional systems and γ/ν , β/ν , etc. are invariant within each universality class.

CHAPTER III

THE XY MODEL AND MAGNETIC DILUTION

3.1 Introduction

Before motivating a study of the XY model let us first define what it is.

The anisotropic Heisenberg model for spin- $\frac{1}{2}$ systems can be written as

$$H = -(4s^2)^{-1} \sum_{ij} \{ J_{ij}^{\perp} (S_i^x S_j^x + S_i^y S_j^y) + J_{ij}^{\parallel} S_i^z S_j^z \} - s^{-1} \sum_i \{ m_{\perp} H^x S_i^x + m_{\parallel} H^z S_i^z \} \quad (3.1.1)$$

The indices i and j run over all lattice sites and S_i^{α} is the α Cartesian component of the spin vector \underline{S} of magnitude s . The exchange "integrals" J_{ij}^{\perp} and J_{ij}^{\parallel} are measures of the spin-spin coupling strength and the external fields H^x and H^z are coupled to the spin system via the coupling constants m_{\perp} and m_{\parallel} .

Three special cases of (3.1.1) can be identified. These are the Ising Hamiltonian (when $J^{\perp} = 0$), the isotropic Heisenberg Hamiltonian (when $J^{\parallel} = J^{\perp}$) and the XY Hamiltonian (when $J^{\parallel} = 0$). Both the Heisenberg and Ising models are well established as models for certain strong ferromagnets and antiferromagnets. The Ising model is also

used as a model for a lattice fluid of classical particles. Recent reviews of the Heisenberg and Ising models are given by Rushbrooke et al. (1974) and Domb (1974) respectively. The XY model has been extensively reviewed by Betts (1974) and much of the description of the XY model in this chapter is gleaned from that article.

In the Sections 2 and 3 following we demonstrate the conditions under which the XY model describes an insulating magnet and a quantum lattice fluid. Section 4 describes what it means to dilute a spin exchange system with classical impurity atoms and what physical situations are described by this process.

3.2 XY Magnetic Insulators

Betts et al. (1970) have shown, using perturbative arguments, how in the presence of a crystal field of particular symmetry, the isotropic Heisenberg Hamiltonian reduces to the XY Hamiltonian. Their argument is as follows. Consider a crystal of magnetic ions of high half odd integer spin embedded in a lattice of non-magnetic ions. The non-magnetic crystalline environment will introduce single ion terms in the spin Hamiltonian. For most symmetries (except cubic) the leading single ion anisotropy is proportional to $(S^z)^2$. If the magnetic ions are assumed to interact according to the isotropic Heisenberg model, then

the Hamiltonian for the complete system is,

$$H = D \sum_i (S_i^Z)^2 - J \sum_{ij} \underline{S}_i \cdot \underline{S}_j \quad (3.2.1)$$

Near the critical region and for $D \gg J > 0$ only the lowest Kramers doublet with $S^Z = \pm 1/2$ will be appreciably populated resulting in an effective spin- $\frac{1}{2}$ system. In a system of two spins for example the XY interaction is

$$H^{XY} = -J(S+1/2)^2/2 \begin{pmatrix} 0 & 0 & 0 & 0 \\ 0 & 0 & 1 & 0 \\ 0 & 1 & 0 & 0 \\ 0 & 0 & 0 & 0 \end{pmatrix} \quad (3.2.2)$$

and the Ising part of the interaction is

$$H^I = -J/4 \begin{pmatrix} 1 & 0 & 0 & 0 \\ 0 & -1 & 0 & 0 \\ 0 & 0 & -1 & 0 \\ 0 & 0 & 0 & 1 \end{pmatrix} \quad (3.2.3)$$

If the magnetic ion is for instance Dy^{3+} then the ratio of the XY non-zero matrix elements to the Ising non-zero matrix elements is approximately 128:1. Clearly then magnets which are XY like can conceivably occur in nature. In fact some cobalt-halide compounds definitely have an antiferromagnetic transition which is theoretically well explained by the XY model. Examples include $CoBr_2 \cdot 6H_2O$ and

$\text{CoCl}_2 \cdot 6\text{H}_2\text{O}$ in two dimensions (de Jongh et al. (1974)). More recently Algra et al. (1976) have investigated the antiferromagnetic transition of the cobalt pyridines $\text{Co}(\text{C}_5\text{H}_5\text{NO})_6(\text{ClO}_4)_2$ and $\text{Co}(\text{C}_5\text{H}_5\text{NO})_6(\text{BF}_4)_2$. For these compounds the magnetic lattice is simple cubic and the specific heat near T_c closely fits the series expansion results of Betts et al. (1971).

Theoretical work by Jasnow and Wortis (1968) on the anisotropic classical Heisenberg model (obtained by taking the limit as $S \rightarrow \infty$ in (3.1.1)) indicates that if $J'' \ll J'$ then the symmetry of the order parameter is likely to be XY like. Universality asserts that this should also be the case for the spin- $\frac{1}{2}$ XY model.

3.3 Quantum Lattice Fluids

Yang and Lee (1952) have shown how the spin- $\frac{1}{2}$ Ising model corresponds to a classical lattice fluid. In this context spin up is identified with the occupancy of a Wigner-Seitz cell by a particle and spin down represents an empty cell. The Ising Hamiltonian is then essentially the potential energy of the system. In a like manner we show below how a quantum lattice fluid is represented by the anisotropic Heisenberg model (following Matsubara and Matsuda (1956)).

Firstly each site (or cell) is assigned two possible states such that

$u_{\underline{r}} = \begin{pmatrix} 1 \\ 0 \end{pmatrix}$ represents an occupied site

and $v_{\underline{r}} = \begin{pmatrix} 0 \\ 1 \end{pmatrix}$ represents a vacant site.

The creation of a particle at the \underline{r} th site can be effected by the operator $a_{\underline{r}}^{\dagger}$ defined by

$$a_{\underline{r}}^{\dagger} v_{\underline{r}} = u_{\underline{r}} \quad \text{and} \quad a_{\underline{r}}^{\dagger} u_{\underline{r}} = 0 \quad (3.3.1)$$

The destruction operator $a_{\underline{r}}$ is the Hermitian adjoint of $a_{\underline{r}}^{\dagger}$, and in terms of matrices we can write

$$a_{\underline{r}}^{\dagger} = \begin{pmatrix} 0 & 1 \\ 0 & 0 \end{pmatrix} \quad \text{and} \quad a_{\underline{r}} = \begin{pmatrix} 0 & 0 \\ 1 & 0 \end{pmatrix} \quad (3.3.2)$$

The number of particles in the \underline{r} th cell is $n_{\underline{r}} = a_{\underline{r}}^{\dagger} a_{\underline{r}}$, which has eigenvalues 0 or 1. Creation and annihilation operators of different sites commute. To ensure that each cell is only singly occupied, operators on the same site obey the anticommutation relations

$$\{a_{\underline{r}}, a_{\underline{r}}\} = \{a_{\underline{r}}^{\dagger}, a_{\underline{r}}^{\dagger}\} = 0 \quad (3.3.3)$$

and

$$\{a_{\underline{r}}, a_{\underline{r}}^{\dagger}\} = 1$$

The connection between $a_{\underline{r}}$ and $a_{\underline{r}}^\dagger$ and the continuum quantum field creation and annihilation operators $\psi^\dagger(\underline{r})$ and $\psi(\underline{r})$ is

$$a_{\underline{r}}^\dagger = \psi^\dagger(\underline{r})v_0^{1/2} \quad \text{and} \quad a_{\underline{r}} = \psi(\underline{r})v_0^{1/2} \quad (3.3.4)$$

and

$$n_{\underline{r}} = v_0 \rho(\underline{r}) = v_0 \psi^\dagger(\underline{r})\psi(\underline{r})$$

where v_0 is the cell volume. The potential energy between two particles at \underline{r} and \underline{r}' is assumed to be

$$v_{\underline{r}\underline{r}'} = \begin{cases} \infty & \underline{r} = \underline{r}' \\ -u_0 & \underline{r} - \underline{r}' = \underline{\delta} \\ 0 & \text{otherwise} \end{cases} \quad (3.3.5)$$

where $\underline{\delta}$ is the nearest neighbour distance. Hence the potential energy operator for the total system is

$$U = -u_0 \sum_{\langle \underline{r}, \underline{r}' \rangle} a_{\underline{r}}^\dagger a_{\underline{r}} a_{\underline{r}'}^\dagger a_{\underline{r}'}$$

The sum in (3.3.6) is over nearest neighbour sites only.

The quantum field theory kinetic energy operator is

$$T = -(\hbar^2/2m) \int \psi^\dagger(\underline{r}) \nabla^2 \psi(\underline{r}) d\underline{r} \quad (3.3.7)$$

where m is the molecular mass. For a discrete lattice the integral is replaced by a sum over sites and the Laplacian by the finite difference operator and ψ 's by a 's. Thus we get

$$\begin{aligned}
T &= -(\hbar^2/2m) \sum_{\underline{r}} a_{\underline{r}}^\dagger (2d/q\delta^2) \sum_{\delta} (a_{\underline{r}+\delta} - a_{\underline{r}}) \\
&= -(\hbar^2 d/2m\delta^2) \left(\sum_{\langle \underline{r}, \underline{r}' \rangle} (a_{\underline{r}}^\dagger a_{\underline{r}'} + a_{\underline{r}} a_{\underline{r}'}^\dagger) - q \sum_{\underline{r}} n_{\underline{r}} \right)
\end{aligned}
\tag{3.3.8}$$

where d is the dimension of the lattice and q the coordination number.

The grand partition function for the complete system is then

$$\begin{aligned}
\Xi(T, \mu) &= \text{Tr} \exp \beta \{ (\mu - \hbar^2 d/m\delta^2) N + \hbar^2 d/qm\delta^2 \sum_{\langle \underline{r}, \underline{r}' \rangle} (a_{\underline{r}}^\dagger a_{\underline{r}'} + a_{\underline{r}} a_{\underline{r}'}^\dagger) \\
&\quad + \mu_0 \sum_{\langle \underline{r}, \underline{r}' \rangle} n_{\underline{r}} n_{\underline{r}'} \}
\end{aligned}
\tag{3.3.9}$$

where

$$N = \sum_{\underline{r}} n_{\underline{r}}$$

Now if we put $a_{\underline{r}} = S_{\underline{r}}^x - iS_{\underline{r}}^y$ and $a_{\underline{r}}^\dagger = S_{\underline{r}}^x + iS_{\underline{r}}^y$ then we can make the identification between (3.3.9) and (3.1.1) by putting

$$2m_{\perp} H^z = \mu + q\mu_0/2 - \hbar^2 d/m\delta^2$$

$$m_{\perp} = 0, J^{\perp} = \hbar^2 d/qm\delta^2$$

and

$$J^{\parallel} = \mu_0/2$$

(3.3.10)

The pure XY model then corresponds to the neglect of the potential energy between particles on adjacent sites.

The above derivation is due to Stephenson (1971) and is outlined in Betts (1974). Historically Matsubara and Matsuda (1956) were the first to derive the anisotropic Heisenberg Hamiltonian as a model for the superfluid-normal fluid transition in He^4 . The XY model of He^4 has been investigated by Ditzian and Betts (1971) and Betts and Lothian (1973) using high temperature series expansions. Their results were in good agreement with the available experimental data for various critical exponents and amplitudes. The results for the critical exponents give $\gamma = 1.33 \pm 0.02$ and a logarithmic divergence of the specific heat (i.e., $\alpha \approx 0$). Dekeyser and Rogiers (1976) confirm this estimate of γ using high temperature series expansions with one more term than those obtained by Betts and co-workers.

3.4 Dilute Models

By dilution of spin exchange lattice models such as the XY model we mean the introduction in the lattice of non-interacting particles. The four common types of impurity dilution are classified as quenched or annealed systems by their thermal distribution and bond or site models by the mode of occupancy of the non-interacting particles.

Bond dilution is when the impurity particles are placed in the "bond" between two lattice sites. Site dilution is achieved by replacing the magnetic ion on a given site by a non-interacting particle. In quenched dilution the impurities are "frozen in" the lattice in a random distribution. On the other hand annealed impurities are thermally mobile and assume their equilibrium distribution at all temperatures.

For crystalline magnets it seems unlikely that annealing of impurities can be achieved since this would imply that the impurity atoms were able to move through the lattice. Quenched impurities in magnetic crystals are physically realisable though. The quenched bond case could correspond in a super-exchange magnet to the replacement of the interstitial ion by an ion that does not allow exchange. The quenched site case corresponds to the replacement of a magnetic ion in a direct exchange magnet by a non-interacting particle.

Annealing of impurities can of course readily occur in fluids. Thus it seems reasonable to use the annealed site model as a model for a diluted lattice gas. There seems to be, however, no mechanism of "exchange" in lattice fluids that could correspond to the super-exchange mode in magnetic crystals, hence bond dilution seems unlikely for lattice fluids.

In the next three subsections the site dilution problems are considered in detail.

3.4.1 Percolation theory

In the next subsection on quenched site dilution we make frequent reference to results from percolation theory. In this subsection we define the percolation problem and its relation to the problem at hand.

Consider a lattice with a fraction p of its sites occupied by magnetic ions. The occupied sites fall into a number of clusters and two such sites belong to the same cluster if there is a chain of nearest neighbour occupied sites connecting them. The mean cluster size will depend on p and one instinctively expects that $S(p)$ will increase linearly with p and be a maximum for $p = 1$. In the case of an infinite lattice however, the cluster size is no longer bounded. There exists, in fact, a critical percolation concentration p_c^* which is the largest value of p for which a given occupied site certainly belongs to a cluster of finite size. For $p > p_c^*$ there is a non-zero probability that a given occupied site belongs to an unbounded cluster. The relation between the percolation problem and the quenched site dilute magnetism is contained in the following statement proved by Rushbrooke and Morgan (1961). The limiting concentration p_c^* of magnetic elements,

below which there is no critical temperature is the same for all such models, whether Heisenberg, XY or Ising and regardless of the spin value concerned. This critical concentration is of course the critical percolation concentration. In fact the properties of the zero temperature Ising model led Kasteleyn and Fortuin (1969) to establish the following analogy between certain percolation functions and the thermodynamic functions of a ferromagnet.

The pair connectedness (which is the probability that two sites belong to the same cluster) is like a pair correlation function. The percolation probability (the fraction of sites contained in infinite clusters) has properties similar to the magnetisation. The mean cluster size $S(p)$ is analogous to the zero field susceptibility. Consequently it is possible to assign critical exponents to these percolation functions. For example

$$S(p) \approx C[(p-p_c^*)/p_c^*]^{-\gamma} p$$

The percolation problem has been extensively reviewed by Essam (1972). Table 3.1 gives the critical percolation concentrations for some common lattices.

Table 3.1 Site percolation critical concentrations for some common lattices

Lattice	Square	Triangular	Simple Cubic	Body Centred Cubic	Face Centred Cubic
P_c^*	0.59 ± 0.01	$1/2$	0.31 ± 0.01	0.24 ± 0.01	0.195 ± 0.005

3.4.2 Quenched site dilution

For magnetic lattice models quenched site dilution is the occupation of a random distribution of lattice sites by non-magnetic impurities. Both the quenched site Heisenberg and Ising models have been studied extensively by many workers.

Exact results known to date are few, and apply only to the Ising model. The most important of these results is due to Griffiths (1969). His result says that the magnetisation fails to be an analytic function of field H at $H=0$ for a range of temperatures above that at which spontaneous magnetisation first appears. Wortis (1974) has observed this occurrence of spurious singularities in M for the one dimensional random dilute bond and site Ising models. Also Rauh (1975, 1976) has studied a randomly dilute spherical model and observed Griffiths singularities. Griffiths and Lebowitz (1968) also have derived some exact, but very general results for the free energy of the annealed site Ising ferromagnet. McCoy and Wu (1968) have studied the two dimensional Ising model with a particular distribution of impurities. Behringer (1957) was the first to investigate the quenched site Heisenberg ($S=\frac{1}{2}$) model and found roughly how T_c varies with the concentration of magnetic ions p . This line of critical points was compared with some

early experimental results of Fallot (1936, 1937) and Forestier (1928) on various alloys with one magnetic component. Brout (1959) also worked on this problem and was the first to point out that Heisenberg like systems can be diluted by either annealing or quenching the impurities. For recent series expansion studies of the quenched site Ising and Heisenberg models, the interested reader is referred to recent papers by Rushbrooke (1971), Rapaport (1972a,b), Rushbrooke et al. (1972), Elliot and Saville (1974) and references therein. Because the Heisenberg, XY and Ising models are independent we will not describe in detail results of previous work on the Ising or Heisenberg quenched site models. Instead, we will quote in later chapters only the results needed for comparison with our own.

3.4.3 Annealed site dilution

Annealed site impurities are not "frozen-in" as are quenched site impurities, but are allowed to assume their thermal equilibrium distribution. It is unrealistic to expect this type of dilution to be realised in crystalline substances. However annealed impurities in a lattice fluid could represent one component of a fluid mixture.

The impurity particles are classical and serve only to occupy lattice site which could otherwise be occupied

by an interacting particle. Since the XY model gives a good description of the superfluid-normal fluid transition in He^4 it is natural to present the annealed site XY model as a model for He^3 - He^4 mixtures. The kinetic mobility and statistics of the He^3 particles are absent, but for temperatures well above the tricritical temperature (where phase separation first occurs) these may not be important considerations. Formally the tricritical point is where the phase separation order parameter, X_3 , and the superfluid order parameter ψ , simultaneously become critical.

To demonstrate that the annealed site spin- $\frac{1}{2}$ XY model has tricritical behavior we establish the equivalence of this system with the Takagi model of He^3 - He^4 mixtures, following Reeve (1976). The argument is similar to that used by Wortis (1974) to identify the Blume-Capel model (Blume (1966), Capel (1966, 1967a,b)) with the spin- $\frac{1}{2}$ annealed site Ising model.

Consider the model with nearest neighbour

Hamiltonian

$$H^T = -J \sum_{\langle ij \rangle} (a_i^\dagger a_j + a_i a_j^\dagger) - H_1 \sum_i S_i^z - H_2 \sum_i (S_i^z)^2 \quad (3.4.1)$$

proposed and solved in the mean field approximation by Takagi (1972). Total spin, $S=1$ for this model. The

operators a_i^\dagger and a_i raise and lower, respectively, the value of the spin projection on the i th site between the values $S^Z = +1$ and $S^Z = 0$ only.

Dekeyser and Rogiers (1975) showed that in the limit as $H_1 - H_2 \rightarrow \infty$, H^T is equivalent to the spin- $\frac{1}{2}$ XY model given by (1.1), with $mH = H_1 + H_2$. However, since the a_i^\dagger and a_i act only in a two dimensional subspace and the S_i^Z are diagonal, we can decompose H^T into the direct sum of two operators. One of these operators is the spin- $\frac{1}{2}$ XY Hamiltonian $H_{N_m}^{xy}$ given by

$$H_{N_m}^{xy} = -J \sum_{\langle ij \rangle} (a_i^\dagger a_j + a_i a_j^\dagger) - mH \sum_i S_i^Z$$

with $mH = H_1 + H_2$, where N_m is the number of particles in the system. The second operator is the one dimensional quantity $N_m(H_2 - H_1)$. Since these operators act in different subspaces of the spin-1 system they commute. Hence we may write the partition function for the Takagi model as

$$Z_T = \sum_{N_m=0}^{N_m=L} \exp\{\beta N_m(H_2 - H_1)\} \text{Tr} \exp\{-\beta H_{N_m}^{xy}\} \quad (3.4.2)$$

where N_m is the total number of lattice sites. Identification of μ , the chemical potential per site, with $H_2 - H_1$ shows that (3.4.2) is precisely the grand partition function of for the spin- $\frac{1}{2}$ annealed site XY problem.

The Takagi model has been extensively studied, via high temperature series expansions, by Dekeyser and Rogiers (1975) and Rogiers, Dekeyser and Quisthoudt (1975). Their results demonstrate, as do mean field calculations, the existence of tricritical behavior qualitatively characteristic of $\text{He}^3\text{-He}^4$ mixtures.

Other thermally dilute systems which have been studied are the Syozi (1965) model (Syozi and Miyazima (1966)) and the bond annealed spin- $\frac{1}{2}$ Ising model (Rapaport (1972) and Cox et al. (1976)).

3.5 Dilution and Critical Phenomena

In this section we relate the general theories given in Chapter II to the problem of dilute lattice models.

The effect of impurities imposed in the XY lattice model will be to lower the critical temperature roughly linearly with increasing impurity concentration. A qualitative plot of $T_c(q)$ versus q , the impurity concentration, is given in figure 3.1.

3.5.1 Scaling theory

The scaling theory outlined in Section predicts that if we approach an arbitrary point P from the high q direction or the high temperature direction the same essential elements should be observed. This is because ordinary

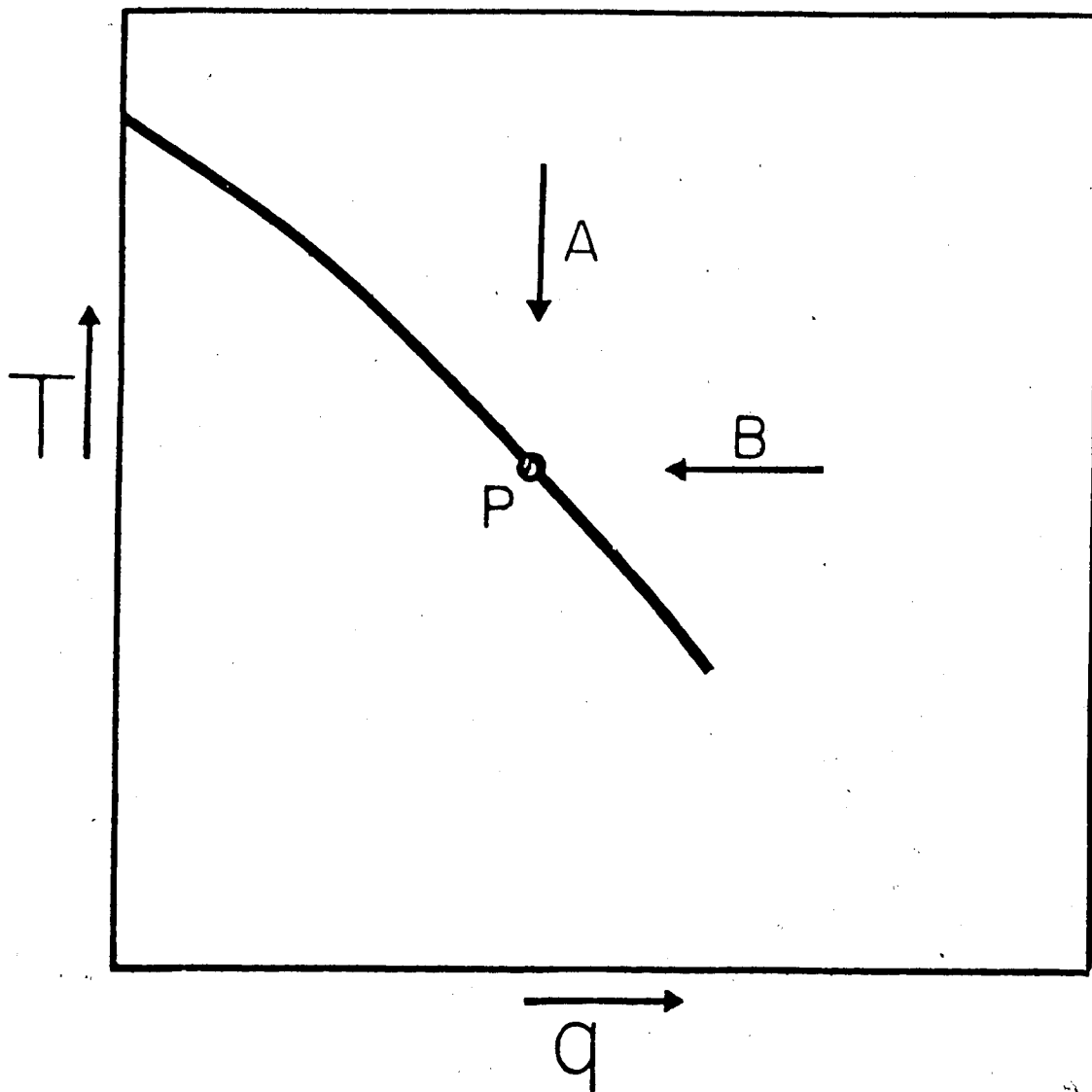


Figure 3.1 Schematic diagram of temperature T versus impurity concentration q for diluted spin-exchange models. The arrow A shows the direction of high temperature approach to the arbitrary point P and the arrow B shows the high q direction.

scaling theory can be applied to the line of critical points, simply by inserting the density (or fugacity) variable as a non scaling parameter in (2.3.1).

3.5.2 Fisher renormalisation

Fisher renormalisation of exponents applies to the annealed site case and will be practically unobservable since $\alpha \simeq 0$.

3.5.3 Universality

According to the universality principle all points along the line of critical points are equivalent. This means that the critical exponents should not vary with q . Weak universality on the other hand demands that ratios like γ/ν be invariant with respect to q .

CHAPTER IV

THE FINITE CLUSTER EXPANSION

4.1 Introduction

Although the first generally applicable expression of the finite cluster theorem is due to Domb (1960), the method of Rushbrooke and Scoins (1955), in turn derived from an application by Fuchs (1942) of cluster integral theory to the Ising problem, is substantially similar.

Nevertheless the power of the method was not fully realised until Domb and Wood (1965) derived the high temperature series for the Heisenberg ferromagnet using the finite cluster technique. Previous to this work though, Rushbrooke and Morgan (1961) and Morgan and Rushbrooke (1961, 1963) developed series expansions in inverse temperature and density for Ising and Heisenberg ferromagnets with quenched site impurities. These were essentially applications of the finite cluster method, a point later elucidated by Rushbrooke (1964).

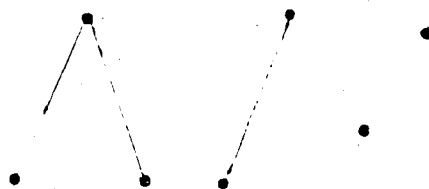
The original derivation of the finite cluster theorem is reviewed in Domb (1974) and parallels the classical cluster integral theory developed by Ursell (1927) and Mayer (1939). This derivation is useful in that it emphasises the equivalence of the finite cluster theorem and the Mayer cluster expansion. However we choose to

follow a more elegant proof due to M. F. Sykes and reported by Essam (1966). Before we can digest this proof though a few graph theoretic definitions are required.

4.2 Definitions of Graph Theory

The definitions presented are outlined in Sykes et al. (1966).

Illustrated below is a graph with seven vertices, three edges (bonds) and four components.



A graph of one component only is called connected, otherwise it is disconnected.

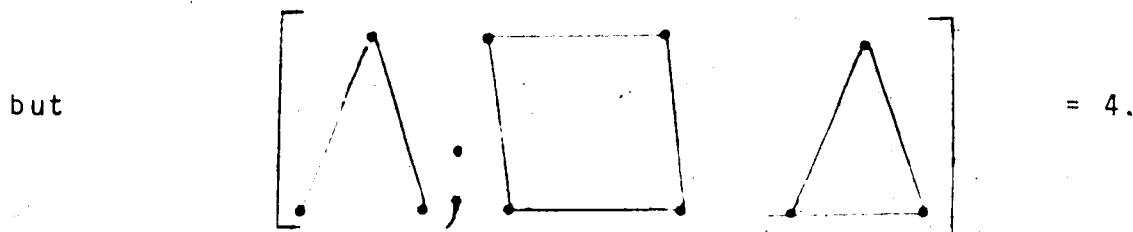
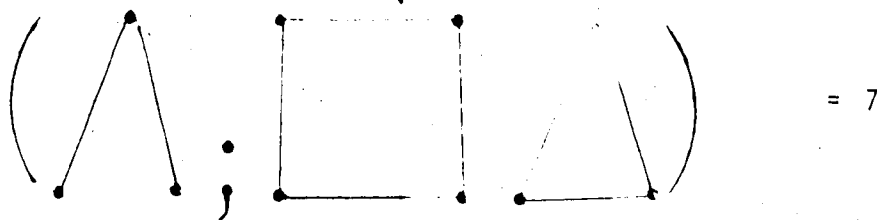
Two graphs G and G' are isomorphic if there is a one-one correspondence between their vertex sets V and V' such that corresponding vertices are joined by edges in one of them only if they are joined in the other.

A graph H is a subgraph of G when the vertex set $V(H)$ is contained in the vertex set $V(G)$ and all the edges of H are edges of G .

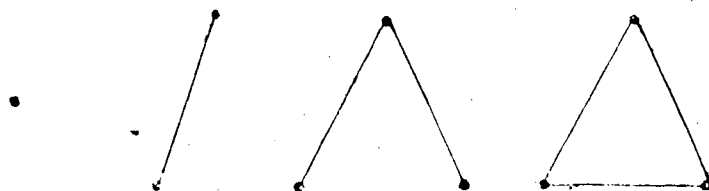
A section graph H of G is a subgraph of G such that its edges are all the edges of G which connect two vertices of H .

Any subgraph G' of G which is isomorphic with a graph g is said to represent a weak embedding of g in G . If the graph G' is a section graph of G then G' represents a strong embedding of g on G . The number of subgraphs of G isomorphic with g , denoted by $(g;G)$, is called the weak lattice constant of g in G . Similarly the number of section graphs of G isomorphic with g is called the strong lattice constant of g on G and is symbolised by $[g;G]$.

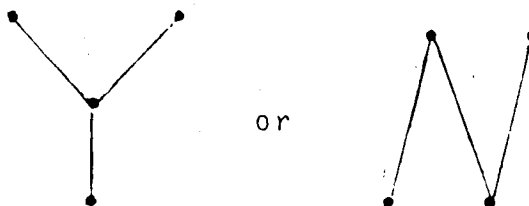
As an example the subgraph



Denoting by, $\{C_i\}$, the complete set of connected graphs, ordered such that $(C_i; C_j) = [C_i; C_j] = 0$ for $i > j$, results in a complete set of connected graphs in dictionary order. The first four elements of such a list must be



followed by either



the choice being inconsequential. The final and most important definition for our purposes is the following.

If $\phi(G)$ is a function defined for any graph G , then $\phi(G)$ is extensive if and only if

$$\phi(G \cup G') = \phi(G) + \phi(G') \quad (4.2.1)$$

where the graph $G \cup G'$ is the graph formed by regarding all the components of G and G' as constituting a single graph.

In the present context a graph G has a vertex set $V(G)$ which represents the sites of a physical lattice having interacting particles on them, while the edges are representative of the interaction between pairs of particles. The function $\Phi(G)$ is any thermodynamic function that can be defined for the graph. For example it may be the free energy, susceptibility, etc.

Armed now with these definitions we can proceed to demonstrate the finite cluster theorem.

4.3 The Finite Cluster Theorem

4.3.1 The theorem

Let $\Phi(G)$ be any function defined for a graph G which has the extensive property (4.2.1). Then

$$\Phi(G) = \sum_{i=1}^k f(C_i) \Pi_i(G)$$

where $C_i \in \{C_i\}$, $\Pi_i(G)$ is either $(C_i; G)$ or $[C_i; G]$ and $f(C_i)$ is a function specified by the C_i only.

4.3.2 The proof

Since $\Phi(G)$ is extensive then from (4.2.1)

$$\Phi(G) = \sum_{j=1}^k \Phi(C_j) \Pi_j^*(G) \quad (4.3.1)$$

where $\Pi_j^*(G)$ is the number of components of G isomorphic with

C_j and k is any integer such that $\Pi_j^*(G) = 0$ for $j > k$. Only connected subgraphs or section graphs need be considered, allowing us to write

$$\Pi_i(G) = \sum_{j=1}^k \Delta_{ij} \Pi_j^*(G)$$

where Δ_{ij} is either $(C_i; C_j)$ or $[C_i; C_j]$ depending on the choice for the lattice constants. The dictionary ordering of $\{C_i\}$ means that $\Delta_{ij} = 0$ for $i > j$ and $\Delta_{ii} = 1$, so that the determinant of (Δ_{ij}) is one and we can write,

$$\Pi_j^*(G) = \sum_{i=1}^k \Gamma_{ij} \Pi_i(G)$$

where $\Gamma_{ij} = (\Delta^{-1})_{ij}$. Substitution of $\Pi_j^*(G)$ back into (4.3.1) gives the desired result, namely

$$\phi(G) = \sum_{i=1}^k f(C_i) \Pi_i(G) \quad (4.3.2)$$

with

$$f(C_i) = \sum_{j=1}^k \phi(C_j) \Gamma_{ji} \quad (4.3.3)$$

This finite cluster theorem holds for both finite and infinite graphs G . An infinite graph is a physical lattice in our case. The lattice constants on a physical lattice are denoted by $[C_i; L]$ and $(C_i; L)$, where L could represent the f.c.c., b.c.c. lattice, etc. They are defined as the number of embeddings of C_i on L per site of

L. Accordingly in the thermodynamic limit the finite cluster expansion is

$$N^{-1} \phi(L) = \lim_{k \rightarrow \infty} \sum_{i=1}^k f(C_i) \cdot \Pi_i(L) \quad (4.3.4)$$

Now in a later section, there are properties of the $f(C_i)$ which enable us to take k finite and retain an exact cluster expansion for $\phi(L)$ in certain independent variables.

4.4 Construction of the Expansion

In practice there are several steps we must follow in order to establish the finite cluster expansion for a specified function $\phi(L)$. These are tabulated as follows:

- (i) Establish a dictionary ordered graph list.
- (ii) Find the matrix elements Δ_{ij} which should usually be the strong embeddings, since this enables the list in (i) to be shorter than that required if the weak embedding scheme is chosen.
- (iii) Obtain the weights $f(C_i)$ in terms of the $\phi(C_i)$ using (4.3.3).
- (iv) Calculate the lattice constants $\Pi_i(L)$.
- (v) Substitute the $f(C_i)$ and $\Pi_i(L)$ into (4.3.2).

In order to clarify the discussion of the previous section we will derive the expansion up to and including clusters of three vertices. The appropriate graph list is

$$C_1 = \bullet$$

$$C_2 = \text{---}$$

$$C_3 = \text{^}$$

and

$$C_4 = \triangle$$

and for convenience we restrict considerations to the strong scheme. Thus $\Delta_{ij} = [C_i; C_j]$ and $\Pi_j(L) = [C_j; L]$. The matrix $(\Delta)_{ij}$ denoted by $\Delta(3)$ is by inspection

$$\Delta(3) = \begin{pmatrix} 1 & 2 & 3 & 3 \\ 0 & 1 & 2 & 3 \\ 0 & 0 & 1 & 0 \\ 0 & 0 & 0 & 1 \end{pmatrix}$$

which has the inverse

$$\Gamma(3) = \begin{pmatrix} 1 & -2 & 1 & 3 \\ 0 & 1 & -2 & -3 \\ 0 & 0 & 1 & 0 \\ 0 & 0 & 0 & 1 \end{pmatrix}$$

The equations (4.3.3) then yields

$$f(C_1) = \phi(C_1)$$

$$f(C_2) = \phi(C_2) - 2\phi(C_1)$$

$$f(C_3) = \phi(C_3) - 2\phi(C_2) + \phi(C_1)$$

$$f(C_4) = \phi(C_4) - 3\phi(C_2) + 3\phi(C_1) \quad (4.4.1)$$

It is worth noting that we could have arrived at (4.4.1) by recursively solving equation (4.3.2) for $G = C_1, G = C_2$, etc. and in practice this method is often preferred since it is easily programmed for a computer and doesn't require knowledge of the Γ_{ij} explicitly. The equations (4.4.1) demonstrate that the $f(C_i)$ depend only on $\phi(C_k)$ with $k \leq i$ and not on $\phi(C_k)$ with $k > i$. This is the essential property which enables perturbation expansions to be constructed.

We shall not detail step (iv), suffice it to say the techniques involved in solving the problem are very

sophisticated (see for instance Martin (1974)). The results we need here, for a lattice of co-ordination number q , are: $[C_1;L] = q$, $[C_2;L] = q/2$, $[C_3;L] = q(q-m-1)/2$ and $[C_4;L] = qm/6$. The lattice L is any of the regular Bravais lattices, namely the face centred cubic (f.c.c.)($q=12$), body centred cubic (b.c.c.)($q=8$), simple cubic (s.c.)($q=6$), plane triangular (p.t.)($q=6$) and the simple quadratic (s.q.)($q=4$). The parameter m is zero except for the close packed f.c.c. ($m=4$) and the p.t. ($m=2$) lattices. These data, together with equation (4.4.1) are substituted into (4.3.2) to give

$$\begin{aligned}
 N^{-1}\phi(L) = & \phi(C_1) + (\phi(C_2) - 2\phi(C_1))q/2 \\
 & + (\phi(C_3) - 2\phi(C_2) + \phi(C_1))q(q-m-1)/2 \\
 & + (\phi(C_4) - 3\phi(C_2) + 3\phi(C_1))qm/6 \\
 & + \dots \dots \dots
 \end{aligned}
 \tag{4.4.2}$$

4.5 Perturbation Expansions from the Finite Cluster Theorem

The derivation of expansions in magnetic ion concentration and inverse temperature for Heisenberg like magnetic models is readily achieved using the finite cluster theorem. By way of example we will derive series in quenched site density, annealed site fugacity and inverse temperature.

Case I: The quenched site problem

In this problem applicable to Heisenberg like ferromagnets, we add to some of the lattice sites non interacting impurities to prevent the occupation of those sites by magnetic ions. The distribution of these impurity atoms is assumed to be at random at all temperatures, physically representing the quenched defects one might conceivably expect in a real crystalline ferromagnet. If the probability of magnetic site occupation is p , then the system is mathematically represented by weighting the factors $f(C_i)$ in (4.3.4) by p^{v_i} where v_i is the number of vertices of C_i . This ensures that all of the vertices of C_i are occupied for $f(C_i)$ to contribute in the expansion, which is

$$\begin{aligned}
 N^{-1} \phi(L) = & p\phi(C_1) + p^2(\phi(C_2) - 2\phi(C_1))q/2 \\
 & + p^3\{(\phi(C_3) - 2\phi(C_2) + \phi(C_1))(q-m-1)q/2 \\
 & + (\phi(C_4) - 3\phi(C_2) + 3\phi(C_1))qm/6\} \\
 & + \dots \dots \dots
 \end{aligned}
 \tag{4.5.1}$$

using (4.4.2) directly.

Clearly (4.5.1) is an exact expansion since C_i contributes only to terms of order v_i and higher in p .

Case II: High temperature expansions

Derivation of series in inverse temperature from (4.4.2) is just as simple as for the previous case, but the exactness of the expansion is not obvious. For this reason we shall demonstrate the method for the specific case of the spin- $\frac{1}{2}$ XY model.

One quantity having the desired extensive property is the dimensionless free energy per site $f(T) = \ln Q / Nk_B T$, where $Q = \text{Tr} \exp\{-\beta H\}$ is the canonical partition function for the system. For the XY model, the method by which we obtain Q for finite clusters is contained in Appendix A. The results we need here are:

$$Q(C_1) = 2$$

$$Q(C_2) = 2 + 2\cosh K$$

$$Q(C_3) = 4 + 4\cosh \sqrt{2}K$$

$$Q(C_4) = 2 + 2\exp(2K) + 4\exp(-K)$$

where $K = \beta J = J/k_B T$ and J is the "exchange integral" between nearest neighbour pairs of magnetic sites. These equations give an expansion in K to third order.

$$\ln Q(C_1) = \ln 2$$

$$\ln Q(C_2) = \ln 2 + K^2/4 + \dots$$

$$\ln Q(C_3) = 3\ln 2 + K^2/2 + \dots$$

$$\ln Q(C_4) = 3\ln 2 + 3K^2/4 + K^3/4 + \dots$$

which are the functions $\phi(C_i)$. From these we get via (4.4.1), $f(C_1) = \ln 2$, $f(C_2) = K^2/4$, $f(C_3) = 0$ and $f(C_4) = K^3/4$. From equation (4.3.2) then we get

$$N^{-1} \ln Q = \ln 2 + qK^2/8 + qmK^3/24 + \dots \quad (4.5.2)$$

Equation (4.5.2) is correct only to second order in K because $f(C_i)$ produces terms of order K^{ℓ_i} or higher, where ℓ_i is the number of bonds in C_i . To obtain an expansion exact to third order would require that all graphs of three bonds or less be present in the dictionary graph list.

Domb (1965) has written down formulae giving, for some different graph topologies, the term in K at which C_i first contributes, K^{ℓ_i} is a lower bound for this.

Obviously we could also expand (4.5.1) in K for the spin- $\frac{1}{2}$ XY model and obtain an expansion in K correct to second order.

Case III: The annealed site problem

This, the last case we shall consider, is somewhat different from the previous cases and is normally applied to lattice fluid problems rather than magnetic crystals. For consistency however we retain the magnetic system terminology.

Just as for the quenched site case we dilute the lattice with non interacting impurities, but allow them to assume their equilibrium temperature distribution. We are thus required to use the grand canonical ensemble, since unlike the quenched site case the density of magnetic ions is itself a thermodynamic function

$$\rho_m = Z_m^{-1} \partial \ln \Xi / \partial Z_m$$

where Ξ is the grand partition function and the fugacity Z_m of the magnetic ions is given by $\exp(\mu_m \beta)$, with μ_m the chemical potential of the magnetic ions.

For continuous media the grand partition function is, for N particles, given by

$$\Xi_N = \sum_{n=0}^N Z^n Q_n$$

where Q_n is the canonical partition function for n particles. On a lattice of discrete sites finite N corresponds to a finite cluster and we may write

$$\Xi(C_j) = \sum_{g_i} Z^{v_i} [g_i; C_j] Q(g_i) \quad (4.5.3)$$

The sum is over all graphs (connected and disconnected) with less than or equal to v_j vertices. Strong embeddings are used in (4.5.3) because they do not allow sites which are connected on C_j to be occupied by sites of g_i which are not, a requirement made necessary by our interpretations of the graphs.

The free energy is constructed by forming $\ln \Xi(C_j)$ for all the C_j as power series in Z_m . As for the quenched site case, if our graph list is complete up to and including graphs of M vertices or less, then the series for $N^{-1} \ln(L)$ will be exact up to order Z_m^M .

For simplicity let us consider the third order approximation for which the list $\{g_i\}$ is

$$g_1 = \bullet$$

$$g_2 = \begin{array}{c} \bullet \\ \bullet \end{array}$$

$$g_3 = \text{---} \text{---}$$

$$g_4 = \triangle$$

$$g_5 = \triangle$$

and

Equation (4.5.3) then gives

$$\Xi(C_1) = 1 + ZQ(C_1)$$

$$\Xi(C_2) = 1 + 2ZQ(C_1) + Z^2Q(C_2)$$

$$\Xi(C_3) = 1 + 3ZQ(C_1) + Z^2(Q(C_1))^2 + 2Z^2Q(C_2) = Z^3Q(C_3)$$

$$\Xi(C_4) = 1 + 3ZQ(C_1) + 3Z^2Q(C_2) + Z^3Q(C_4)$$

where we have used $Q(g_2) = Q(C_1)Q(C_1)$.

Proceeding as before and using $\phi(C_i) = \ln \Xi(C_i)$ gives the weights $f(C_i)$ as

$$f(C_1) = ZQ(C_1) - Z^2(Q(C_1))^2/2 + Z^3(Q(C_1))^3/3$$

$$f(C_2) = Z^2(Q(C_2) - (Q(C_1))^2) + Z^3(2(Q(C_1))^3 - 2Q(C_1)Q(C_2))$$

$$f(C_3) = Z^3((Q(C_1))^3 - 2Q(C_1)Q(C_2) + Q(C_3))$$

$$f(C_4) = Z^3((Q(C_1))^3 - 3Q(C_1)Q(C_2) + Q(C_4))$$

up to third order. The resulting expansion is

$$\begin{aligned} N^{-1} \ln \Xi(L) &= Z_m Q(C_1) + Z_m^2 \{ (Q(C_2) - (Q(C_1))^2)q/2 - (Q(C_1))^2/2 \} \\ &\quad + Z_m^3 \{ q(q-m-1)/2 ((Q(C_1))^3 - 2Q(C_1)Q(C_2) + Q(C_3)) \\ &\quad + qm/6 (2(Q(C_1))^3 - 3Q(C_1)Q(C_2) + Q(C_4)) \} \end{aligned}$$

$$\begin{aligned}
 & + q/2 (2(Q(C_1))^3 - 2Q(C_1)Q(C_2)) + (Q(C_1))^3/3) \\
 & + \dots
 \end{aligned}
 \tag{4.5.4}$$

Although the exactness of the expansion is again apparent, it is not a trivial task to verify this generally. Nevertheless the previously mentioned analogy of the finite cluster and the classical Mayer expansion indicates that a fugacity expansion is not unexpected. The earlier method of Rushbrooke and Scions (1955) does give a little clearer insight into this property which has also been demonstrated by Essam (1967) for the "hard square" lattice fluid model.

Series expansions for thermodynamic expectation values are extensive and so there is no difficulty in obtaining expansions for thermodynamic functions for the quenched site and high temperature cases.

Tentatively let us define

$$\langle O \rangle_N = \frac{1}{\Xi_N} \sum_{n=0}^N z^n \text{Tr } O_n \exp(-\beta H_n) \tag{4.5.5}$$

as the grand canonical expectation value for the operator O over N particles, where O_n is the operator for the n particles with interaction Hamiltonian H_n . Symbolically we can express this as

$$\langle O \rangle_N = \text{Tr}_{\{n, H_n\}} O_n \exp(-\beta(H_n - \mu n)) / \text{Tr}_{\{n, H_n\}} \exp(-\beta(H_n - \mu n))$$

which is formally equivalent to

$$\langle O \rangle_N = -\beta^{-1} \lim_{\lambda \rightarrow 0} \frac{\partial}{\partial \lambda} \{ \ln \text{Tr}_{\{n, H_n\}} \exp(-\beta(H_n - \mu n + \lambda O_n)) \}$$

Now if the operator $P_n = H_n - \mu n + \lambda O_n$ in the exponent is additive in the sense that

$$P(S_1 \cup S_2) = P(S_1) + P(S_2)$$

where S_1 and S_2 are two independent systems, then the quantity $\ln \text{Tr}_{\{n, H_n\}} \exp(-\beta P_n)$ is extensive since the commutator $[P(S_1), P(S_2)] = 0$. The additive property of P holds for all the quantities we consider because O_n can usually be written in the form $\sum_{ij} O_{ij}$, with operators not physically connected on the lattice not interacting.

Equation (4.5.5) then is a good choice of definition and is the same as

$$\langle O \rangle_N = \sum_{n=0}^{\infty} z^n \bar{O}_n / \Xi_n \quad (4.5.6)$$

where \bar{O}_n is the unnormalised canonical expectation value of O over n particles. We note here that the usual definition of the grand canonical expectation value $\langle O \rangle_N$ as found in standard texts (for instance Huang (1963)) is not extensive. This is because the normalised canonical expectation value of O_n is usually used in (4.5.6) instead of the unnormalised quantity \bar{O}_n .

Equation (4.5.5) then is a good choice of definition, but is not the same as is usually used. For a graph G the equivalent definition is

$$\langle O(G) \rangle = \sum_{g_i} z^{V_i} [g_i; G] \bar{O}(g_i) / \Xi(G) \quad (4.5.7)$$

The unnormalised canonical expectation values $\bar{O}(g_i)$ are not extensive and add like

$$\bar{O}(G \cup G') = (\bar{O}(G)/Q(G) + \bar{O}(G')/Q(G')) Q(G)Q(G')$$

remembering that $Q(G \cup G') = Q(G)Q(G')$.

As an example we get for the graph C_3 ,

$$\langle O(C_3) \rangle = \frac{3z\bar{O}(C_1) + z^2(2\bar{O}(C_1)Q_2(C_1) + 2\bar{O}(C_2)) + z^3\bar{O}(C_3)}{1 + zQ(C_1) + z^2((Q(C_1))^2 + Q(C_2)) + z^3Q(C_3)}$$

Expanding $\langle O(C_i) \rangle$ for all the graphs C_i in powers of Z results in an exact series expansion for $N^{-1}\langle O(L) \rangle$ as we had before for $N^{-1}\ln \Xi(L)$.

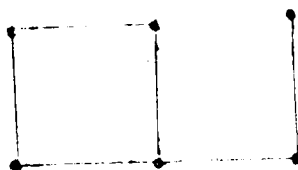
4.6 Inversion of the Finite Cluster Theorem

In Section 4 it was mentioned that the equation (4.3.3) is commonly solved by recursion of (4.3.2). However in principle it is possible to invert (4.3.2) analytically to obtain the theorem as

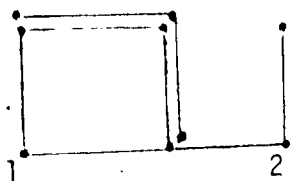
$$N^{-1}\phi(L) = \sum_{C_i} \phi(C_i)A(C_i;L) \quad (4.6.1)$$

This result was established by Rushbrooke (1964) for the quenched site problem, but is true in general. One other definition is necessary before explaining his result.

The perimeter s of a graph G' embedded in a graph G is the number of vertices of G not themselves in G' , but connected to at least one vertex of G' . An example is the graph C_3 embedded into



as



which has perimeter $s=2$ (the sites labelled 1 and 2). The number of ways a graph C_i can be strongly embedded in a graph G , with perimeter s is usually denoted by $[C_i; G], s$.

Rushbrooke's result is then

$$A(C_i; L) = \sum_s p^{\sum_i v_i} (1-p)^s [C_i; L], s \quad (4.6.2)$$

The variable p is the quenched site probability and the series is truncated at s or m , where m is the maximum number of vertices considered in the initial graph list. The result (4.6.2) is valid when $p=1$, so the finite cluster

expansion becomes

$$N^{-1}\phi(L) = \sum_{C_i} \phi(C_i) (-)^{m-v_i} \sum_s \binom{s-1}{m-v_i} [C_i; L], s \quad (4.6.3)$$

where s must be greater than or equal to $m - v_i + 1$ or the term doesn't contribute.

Counting the perimeter for each lattice embedding is more difficult than the normal lattice constant problem. However we have chosen to use (4.6.3) since it eliminates the tedious recursion which must be performed each time we change the temperature in a density or fugacity expansion. Tables of strong lattice constants and perimeter counts for the f.c.c., b.c.c., s.c., p.t. and s.q. lattices can be found in Appendix B.

4.7 Advantages of the Method

The finite cluster theorem is not the only method enabling density expansions to be generated, but it is as yet the most powerful.

In the terminology of magnetic systems the following advantages can be listed.

- (i) An expansion in density or fugacity contains complete temperature information.
- (ii) For the quenched site case an expansion in inverse temperature contains complete density information.

- (iii) When used in conjunction with the XY model all series contain complete parallel field information.
- (iv) Using the expansion in the strong scheme necessitates a shorter graph list than most other methods.

CHAPTER V

THE QUENCHED SITE

5.1 Introduction

In this chapter we present the results of an investigation into the quenched site spin- $\frac{1}{2}$ XY model on the regular three dimensional Bravais lattices.

The plan of this chapter is as follows. In Section 2 we discuss first the generation of series expansions in p , the concentration of magnetic atoms, for the zero field free energy and for the zero field fluctuation in the long range order. The coefficients are determined for arbitrary temperature. Next we discuss the generation of high temperature expansions for the same two quantities.

The methods of analysis are outlined in Section 3.

In Section 4 we investigate the behavior of the critical exponents of the order parameter fluctuation. One issue we consider is whether the exponent, $\gamma(p)$ for approach to the second order line at constant p is in fact a function of p . We also consider whether the exponent $\bar{\gamma}(T)$ for approach to the second order line at constant T depends on T .

Section 5 deals with lattice dependent critical properties, particularly the location in the T, p plane of the second order line and the amplitude of the critical singularity of the order parameter fluctuation.

Section 6 contains summary and discussion.

5.2 Generation of Series

In the present investigation we have generated two types of series, high temperature series and low concentration series for each of two quantities, the zero field free energy and the zero field fluctuation in the long range order.

The method of obtaining these series is explained in detail in Chapter IV. The Hamiltonian for the system is

$$-\beta H = K \sum_{\langle ij \rangle} (a_i^\dagger a_j + a_i a_j^\dagger) \quad (5.2.1)$$

and the method by which we diagonalise the Hamiltonian for finite clusters is given in the appendix. In Equation (5.2.1) $K = \beta J$.

The expansion for $Y(p, K)$, the fluctuation in the long range order, in terms of p , the concentration of magnetic ions, is of the form

$$Y = p + \sum_{\ell=2}^{\infty} \bar{c}_\ell(K) p^\ell. \quad (5.2.2)$$

The $\bar{c}_i(K)$ are not of simple analytic form but can be obtained numerically to arbitrarily high precision for a given temperature. In Tables 5.1, 5.2 and 5.3 are tabulated for a selected set of reduced temperatures, $t = K_c/K$, \bar{c}_2 through \bar{c}_7 for the three cubic lattices.

The high temperature expansions of the free energy for the f.c.c. (F), b.c.c. (B) and s.c. (S) lattices are respectively

$$\begin{aligned}
 f_F(p, K) = & \ln 2 + \frac{1}{2} p^2 K^2 + 2p^3 K^3 + \left(-\frac{1}{16} p^2 - \frac{3}{8} p^3 + \frac{1}{8} p^4\right) K^4 \\
 & + \left(-p^3 - 5p^4 + 10\frac{1}{2} p^5\right) K^5 + \left(\frac{1}{2} + \frac{11}{120} p^3 - \frac{237}{80} p^4 - 17\frac{1}{4} p^5 + 30\frac{5}{16} p^6\right) K^6 \\
 & + \left(\frac{17}{40} p^3 + 3\frac{11}{20} p^4 - 8\frac{13}{120} p^5 - 61p^6 + 96\frac{3}{8} p^7\right) K^7 + \dots
 \end{aligned}
 \tag{5.2.3}$$

$$\begin{aligned}
 f_B(p, K) = & \ln 2 + p^2 K^2 + \left(-\frac{1}{24} p^2 - \frac{7}{12} p^3 + \frac{1}{2} p^4\right) K^4 \\
 & + \left(\frac{1}{360} p^2 + \frac{7}{60} p^3 - \frac{29}{120} p^4 - 3\frac{1}{2250} p^5 + 4\frac{5}{8} p^6\right) K^6 + \dots
 \end{aligned}
 \tag{5.2.4}$$

$$\begin{aligned}
 f_S(p, K) = & \ln 2 + \frac{3}{4} p^2 K^2 + \left(-\frac{1}{32} p^2 - \frac{5}{16} p^3 + \frac{3}{8} p^4\right) K^4 \\
 & + \left(\frac{1}{480} p^2 + \frac{5}{80} p^3 + \frac{1}{32} p^4 - \frac{1}{2} p^5 + \frac{11}{16} p^6\right) K^6
 \end{aligned}
 \tag{5.2.5}$$

Table 5.1 Coefficients $\bar{c}_l(K)$ in (5.2.2) for the face centred cubic lattice, $K_C^F(1) = 0.2210$

t	\bar{c}_2	\bar{c}_3	\bar{c}_4	\bar{c}_5	\bar{c}_6	\bar{c}_7
1.0	1.3206	1.4540	1.5754	1.6761	1.7643	1.8438
0.9	1.4686	1.7739	2.1147	2.4724	2.8583	3.2790
0.8	1.6456	2.1894	2.8864	3.7251	4.7505	6.0076
0.7	1.8804	2.7905	4.1294	5.9626	8.5007	12.0055
0.6	2.1834	3.6373	6.1045	9.9416	15.9742	25.3892
0.5	2.6097	4.9290	9.5688	17.8192	32.7635	59.4336
0.4	3.2360	6.9316	15.9800	34.3539	73.5759	154.345
0.3	4.2321	9.9680	29.0983	71.0295	185.052	450.262
0.2	6.0287	13.1298	64.5183	138.079	615.889	1310.94
0.1	.6275	2.2292	267.210	-561.020	8330.10	-35342.6

Table 5.2 Coefficients in (5.2.2) for the body centred cubic lattice taking $K_C^B(1) = 0.344$

t	\bar{c}_2	\bar{c}_3	\bar{c}_4	\bar{c}_5	\bar{c}_6	\bar{c}_7
1.0	1.3649	1.4145	1.6003	1.6556	1.7775	1.8331
0.8	1.6967	2.0953	2.9042	3.6002	4.6957	5.8156
0.6	2.2361	3.3507	6.0300	9.1863	15.2076	23.2840
0.4	3.2476	5.8527	15.3179	28.3515	65.4839	124.193
0.2	5.5760	8.1090	61.5423	44.0514	657.957	-170.553

Table 5.3 coefficients in (5.2.2) for the simple cubic lattice taking $K_C^S(1) = 0.495$

t	\bar{c}_2	\bar{c}_3	\bar{c}_4	\bar{c}_5	\bar{c}_6	\bar{c}_7
1.0	1.4554	1.4152	1.6211	1.6646	1.7849	1.8340
0.8	1.7993	2.0114	2.8415	3.4344	4.4364	5.3102
0.6	2.3438	2.9792	5.5891	7.9332	13.0036	19.0076
0.4	3.3018	4.2826	13.3063	18.8738	49.9002	72.7894
0.2	5.0684	2.5483	49.7399	-29.1445	542.644	-1029.774

The high temperature expansions of the order parameter fluctuation on the same three lattices are

$$\begin{aligned}
 Y_F(\quad)/\rho &= 1 + 6pK + 33p^2K^2 + \left(-\frac{1}{2}p - 11p^2 + 175\frac{1}{2}p^3\right)K^3 \\
 &+ \left(-17p^2 - 106p^3 + 918\frac{3}{4}p^4\right)K^4 \\
 &+ \left(\frac{1}{20}p + 1\frac{1}{10}p^2 - 148\frac{2}{5}p^3 - 789\frac{3}{4}p^4 + 4766\frac{5}{8}p^5\right)K^5 \\
 &+ \left(7\frac{14}{15}p^2 + 71\frac{5}{6}p^3 - 1102\frac{43}{80}p^4 - 5284p^5 + 24589\frac{5}{16}p^6\right)K^6 \\
 &+ \left(-\frac{17}{3360}p + 2\frac{157}{240}p^2 + 150\frac{127}{336}p^3 + 829\frac{251}{336}p^4 \right. \\
 &\quad \left. - 7395\frac{83}{480}p^5 - 33287\frac{5}{16}p^6 + 126344\frac{203}{224}p^7\right)K^7
 \end{aligned}$$

(5.2.6)

$$\begin{aligned}
 Y_B(p,K)/\rho &= 1 + 4pK + 14p^2K^2 + \left(-\frac{1}{3}p - 4\frac{2}{3}p^2 + 49p^3\right)K^3 \\
 &+ \left(-4\frac{2}{3}p^2 - 23\frac{1}{3}p^3 + 165\frac{1}{2}p^4\right)K^4 \\
 &+ \left(\frac{1}{30}p + 1\frac{2}{5}p^2 - 21\frac{2}{5}p^3 - 116\frac{1}{4}p^4 + 561\frac{1}{4}p^5\right)K^5 \\
 &+ \left(1\frac{29}{90}p^2 + 14\frac{31}{45}p^3 - 104\frac{17}{72}p^4 - 484\frac{5}{6}p^5 + 1875\frac{7}{8}p^6\right)K^6 \\
 &+ \left(-\frac{17}{5040}p - \frac{119}{360}p^2 + 8\frac{8}{21}p^3 + 93\frac{213}{280}p^4 \right. \\
 &\quad \left. - 427\frac{457}{720}p^5 - 1996\frac{1}{24}p^6 + 6287\frac{11}{16}p^7\right)K^7
 \end{aligned}$$

(5.2.7)

$$\begin{aligned}
Y_S(p,K)/p = & 1 + 3pK + 7\frac{1}{2} p^2 K^2 + (-\frac{1}{4} p - 2\frac{1}{2} p^2 + 18\frac{3}{4} p^3) K^3 \\
& + (-2\frac{1}{4} p^2 - 8\frac{3}{4} p^3 + 45\frac{3}{8} p^4) K^4 \\
& + (\frac{1}{40} p + \frac{3}{4} p^2 - 7\frac{1}{2} p^3 - 29\frac{5}{8} p^4 + 110\frac{7}{16} p^5) K^5 \\
& + (\frac{17}{24} p^2 + 5\frac{23}{30} p^3 - 24\frac{89}{160} p^4 - 87\frac{11}{16} p^5 + 264\frac{15}{32} p^6) K^6 \\
& + (-\frac{34}{13440} p - \frac{17}{96} p^2 + 2\frac{74}{105} p^3 + 23\frac{2809}{3360} p^4 \\
& - 72\frac{529}{960} p^5 - 255\frac{9}{32} p^6 + 635\frac{1155}{1344} p^7) K^7
\end{aligned}$$

(5.2.8)

5.3 Methods of Series Analysis

Given the first n terms of the power series representation of a function $F(Z)$ we wish to determine the radius of convergence Z_c of that power series and the asymptotic form of $F(Z)$ as $Z \rightarrow Z_c$. The two most common methods employed in critical phenomena are the ratio method and the method of Padé approximants.

5.3.1 The ratio method

Suppose that the coefficients in the series

$$F(Z) = \sum_l a_l Z^l \quad (5.3.1)$$

are known to degree n and are of the same sign. Assuming

that all the a_ℓ have the same sign, the sequence of ratios $r_\ell = a_{\ell+1}/a_\ell$ must approach the radius of convergence Z_c of $F(Z)$ as $\ell \rightarrow \infty$. If we further assume that $F(Z)$ has the asymptotic form

$$F(Z) \sim A(1 - Z/Z_c)^{-g} \quad (5.3.2)$$

as $Z \rightarrow Z_c$ then the ratios must have the asymptotic form

$$r_\ell \sim Z_c^{-1}(1 + (g-1)/\ell) \quad (5.3.3)$$

The radius of convergence of (5.3.1) is the first singularity from the origin in the complex Z plane. A plot of r_ℓ versus $1/\ell$ will yield Z_c^{-1} as the intercept on the $1/\ell = 0$ axis and the slope will give $Z_c^{-1}(g-1)$, provided the form (5.3.2) is correct. By expanding (5.3.2) as a series in Z the asymptotic form of the a_ℓ for large ℓ is determined as

$$a_\ell \sim Ag(g+1) \dots (g+\ell-1)/\ell! Z_c^\ell \quad (5.3.4)$$

from which the amplitude A can be obtained using the previous estimates for g and Z_c .

5.3.2 Padé approximants

The ratio method is usually used to give preliminary estimates for the position of the critical point and the exponent g . A more widely used method, especially for series of moderate length, is the method of Padé approximants.

A $[N/D]$ Padé approximant is the ratio of two polynomials of degree N and D , so that

$$[N/D] = \frac{n_0 + n_1 Z + n_2 Z^2 + \dots + n_N Z^N}{1 + d_1 Z + d_2 Z^2 + \dots + d_D Z^D} \quad (5.3.5)$$

The $N+D+1$ unknown coefficients of equation (5.3.5) are equated to the first $N+D+1$ coefficients of the series (5.3.1).

If the first L terms of $F(Z)$ are known, then we must have $N+D+1 \leq L$. Since the singularities of the Padé approximant consists of simple poles only we should represent by Padé approximants functions which have simple poles only. If the function to be analysed has the simple form (5.3.2) then the functions $[F(Z)]^{1/g}$ and $d \ln F(Z)/dZ = [F(Z)]^{-1} dF(Z)/dZ$ have simple poles. If g is known then poles of Padé approximants to $[F(Z)]^{1/g}$ give estimates of Z_c and the residues of the poles closest to Z_c give estimates of $A^{1/g}$. If g is not known then the location of poles of Padé approximants to $d \ln F(Z)/dZ$ give estimates of Z_c and the corresponding residues give estimates of g .

5.4 Critical Exponent Behavior

At the phase boundary the fluctuation in the long range order (or equivalently the initial susceptibility) of the spin- $\frac{1}{2}$ XY model is expected to diverge strongly. For the purposes of series analysis we assume a singularity of the simple form

$$\chi(p, K) \approx C(p) [1 - K/K_C(p)]^{-\gamma(p)} \quad (5.4.1)$$

for approach along a path of constant p in the K - p plane. For approach along a line of constant temperature the singularity is assumed to have the form

$$\chi(p, K) \approx \bar{C}(K) [1 - p/p_C(K)]^{-\bar{\gamma}(K)} \quad (5.4.2)$$

Admittedly more complicated behavior cannot be ruled out. Indeed various more complicated types of phase transition behavior have been established (McCo. and Wu (1968), Griffiths (1969)) or made plausible (Suzuki (1974), Harris (1974)) for other models.

Most previous analysis has concentrated on the high temperature series, for which the behavior (5.4.1) is assumed (Rusbrooke et al. (1972), Rapaport (1972a) and references therein). Accordingly, we consider the high temperature series first. As critical exponents are lattice independent and as high temperature series generally behave best on the f.c.c. lattice we concentrate on that lattice in attempting to determine $\gamma(p)$ and $\bar{\gamma}(K)$. Our results on the b.c.c. and s.c. lattice are consistent with but less precise than those on the f.c.c. lattice.

Detailed analysis of a 9 term high temperature series for the fluctuation of the pure XY model on the f.c.c.

lattice yielded $\gamma(1) = 1.33 \pm 0.02$ and $K_C(1) = 0.2210 \pm 0.0010$ (Betts et al. (1970), Betts (1974)). Naturally the analysis of the seven term high temperature series for $Y(p,K)$ for the dilute XY magnet will yield less precise results.

Assuming the validity of (5.4.1) estimates of $\gamma(p)$ can be obtained from Padé approximants to the logarithmic derivative of the high temperature series for $Y(p,K)$. The results of such analysis for a selection of values of p for the high degree, central approximants are displayed in Table 5.4.

The most noticeable feature of Table 5.4 is the increasing scatter of the $\gamma(p)$ estimates as p decreases. This scatter, even at $p = 1$, is sufficiently great to indicate that the high temperature series have not yet settled down to their asymptotic behavior. If, nevertheless, some "best" estimate of $\gamma(p)$ be extracted from Table 5.4 and plotted against p then the resulting curve falls roughly halfway between the similar curves of Rushbrooke et al. (1972) for the spin- $\frac{1}{2}$ Ising and Heisenberg models. Given that $\gamma(p)$ increase as p decreases for all these models, then the behavior XY model is as expected from simple interpolation. However we do not believe that the Padé approximant evidence, for the XY model, is sufficient to establish firmly a dependence of γ on p .

Table 5.4 Estimates of the critical exponent, $\gamma(p)$, from $[N/D]$ Padé approximants to series for $d \log Y(p,K)/dK$ on the f.c.c. lattice

$[N/D]$	$p=1.0$	$p=0.9$	$p=0.8$	$p=0.7$	$p=0.6$
[1/5]	1.36	1.44	1.61	2.19	-
[2/4]	1.36	1.43	1.55	1.81	2.89
[3/3]	1.27	1.31	1.38	1.50	1.76
[4/2]	1.52	1.83	3.52	-	-
[1/4]	1.44	-	-	1.14	1.15
[2/3]	1.23	1.25	1.30	1.37	1.53
[3/2]	1.08	1.08	1.07	1.06	1.04

Ratio plots also indicate that the high temperature series for $Y(p,K)$ have not yet reached their asymptotic form.

The low concentration expansions of $Y(p,K)$ tell a rather different story. We have been able to analyse these series by both ratio and Padé approximant methods for a set of values of $t = T/T_C(1)$. For $0.7 < t < 1.0$ the ratio plots are remarkably linear. Figure 5.1 illustrates the behavior of the ratios for a typically good series, at $t = 0.9$. Table 5.5 summarizes the results of the ratio analysis. The assigned errors are confidence limits obtained by examining the range of plausible straight line fits to the points on the ratio plot.

Alternative estimates of $\bar{\gamma}(t)$ are obtained from the residues of Padé approximants to low concentration series expansions of $Y(p,K)$ on the f.c.c. lattice. The results of such analysis for degree 4 and 5 approximants is displayed in Table 5.6. Confidence limits could be assigned on the basis of the degree of consistency among different Padé approximants to the same series. Note that the central estimates drift slowly upward, as t decreases. The estimates from high denominator degree approximants drop while those from high numerator degree rise sharply as t decreases.

The ratio estimates of $\bar{\gamma}(t)$ and the estimates from central Padé approximants agree well with one another.

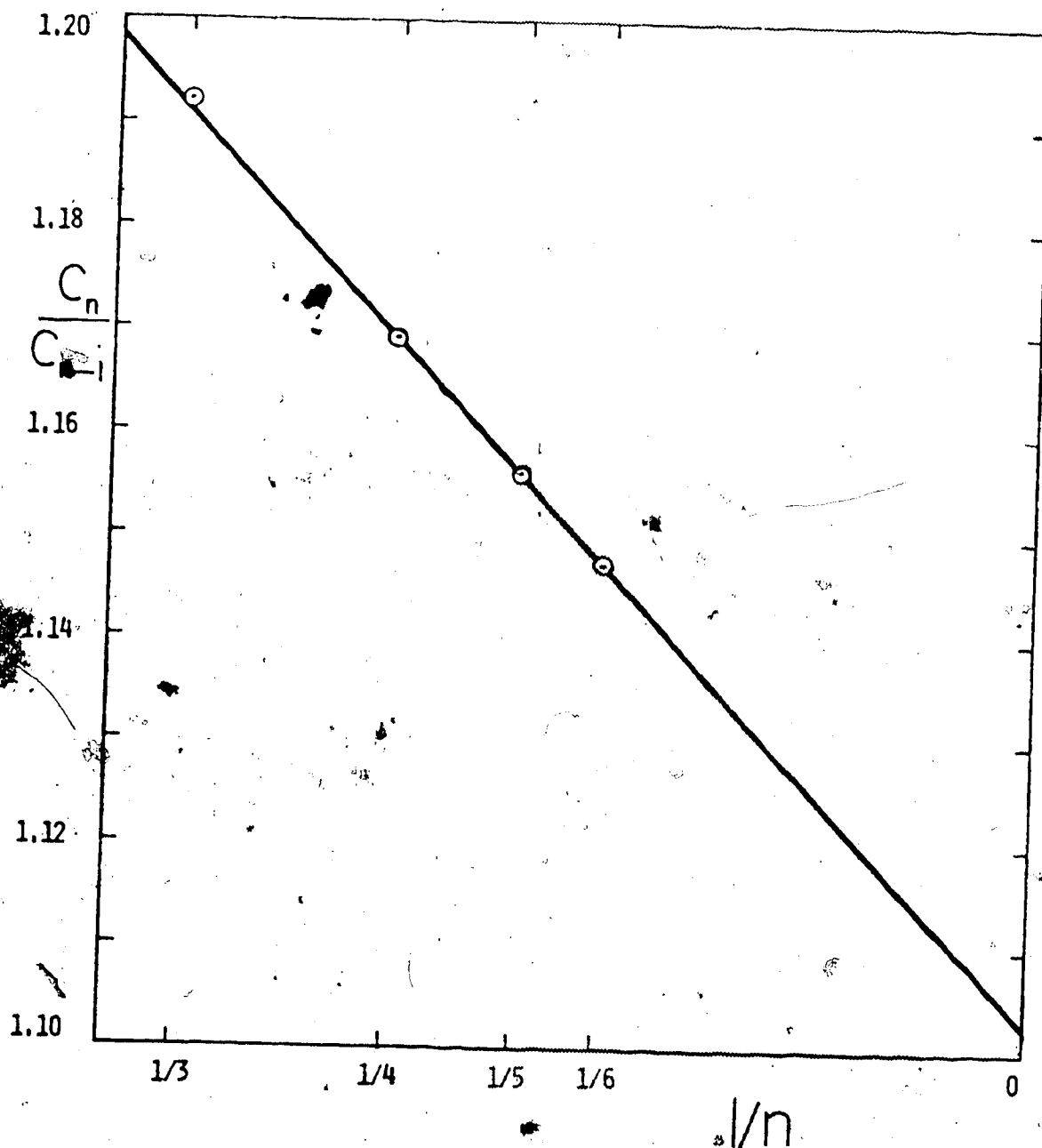


Figure 5.1. Ratio of coefficients \bar{c}_n/\bar{c}_{n-1} in the low p expansion of the fluctuation $Y(p, K)$ versus $1/n$ for $t \equiv 0.221/K = 0.9$ on the f.c.c. lattice.

Table 5.5 Estimates of the critical concentration, p_c , and critical exponent $\bar{\gamma}(t)$ from ratio plots of the low concentration expansion of $\gamma(p,K)$

$t=T/T_C(1)$	1.0	0.9	0.8	0.7	0.6	0.5
p_c	0.9930	0.9071	0.8237	0.743	0.666	0.588
	± 0.0010	± 0.0010	± 0.0015	± 0.002	± 0.003	± 0.005
$\bar{\gamma}$	1.23	1.24	1.25	1.30	1.35	1.40
	± 0.01	± 0.01	± 0.01	± 0.02	± 0.03	± 0.05

Table 5.6 Estimates of the critical exponent, $\bar{\gamma}(t)$, from [N/D] Padé approximants to series for $d \log Y(p, K)/dp$ on the f.c.c. lattice

[N/D]	t=1.0	t=0.9	t=0.8	t=0.7	t=0.6	t=0.5
[0.5]	1.22	1.13	1.05	0.97	0.89	0.79
[1/4]	1.23	1.25	1.28	1.32	1.39	1.55
[2/3]	1.23	1.24	1.27	1.30	1.35	1.41
[3/2]	1.23	1.24	1.26	1.30	1.34	1.40
[4/1]	1.24	1.39	1.57	1.85	2.34	3.82
[0/4]	1.23	1.14	1.06	0.99	0.94	0.94
[1/3]	1.23	1.25	1.28	1.33	1.41	1.57
[2/2]	1.22	1.24	1.25	1.28	1.31	1.36
[3/1]	1.21	1.33	1.45	1.58	1.62	1.34

Naively one would conclude that for the undiluted spin- $\frac{1}{2}$ -XY model $\bar{\gamma} = 1.23 \pm 0.01$ while as the critical temperature drops due to dilution the critical exponent $\bar{\gamma}(t)$ increases to reach a value $\bar{\gamma} = 1.4 \pm 0.1$ at $t = 0.5$ (or at $p = 0.5$).

Both features are somewhat unsettling. For the pure $S = 1/2$ XY model $\gamma = 1.33 \pm 0.02$ (and for the $S = \infty$ XY model $\gamma = 1.31 \pm 0.02$, Ferer and Wortis (1972)). The equality of γ and $\bar{\gamma}$ for the undiluted model seems rather firmly excluded. According to prevailing views of critical behavior, near a line of second order transitions (Griffiths and Wheeler (1970), Griffiths (1973)) one would expect the free energy and thus $Y(p,K)$ to be a generalized homogeneous function of an appropriate pair of independent variables, $\lambda(p,K)$ and $g(p,K)$. A special direction in the p,K plane is defined by the tangent to the second order transition line, $K = K_C(p)$. The $\lambda = 0$ axis then must be chosen tangential to the second order line at the point of interest (here, at $p=1$) and the $g = 0$ axis is then in any direction making a finite angle with the tangent. If $Y(\lambda,g)$ were a homogeneous function of its arguments then $\gamma(1)$ and $\bar{\gamma}(1)$ would have to be equal, contrary to our findings.

Secondly, ideas of universality or smoothness (Griffiths (1970), Kadanoff (1971), Betts et al. (1971), Ferer and Wortis (1972)) would require $\bar{\gamma}(t)$ to be independent

of p . The estimates of $\bar{\gamma}(t)$, particularly from the ratio plots, cannot readily be reconciled with a constant $\bar{\gamma}$. Smoothness would also require $\gamma(p)$ to be independent of p , but our high temperature series results are not precise enough to rule out a constant γ .

The above results are all based on the f.c.c. lattice. However the corresponding results for the b.c.c. and s.c. lattices, though less precise, are in accord with the f.c.c. results.

5.5 Lattice Dependent Critical Properties

From the series we have generated, if they be long enough, we can derive a number of critical properties which are lattice dependent. In principle we can estimate for the f.c.c., b.c.c. and s.c. lattices the amplitudes $C(p)$ and $\bar{C}(t)$ as defined by (5.4.1) and (5.4.2) respectively, analogous amplitudes $A(p)$ and $\bar{A}(t)$ for the specific heat, and the location of the second order line, $p_c(t)$ or $t_c(p)$.

To locate the second order line, $p_c(t)$, we use the more regular low concentration expansions for $Y(p,K)$ rather than the high temperature expansions. If $\bar{\gamma}(t)$ were given the most precise series estimates of $p_c(t)$ would be obtained from Padé approximants to $Y^{1/\bar{\gamma}}$. Now in Section 4 we have noted some apparent t dependence of the estimates of $\bar{\gamma}$. However a 10% error in $\bar{\gamma}$ yields only approximately a 1%

error in p_c , which allows us to determine $p_c(t)$ with reasonable precision. We adopt a uniform value of $\bar{\gamma}(t)=4/3$. This represents a reasonable mean value of $\bar{\gamma}$ extracted from Tables 5.4 and 5.5, and also this is very close to the value of $\gamma(1)$ estimated from high temperature series.

Over most of the range $0.3 \leq t \leq 1.0$ estimates of $p_c(t)$ from higher degree central Padé approximants to $\gamma^{3/4}$ are well converged, and we have taken as the best estimate of p_c the average of the $[1/5]$, $[2/4]$, $[3/3]$, $[4/2]$, $[1/4]$, $[2/3]$, $[3/2]$ and $[2/2]$ approximants. Our confidence limits, given $\bar{\gamma}=4/3$, are a fraction of a percent over the above range. The quality of the series deteriorates rapidly for $t < 0.3$ however.

Our results for $p_c(t)$ are displayed in Figure 5.2 for all three lattices. For comparison we have also plotted the mean field result, $p_c = t$, the results for the $S=1/2$ Ising model on the f.c.c. lattice (Rapaport (1972a)) and the results for the $S=1/2$ Heisenberg model on the f.c.c. lattice (Rushbrooke et al. (1972)). Rapaport was able to extend the Ising model curve down to $t=0$ while Rushbrooke et al. were unable to extend the Heisenberg model results below $t=0.4$. For the f.c.c. and b.c.c. lattices we have been able to estimate p_c for $t \geq 0.2$, and as the curves are so smooth we feel confident in extrapolating them to $t=0$. Also plotted in

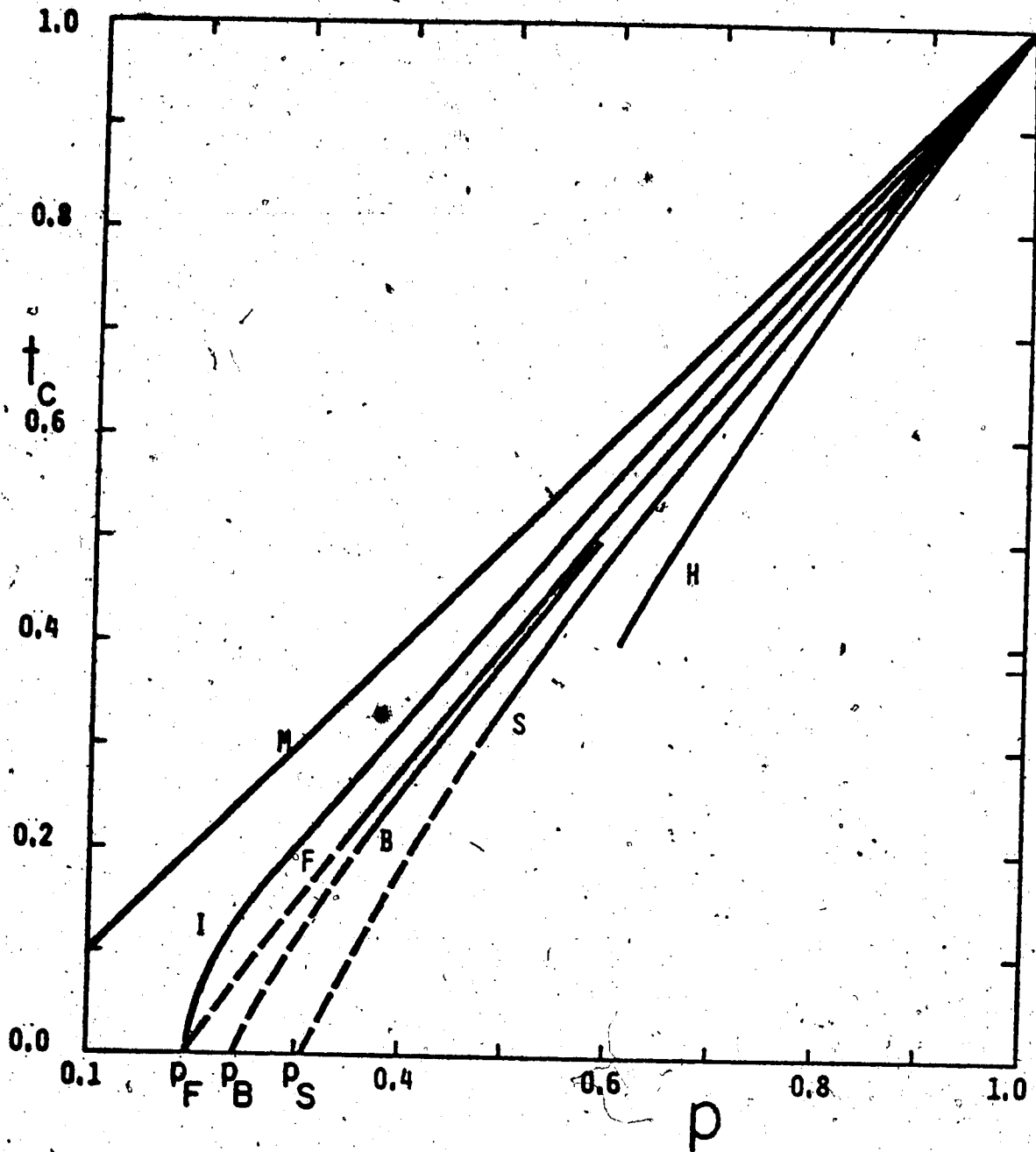


Figure 5.2 Critical temperature, $t_c = T_c(p)/T_c(0)$ versus p for the mean field approximation (M), the spin- $\frac{1}{2}$ Ising model on the f.c.c. lattice (I), the spin- $\frac{1}{2}$ Heisenberg model on the f.c.c. lattice (H), and the spin- $\frac{1}{2}$ XY model on the f.c.c. (F), b.c.c. (B) and s.c. (S) lattices.

Figure 5.2 are the critical probabilities for the site percolation problem (Essam (1972) and references therein).

The $p_c(t)$ curve for the Ising model, as already noted by Rapaport, appears to intersect the p axis at the site percolation critical value, p_c^S , with infinite slope. In contrast the XY model curves appear to intersect the p axis with finite slope. Of course for any lattice model of dilute magnetism we must have $p_c(0) > p_c^S$ because there are no infinite clusters for $p < p_c^S$. For the Ising and the XY models the inequality seems to be an equality. The finiteness of dt/dp at $t=0$ for the XY model as opposed to the infinite slope for the Ising model reflects the difference in character of the elementary excitations. It requires a finite energy to overturn spins and thence reduce the Ising model magnetisation while the XY model presumably has spin wave like excitations of vanishing energy.

For the Heisenberg model curve to intersect the p axis at p_c (if it do so) it must have a range of upward curvature, as discussed by Morgan and Rushbrooke (1963). In contrast the Ising and XY models seem to have downward curvature only throughout their whole range.

Finally we present in Table 5.7 our best estimates of the terminal gradients at both ends of the $p_c(t)$ curves for the XY models and for comparison the figures for the $S=1/2$ Ising and Heisenberg models (Rushbrooke et al. (1972)).

Table 5.7 Terminal gradients, $t'_c(1)$ and $t'_c(p_c)$, of the phase transition curve $t_c(p)$, for the $S=1/2$ Ising, XY and Heisenberg models

Gradient	Model and Lattice			
	$I_F(1/2)$	$XY_F(1/2)$	$XY_B(1/2)$	$XY_S(1/2)$ $H_F(1/2)$
$t'_c(1)$	1.05	1.164	1.15	1.22
	± 0.02	± 0.005	± 0.01	± 0.02
				± 0.03
$t'_c(p_c)$	∞	1.3	1.6	2.0
		± 0.2	± 0.3	± 0.6

Residues of Padé approximants to $\gamma^{3/4}$ yield critical amplitudes $\bar{C}(K)$ or $\bar{C}(t)$, assuming the validity of (3.2) and continuing to adopt the universal value $\bar{\gamma}(t) = 4/3$. The results are of course not so well converged as those for $p_c(t)$ from the poles of the same Padé approximants. Given the foregoing assumptions we obtain estimates of the amplitudes $\bar{C}_X(t)$ ($X = F, B$ or S) with a typical confidence limit of 2 or 3% over the range $0.5 \leq t \leq 1.0$.

Figure 5.3 exhibits $\bar{C}(t)$ for the three lattices. A somewhat unusual feature is that all three curves intersect at $t = 0.8$ and $\bar{C} = 0.95$. We do not however attach any particular significance to this feature.

Attempts to analyse the specific heat series have not been successful. This is not surprising in view of the shortness of the series and the well known intractability of specific heat series in general.

5.6 Discussion and Summary

In Section 2 we have discussed the generation of series expansions for, f , the zero field free energy and, Y , the zero field fluctuation in the long range order or transverse magnetisation of the spin- $\frac{1}{2}$ XY model with quenched site dilution. Low magnetic ion concentration series of degree seven in concentration, p , have been generated for both $f(p,K)$ and $Y(p,K)$ for arbitrary K , the inverse temperature

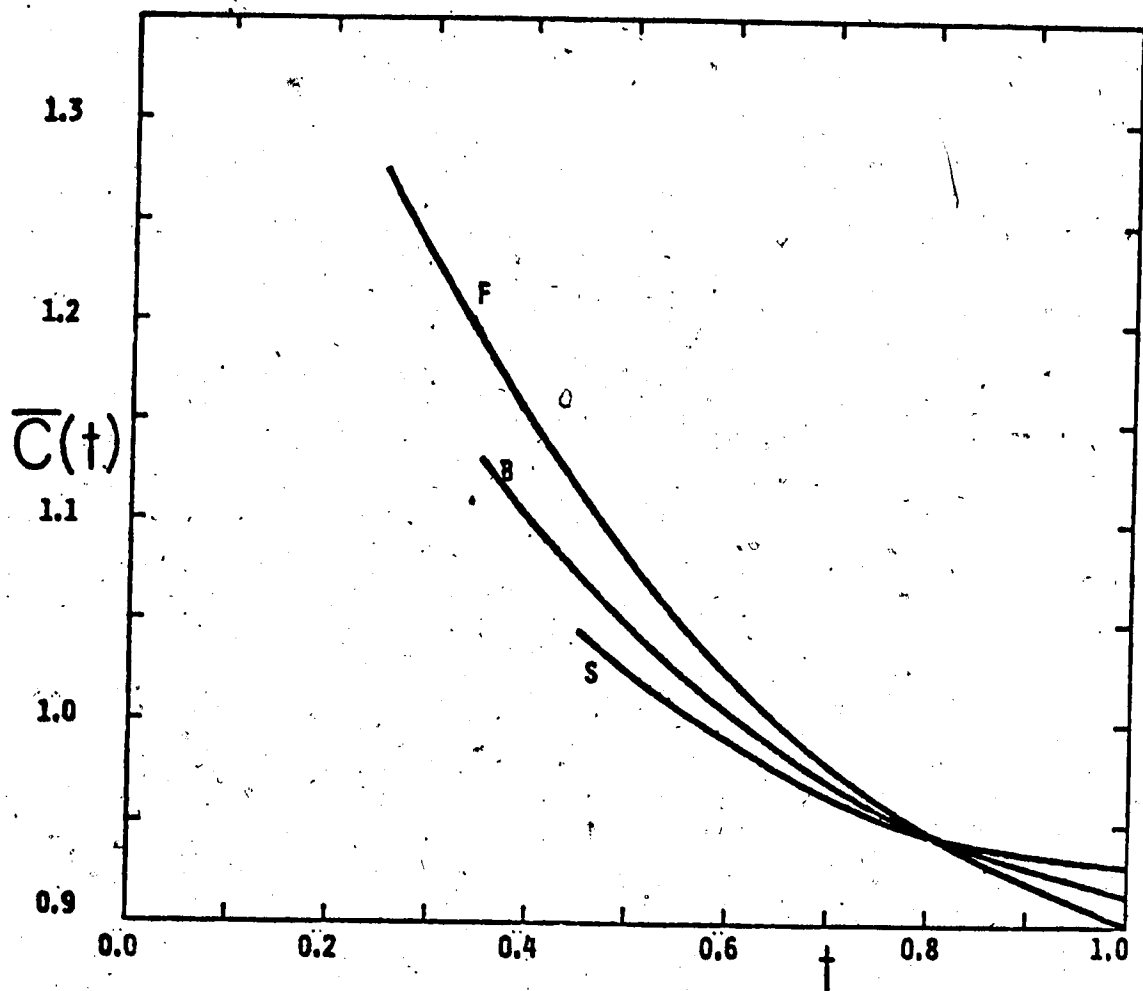


Figure 5.3 The amplitude $\bar{C}(t)$ of the order parameter fluctuation versus $t = T/T_c(1)$ for the f.c.c. (F), b.c.c. (B) and s.c. (S) lattices.

variable and coefficients for Y for selected values of K are tabulated in Section 2. Using the low concentration series high temperature series of degree seven in x have been generated for f and Y for arbitrary p . The resulting series are listed in Section 2 also. In Section 4 above we have reported the results of analysis of the high temperature series for $Y(p,K)$, which are not conclusive but point toward a p dependent $\bar{\gamma}$. The low p series for $Y(p,K)$ are however more regular and yield an apparent p dependence of $\bar{\gamma}$ as illustrated in figure 5.2.

Assuming a "best" value of $\bar{\gamma} = 1.33$ we have determined the second order phase transition line $p_c(t)$ from the low p series for $Y(p,K)$ for all three lattices. The results are displayed in figure 5.3 with for comparison the $p_c(t)$ curves for the Ising and Heisenberg models. One interesting feature of the XY model curves, in common with the Ising model curve, is the downward curvature everywhere. Another interesting feature is that the XY curves seem to intersect the p axis at the appropriate percolation probabilities. In contrast with the Ising model, the XY curves have finite slope at $T = 0$. It is not possible to say if the Heisenberg model curve intersects the p axis at the percolation probability, but if it does then it must have a region of upward curvature.

The linear behavior of $T_c(p)$ as a function of p near the percolation concentration p_c^* has been verified by Stauffer (1976). He has used the spin-wave argument of Shender and Shklovskii (1975), together with de Gennes' (1976) scaling law for the conductivity of a random resistor network, to arrive at the relation $T_c(p) \propto (p - p_c^*)$ as $p \rightarrow p_c^*$.

Scaling theory for dilute magnets in the percolation limit has recently been investigated by Essam et al. (1976) and Stauffer (1975). In particular the results of Stauffer obtained using cross-over considerations similar to those used in Section 2.3, predict the divergence of the amplitudes $\bar{C}(t)$ as $t \rightarrow 0$ shown in figure 5.3. Finally we note that Cox et al. (1976) have verified that for the quenched bond Ising model the ratio γ/ν doesn't depend on p , the concentration of allowed bonds, whereas γ does. This would seem to verify the weak universality hypothesis of Suzuki in this case.

CHAPTER VI

THE ANNEALED SITE PROBLEM

6.1 Introduction

The nearest neighbour spin- $\frac{1}{2}$ XY model in a parallel magnetic field H is defined by the interaction Hamiltonian,

$$H^{XY} = -J \sum_{\langle ij \rangle} (a_i^\dagger a_j + a_i a_j^\dagger) - mH \sum_i S_i^z \quad (6.1.1)$$

The system we consider in this chapter is governed by the Hamiltonian (6.1.1), but the lattice contains impurity atoms which are thermally mobile. The possible existence of a tricritical point for this model is discussed in Section 3.3.

The plan of this chapter is as follows. In Section 2 we tabulate some of the series expansions used in the analysis. Section 3 contains the analysis of the series for the three cubic Bravais lattices when $H=0$ and for the f.c.c. lattice for some non-zero values of H . In Section 4 we relate the spin- $\frac{1}{2}$ annealed site XY model to He^3 - He^4 mixtures and show how the λ -lines may be obtained in terms of experimental variables. Attempts to locate the tricritical point for the f.c.c. lattice when $H=0$ are outlined in Section 5. A short discussion and summary are contained in Section 6.

6.2 Generation of Series

The series for the fluctuation in order parameter and for the grand partition function are generated by the method outlined in Section 4.5. Series in magnetic site fugacity z may be converted to series in magnetic ion density n_m by using the formula

$$N_m(K, h, z) = z \partial \ln \Xi(K, h, z) / \partial z \quad (6.2.1)$$

where $K = \beta J$ and $h = mH/J$.

The expansion for $Y(K, h, z)$, the fluctuation in long range order, in powers of z when $h=0$ is of the form

$$Y = 2z + \sum_{\ell=2} b_{\ell}(K) z^{\ell} \quad (6.2.2)$$

The coefficients $b_{\ell}(K)$ are not analytic, but are obtainable to arbitrarily high precision for a given value of K .

Tabulated in Table 6.1 are the coefficients b_{ℓ} , $\ell=2, \dots, 7$ for the f.c.c. lattice for selected values of normalised temperature $t = K_c(1)/K$.

The series (6.2.2) may be converted to a series in magnetic ion concentration n_m as discussed above. In zero field this may be written as

$$Y = n_m + \sum_{\ell=2} a_{\ell}(K) n_m^{\ell} \quad (6.2.3)$$

Table 6.1 Coefficients $b_p(K)$ for the f.c.c. lattice in zero field,
for the series (6.2.2). $K_c(1) = 0.221$

t	b_2	b_3	b_4	b_5	b_6	b_7
1.0	1.9358	-1.2630	1.1926	-1.3857	1.9888	-3.2288
0.9	2.6813	- .4062	1.1442	-1.3613	2.3083	-3.7793
0.8	3.6378	1.3444	2.4022	- .7324	3.3345	-3.8286
0.7	4.9093	4.7995	7.7653	5.5331	11.7095	5.1372
0.6	6.6866	11.7740	25.9281	43.1178	87.0688	145.7512
0.5	9.3396	26.7956	87.3456	250.4336	744.9749	2121.034
0.4	14.6213	72.9081	400.0496	2070.660	1077.32	55196.95
0.3	22.1367	174.9005	1530.828	13018.64	111720.1	953356.7

The coefficients a_l , $l=2, \dots, 7$ for the f.c.c. lattice are tabulated in Table 6.2 for selected values of t .

6.3 Second Order Transition Lines

In order to determine the locus of critical densities n_m^c as a function of temperature we rely solely on the analysis of the series for the fluctuation in order parameter. The only other available function expected to diverge at the second order phase boundary (and then only weakly) is the specific heat, for which the series we obtained failed to yield consistent results. As is usual, we assume a divergence for $Y(K, h, n_m)$ near the critical density with the form

$$Y(K, h, n_m) \approx \bar{C}(K, h) [1 - n_m/n_m^c(K, h)]^{-\bar{\gamma}(K, h)} \quad (6.3.1)$$

where the path of approach in the Kn_m plane is along lines of constant K and h , with $h = mH/J$.

Both the ratio method and Padé approximant techniques have been used to locate n_m^c for fixed values of $t = K_c(n_m = 1)/K$. In general the results of the analysis are very similar to those presented in I for the quenched site case. In particular, ratio analysis and the residues of Padé approximants to $d \ln Y(K, h, n_m)/dn_m$ for the f.c.c. lattice show that the apparent value of $\bar{\gamma}(K, h=0)$ varies from

Table 6.2 Coefficients $a_\ell(K)$ for the f.c.c. lattice in zero field, for the series (6.2.3). $K_c(1) = 0.221$

t	a_2	a_3	a_4	a_5	a_7	a_7
1.0	1.3368	1.4784	1.5984	1.6964	1.7820	1.8589
0.9	1.4885	1.8099	2.1559	2.5164	2.9044	3.3264
0.8	1.6790	2.2660	3.0059	3.8978	4.9922	6.3383
0.7	1.9258	2.9183	4.3708	6.3762	9.1760	13.0718
0.6	2.2601	3.9019	6.7242	11.2226	18.4543	29.9775
0.5	2.7392	5.4850	11.1818	21.8379	42.0208	79.5784
0.4	3.6384	8.8727	23.3351	56.8355	137.9683	325.2112
0.3	.48310	13.8362	48.4571	143.5603	453.5246	1310.580

from $\bar{\gamma} = 1.21 \pm .01$ for $t = 1.0$ to $\bar{\gamma} = 1.5 \pm 0.1$ for $t = 0.5$. Values of $\bar{\gamma}$ from some fourth and fifth order Padé approximants to $d \ln Y(K, h, n_m) / dn_m$ are presented in Table 6.3. Estimates of $\bar{\gamma}$ are scattered for $t < 0.4$.

The value of $\bar{\gamma}(t=1)$ agrees within the error range with the value $1.23 \pm .01$ found for the quenched site case. On the other hand, high temperature series analysis for the pure case gave $\gamma = 1.333 \pm .002$ (Betts, Elliott and Lee (1970), Dekeyser and Rogiers (1975)). According to the same arguments from scaling theory presented in Chapter 5, this value of γ is expected to equal $\bar{\gamma}(t=1)$ for the annealed site case. If indeed $\bar{\gamma}(t=1)$ is less than γ , as our estimate indicates, the reason is not apparent. Fisher (1968) has also argued that the observed value of $\bar{\gamma}(t=1)$ will be greater than γ if α is non-zero, regardless of the sign of α . Also if the specific heat has a logarithmic divergence at the second order phase boundary then the observed value of $\bar{\gamma}(t=1)$ should equal γ .

The variation of $\bar{\gamma}$ with t was also apparent for the quenched site problem. The ramifications of this result with regard to universality were discussed in Chapter 6. For the quenched site case however, the magnetic ion concentration is not a thermodynamic variable, so any t dependence of $\bar{\gamma}$ is not necessarily a violation of universality.

Table 6.3 Estimates of the critical exponent $\bar{\gamma}(K)$ from $[N/D]$ Padé approximants to series for $d \ln Y(K, h, n_m) / dn_m$ on the f.c.c. lattice for $h=0.0$, $t=K_c(n_m=1)/K$

$[N/D]$	$t=1.0$	$t=0.9$	$t=0.8$	$t=0.7$	$t=0.6$	$t=0.5$	$t=0.4$
[1/4]	1.21	1.24	1.27	1.30	1.28	1.71	3.91
[2/3]	1.21	1.24	1.27	1.32	1.40	1.52	1.75
[3/2]	1.21	1.24	1.27	1.32	1.38	1.48	1.63
[1/3]	1.21	1.24	1.28	1.33	1.43	1.61	2.63
[2/2]	1.21	1.23	1.26	1.30	1.35	1.41	1.49

However, for the annealed site problem the magnetic ion concentration is a thermodynamic variable and any variation of $\bar{\gamma}$ with t does imply a violation of universality.

For the b.c.c. and s.c. lattices in zero field and for the f.c.c. lattice in non-zero field, the estimates of $\bar{\gamma}(K, h)$ are, as expected, not so consistent as for the f.c.c. lattice in zero field. Table 6.4 contains the values of $\bar{\gamma}(h)$ from Padé approximants to $d \ln Y(K, h, n_m) / dn_m$ for $t = 0.8$ and various values of h for the f.c.c. lattice. The various Padé approximants show no apparent variation of $\bar{\gamma}$ with h for $h \leq 0.4$. For the largest value of h considered, $h = 1.0$, the estimates of $\bar{\gamma}$ are more scattered, but there is still no significant average deviation from the estimates of $\bar{\gamma}$ at $h = 0$. Constancy of the high temperature exponent γ with variation in h for the pure spin- $\frac{1}{2}$ XY model was also observed by Dekeyser and Rogiers (1975). In other words $\bar{\gamma}(K, h)$ appears to be universal with respect to H , but not with respect to T .

To locate the second order transition surface $n_m^C(t, h)$, we use estimates of n_m^C from Padé approximants to $[Y(K, h, n_m)]^{1/\bar{\gamma}}$, assuming a constant value of $\bar{\gamma} = 4/3$ (see Chapter 5) for the three dimensional lattices. Estimates of n_m^C from the fifth and sixth order Padé approximants are tabulated in Table 6.5 for the f.c.c. lattice with $h=0$ and various values of t . In general the estimates of n_m^C from

Table 6.4 Estimates of the critical exponent $\bar{\gamma}(h)$ from $[N/D]$ Padé approximants to series for $d \ln Y(K, h, n_m) / dn_m$ on the f.c.c. lattice for $K_c(n_m=1)/K = 0.8$, $h=H/J$

$[N/D]$	$h=0.0$	$h=0.2$	$h=0.4$	$h=1.0$
[1/4]	1.27	1.28	1.27	1.25
[2/3]	1.27	1.27	1.27	1.24
[3/2]	1.27	1.27	1.27	1.29
[1/3]	1.28	1.28	1.30	1.21
[2/2]	1.26	1.26	1.27	1.19

Table 6.5 Estimates for the critical density n_m^c from [N/D] Padé approximants to series for $[Y(K, h, n_m)]^{3/4}$ on the f.c.c. lattice for $h=0.0$

[N/D]	[1/5]	[2/4]	[3/3]	[4/2]	[2/3]	[3/2]
t=1.0	1.0074	1.0038	1.0034	1.0045	1.0078	1.0383
t=0.9	0.9193	0.9164	0.9160	0.9172	0.9194	0.9273
t=0.8	0.8304	0.8288	0.8286	0.8294	0.8304	0.8326
t=0.7	0.7405	0.7404	0.7404	0.7404	0.7404	0.7407
t=0.6	0.6495	0.6487	0.6477	0.6494	0.6485	0.6486
t=0.5	0.5527	0.5518	0.5484	0.5566	0.5541	0.5548
t=0.4	0.4457	0.4371	0.4353	0.4453	0.4400	0.4411
t=0.3	0.3734	0.3668	0.3661	0.3732	0.3674	0.3676

this method are rather insensitive to small variations in the choice of $\bar{\gamma}$. This supports our adoption of a universal value for $\bar{\gamma}$ for the purpose of obtaining a transition surface.

Zero field second order transition lines in the t_n plane for the three cubic Bravais lattices are exhibited in Figure 6.1. A comparison of these lines with the equivalent set for the quenched site case (Figure 5.2) indicates that the line of critical density of magnetic sites is of opposite curvature to the line for the annealed site problem on the same lattice. The terminal gradients of these transition curves at $t=1$ match those for the quenched site case for each lattice.

6.4 He³-He⁴ Mixtures

Up to now we have interpreted the annealed site problem in terms of magnetic variables. However the problem is physically better suited to a lattice quantum fluid, for example He³-He⁴ mixtures in which the He³ particles are approximated by classical non-interacting particles. If we let n_3 and n_4 be the respective densities of He³ and He⁴ particles per lattice site and make the identifications

$$n_3 = 1 - n_m \quad (6.4.1)$$

$$n_4 = n_m (1 \pm \langle S_z \rangle) / 2 \quad (6.4.2)$$

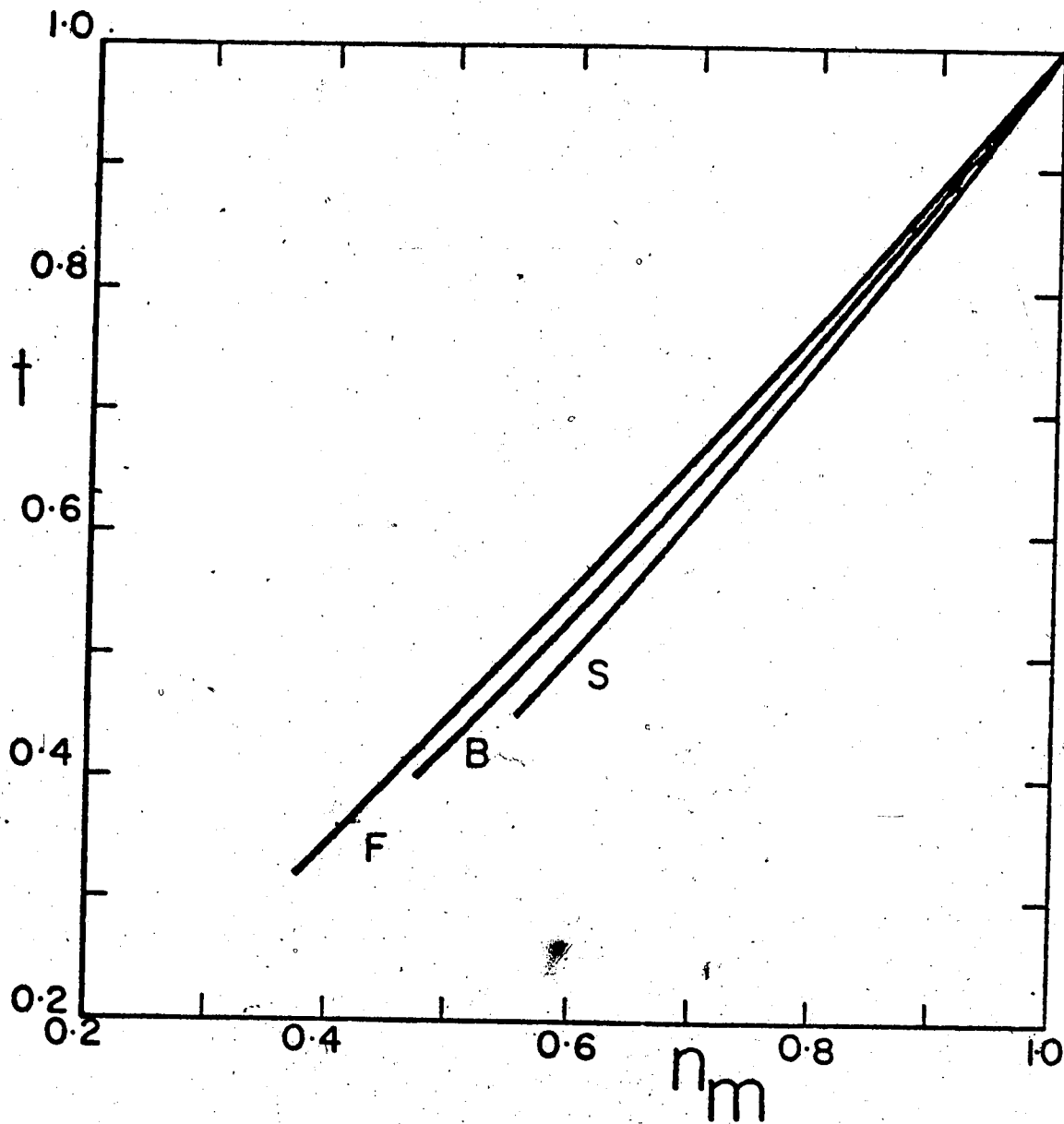


Figure 6.1 Critical temperature $t = K_c(n_m=1)$ versus n_m for the f.c.c. (F), b.c.c. (B) and s.c. (S) lattices from poles of Padé approximants to $[Y(K, h=0, n_m)]^{3/4}$.

we can obtain the density per site $n = n_3 + n_4$ and the He^3 concentration $x_3 = n_3/n$ in terms of our natural variable n_m . The choice of sign in (5.2) arises from the observation that $\langle S_z(H) \rangle = - \langle S_z(-H) \rangle$, while the Hamiltonian (6.1.1) remains invariant under change of sign of magnetic field. Provided that the expansion of $\langle S_z(K,h) \rangle$ as a series in n_m is well converged for each value of K , h and n_m on the critical line we can find the λ -lines as contours of constant n in the tx_3 plane. In practice we have been able to do this only for the f.c.c. lattice using data from the $Y(K,h,n_m)$ series for $h < 1.0$, enabling us to find part of the λ -line for $n = 0.65 \pm .02$. In figure 6.2 the second order transition lines in the tx_3 plane for $h=0$, $+1.0$ and -1.0 are displayed for the f.c.c. lattice, while the dashed curve shows the λ -line for $n \approx 0.65$. The lines of constant h in Figure 6.2 have confidence limits in the x_3 variable of 2-3%, while the constant n curve has confidence limits of about 6% in each ordinate value.

The series we have obtained for $Y(K,h,n_m)$ in powers of n_m are generally well behaved for $0.4 \leq t \leq 1.0$ and $|h| \leq 1.0$. On the other hand the series for $Y(K,h,z)$ in powers of z can be analysed consistently in the region $0.2 \leq t \leq 0.6$.

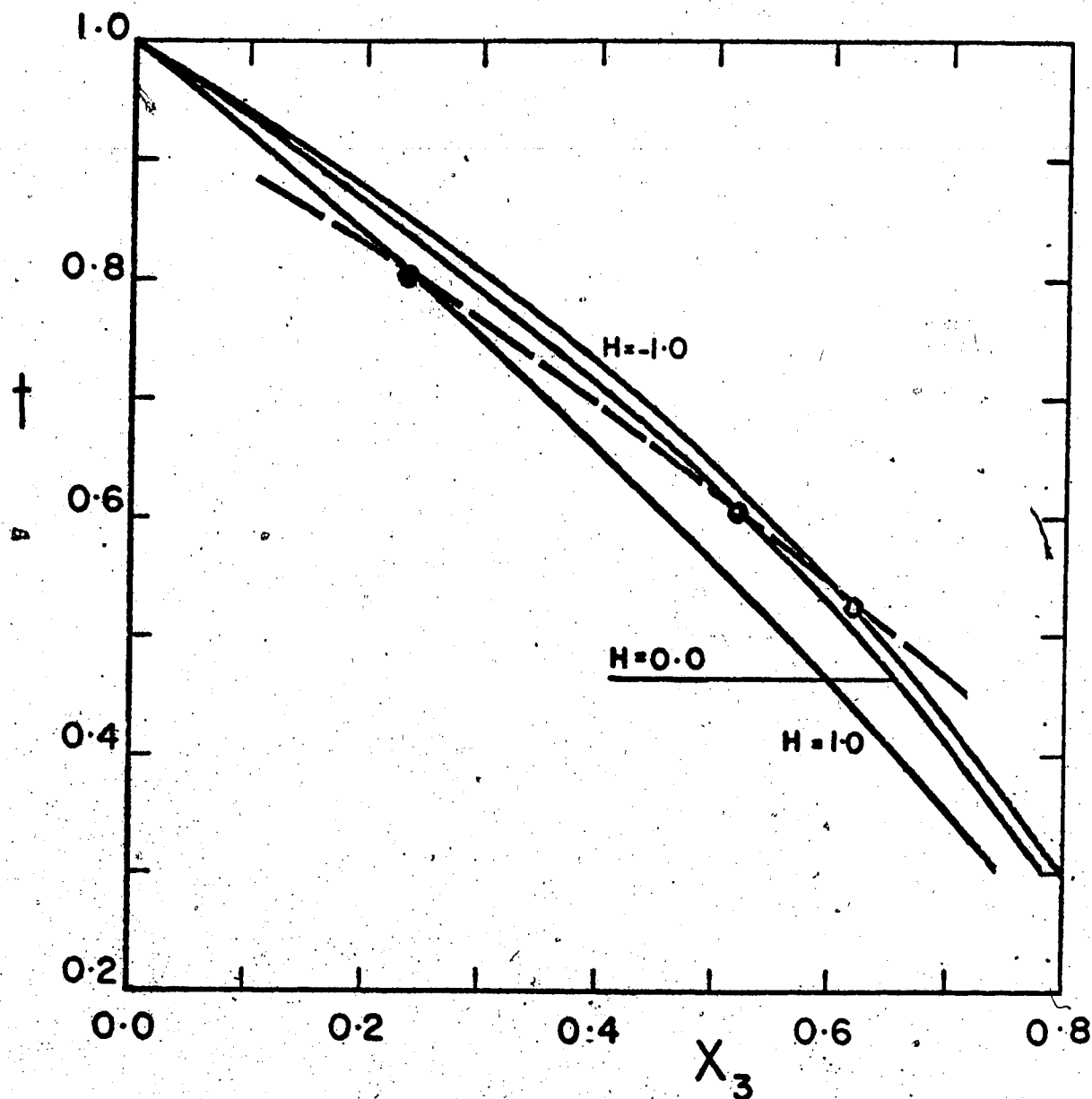


Figure 6.2 Critical temperature $t = K_c(x_3=0)/K$ versus x_3 for the f.c.c. lattice with $h=H/J = +1.0, 0.0$ and -1.0 from Padé approximants to $[Y(K, h, n)]^{3/4}$. The dashed curve is the λ -line for $n \approx 0.65$.

- For the series in fugacity we assume the asymptotic form for Y , near z_c , given by

$$Y(K,h,z) \approx C(K,h)[1 - z/z_c(K,h)]^{-\gamma(K,h)} \quad (6.4.3)$$

and analyse the series using Padé approximants to $d \ln Y(K,h,z)/dz$ and $[Y(K,h,z)]^{3/4}$. The second order transition line in the tz plane for the f.c.c. lattice in zero field is shown in Figure 6.3. The estimates of γ from the analysis are not consistent except for near the region of what we believe to be the tricritical point. The poles nearest to the origin of Padé approximants to $d \ln Y(K,h,z)/dz$ are located at z_c and $-z_c - \delta$, with $\delta > 0$ but small. The effect of the pole near $-z_c$ was successfully eliminated by transforming the expansion variable z to \bar{z} via the equation

$$z = \bar{z}/(2 - \bar{z}/z_c) \quad (6.4.4)$$

The effect of the transformation (6.4.4) is to leave the point z_c invariant and remove the point $-z_c$ to $-\infty$. Estimates of z_c were obtained from the poles of Padé approximants to $[Y(K,h,z)]^{3/4}$ for each temperature considered. Ratios of the coefficients $\bar{b}_l(K,h)$ of the transformed series $Y(K,h,\bar{z})$ are remarkably linear when plotted against $1/l$. Estimates of $\gamma(t)$ from Padé approximants to $d \ln Y(K,h,\bar{z})/d\bar{z}$ are given in Table 6.6 for the f.c.c. lattice in zero field for selected

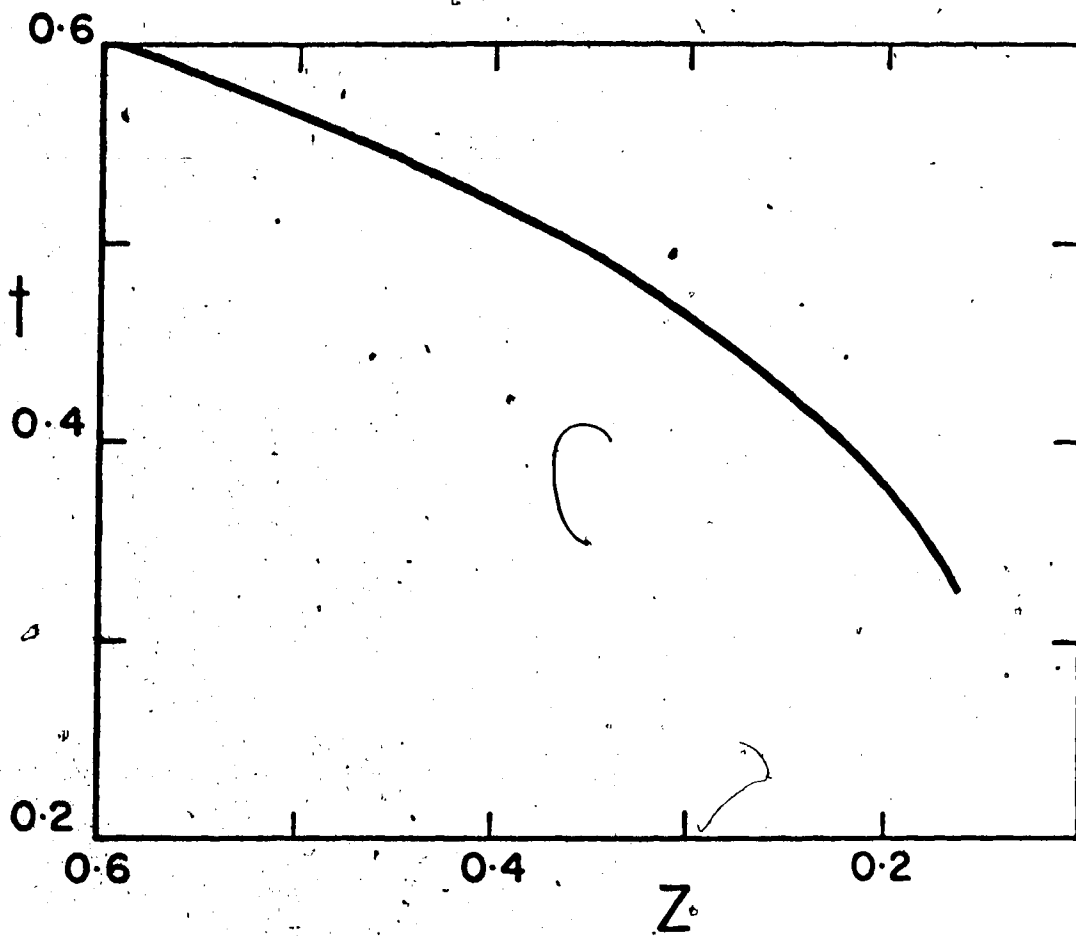


Figure 6.3 Critical temperature $t_c = K_c(z \rightarrow \infty)/K$ versus z for the f.c.c. lattice with $h=0.0$ from the poles of Padé approximants to $[Y(K, h, z)]^{3/4}$.

Table 6.6 Estimates of $\gamma(K)$ from $[N/D]$ Padé approximants to the transformed series $d \ln Y(K, h, \bar{z}) / d \bar{z}$ on the f.c.c. lattice for $h=0.0$, $t=K_c(\bar{z}+\infty)/K$

[N/D]	t=0.60	t=0.55	t=0.50	t=0.45	t=0.40
[1/4]	1.384	1.425	0.765	1.193	1.138
[2/3]	1.380	1.400	1.412	1.272	1.159
[3/2]	1.377	1.401	1.886	1.181	1.135
[1/3]	1.433	1.252	1.244	1.200	1.126
[2/2]	1.371	1.373	1.234	1.200	1.125

values of $t \leq 0.6$. For $t > 0.6$ the series are not well behaved and a suitable transformation could not be found to smooth the ratio plots. However the estimates of $\bar{\gamma}(K,h)$ from the series in n_m should be the same as from the series in z , since conversion from one series to the other involves only a transformation of variable. Near the tricritical point though, series for $Y(K,h,z)$ are expected to behave differently than the series for $Y(K,h,n_m)$.

In the next section we use the series $Y(K,h,z)$ to try to locate the tricritical point in the tz plane.

6.5 The Tricritical Point

A tricritical point, as defined by Griffiths (1970), is characterised by the existence of two competing order parameters which simultaneously become critical.

The phase diagram for $\text{He}^3\text{-He}^4$ mixtures in the tz plane, where z is the fugacity of one of the species, is a single continuous line, which has a tricritical point at $Z = Z_t$ and $T = T_t$. For $T > T_t$ the transition is from the superfluid to the normal-fluid state of He^4 . When T is less than T_t the transition is first order and the line defines the phase boundary of the He^4 -rich and He^3 -rich phases. In general all critical exponents are expected to have values at the tricritical point different from their values at the second order phase boundary. According to the

tricritical scaling theory developed by Riedel (1972, 1974) and Griffiths (1973) there are two different sets of tricritical exponents. Which of these sets is applicable depends on the path of approach to the tricritical point and on what variables the quantity of interest is expressed in. For our immediate purpose it is sufficient to note that for fixed K and h if we approach the tricritical point using low fugacity series, the exponents are denoted α_t, γ_t , etc. and have the mean field values $\alpha_t = 1/2$ and $\gamma_t = 1$. If on the other hand we use the low density series the exponents are symbolised by α_u, γ_u , etc. and have the mean field values $\alpha_u = -1$ and $\gamma_u = 2$. Experiments on $\text{He}^3\text{-He}^4$ mixtures by Goellner et al. (1973) suggest that the tricritical exponents have the classical values given above.

The location of the tricritical point using series expansions has been attempted for many different models. Systems for which are available expansions for the free energy about both the completely ordered and disordered states are relatively easily analysed. In such cases, for instance the Blume-Capel model as studied by Saul et al. (1974), the first order phase boundary may be located by equating the two branches of the free energy. Unfortunately, for the spin- $\frac{1}{2}$ XY model the nature of the ground state is entirely unknown, so that only expansions about the disordered state may be

obtained. As yet no precise method has been devised for finding a tricritical point using series expansions of functions derived from only one branch of the free energy.

For the spin- $\frac{1}{2}$ XY annealed site model we have used two methods to locate the tricritical point, both of which assume classical tricritical exponents. The first approach we have used is to locate the point in the tz plane where $\gamma = 1$. Estimates of $\gamma(K)$, for the f.c.c. lattice for different values of t , from residues of Padé approximants to $d \ln Y(K, h=0, z) / dz$ are displayed in Table 6.7. As can be seen from Tables 6.4 and 6.5 the value of γ appears to approach the mean field value ($\gamma = 1$) very slowly as a function of temperature. Between $0.32 < t < 0.29$ γ varies only slightly from the mean field value. If we assume a tricritical temperature $t_t = 0.31 \pm .02$ then we find using the transition line of figure 6.3 that $z_t = 0.11 \pm .02$ and from Figure 6.2 $x_t = 0.80 \pm .02$.

In addition to the fluctuation in order parameter the quantity

$$w(K, h, z) = z \partial n_m(K, h, z) / \partial z \quad (6.5.1)$$

is expected to diverge strongly at the tricritical point. The quantity $w(K, h, z)$ can reasonably be expected to behave as a concentration susceptibility because $n_m(K, h, z)$ is a good

Table 6.7 Estimates of $\gamma(K)$ from $[N/D]$ Padé approximants to series for $d \ln Y(K, h, z) / dz$ on the f.c.c. lattice for $t = K_c(z \rightarrow \infty) / K$ near the tricritical point and $h=0.0$

$[N/D]$	$t=0.320$	$t=0.310$	$t=0.305$	$t=0.300$	$t=0.290$
[1/4]	1.030	1.014	1.004	0.993	0.969
[2/3]	1.035	1.019	1.009	0.997	0.974
[3/2]	1.028	1.012	1.002	0.991	0.967
[1/3]	1.010	0.992	0.981	0.968	0.941
[2/2]	1.007	0.989	0.976	0.963	0.935

order parameter for the first order transition in the tz plane. $w(K,h,z)$ is readily constructed from $\ln \Xi(K,h,z)$ as a series in z using the relation (6.2.1). We write then the asymptotic form for $w(K,h,z)$ as $z \rightarrow z_t$ from below as

$$w(K,h,z) \sim A(K,h)[1 - z/z_t(K,h)]^{-\lambda_t} \quad (6.5.2)$$

where we use the exponent notation developed from tricritical scaling theory.

Residues of Padé approximants to $d \ln w(k,h=0,z)/dz$ for the f.c.c. lattice at the point $t_t = 0.31$ yield an estimate of $\lambda_t = 0.32 \pm .10$. This estimate of λ_t is somewhat lower than the classical value $\lambda_t = 1/2$, but because of the uncertainty in the estimate of t_t and the limited length of the series we cannot justifiably conclude that $\lambda_t \neq 1/2$. Values of the exponent α_t for the specific heat could not be consistently estimated. Using the above method Rogiers, Dekeyser and Quisthoudt (1975) concluded that $x_t \approx 0.8$ and that the exponents γ_t , λ_t and α_t are apparently classical.

The second method we have used involves locating the transition line from Padé approximants to $[w(K,h,z)]^{1/\lambda_t}$ assuming $\lambda_t = 1/2$. If the curve obtained in the tz plane from this method meets the transition line obtained from Padé approximants to $[Y(K,h,z)]^{1/\gamma}$ with $\gamma = 4/3$, then we identify the point of intersection with the tricritical point. This

method was used by Plischke and Betts (1975) to locate the tricritical point of the Cheng-Schick model (Cheng and Schick (1973)). We have found however, that the line of critical points predicted from Padé approximants to $[w(K, h=0, z)]^2$ for the f.c.c. lattice for $t <$ differs only marginally from the second order line predicted from Padé approximants to $[Y(K, h=0, z)]^{3/4}$ displaying in figure 6.3. For $0.28 < t < 0.31$, the poles of the central Padé approximants to w^2 and $Y^{3/4}$ are the same to within 0.03%.

Consequently have been unable to make an estimate of t_t using this method. However, we note that the region of approximate degeneracy of the two critical lines ($0.28 < t < 0.31$) is where the exponent $\gamma_t \approx 1$.

6.6 Summary and Discussion

The annealed site spin- $\frac{1}{2}$ XY model has been studied on three cubic lattices. Series expansions up to seventh order in magnetic site fugacity and magnetic ion density have been derived for the fluctuation in order parameter. These series have been analysed in two types of variable, one applicable to magnetic systems and the other suited to He³-He⁴ mixtures. The tricritical point has been approximately located in the tz plane. The λ -line obtained for $n=0.65$ in the tx_3 plane lies between the λ -lines presented by Rogiers, Dekeyser and Quisthoudt (1975) for $n=0.5$ and $n=0.8$ for the

Takagi model. Also we have been able to compare directly the second order transition curve for the f.c.c. lattice with $H=0$ in the tz plane with that for the Takagi model obtained by Rogiers (1974). These two lines agree within the confidence limits.

The estimates of $\bar{\gamma}$ we have obtained in the pure limit, $t=1$, do not agree with estimates of γ assessed from high temperature series for the pure spin- $\frac{1}{2}$ XY model. Our estimate of $\bar{\gamma}(t=1)$ is apparently the same as previously obtained for the XY model with quenched site impurities.

As Rogiers, Dekeyser and Quisthoudt (1975) noted, the Takagi model (and hence the spin- $\frac{1}{2}$ XY annealed site model) does not predict quantitatively the phase diagram of $\text{He}^3\text{-He}^4$ mixtures in the tx_3 plane. The ability of the Cheng-Schick model of $\text{He}^3\text{-He}^4$ mixtures to match the experimental phase diagram (Goellner et al. (1973)) was established by Plischke and Betts (1975). The Cheng-Schick model allows kinetic mobility of the He^3 particles and contains the correct fermi statistics for these particles. Both of these properties are lacking in the Takagi model where the He^3 atoms are approximated by classical particles with infinite mass.

CHAPTER VII

THE TWO DIMENSIONAL MODELS

7.1 Introduction

Because of the controversy concerning the existence of phase transitions in two dimensional quantum systems, we consider the two dimensional quenched and annealed s XY models in a separate chapter.

In Section 2 the exact result of Mermin and Wagner (1966), concerning the existence of long range order in two dimensional models is briefly explained. Also in Section 2 the possible existence of a Stanley-Kaplan type transition in such models is examined. In Section 3 we present the results of Betts, Elliot and Ditzian (1970) of a high temperature series analysis for the XY model on the triangular lattice. Our results from low density series for the quenched and annealed site XY models on the triangular lattice are presented in Section 4. A brief discussion and summary are contained in Section 5.

7.2 Exact Results and Conjectures

Stanley and Kaplan (1966) analysed the high temperature susceptibility series of Rushbrooke and Wood (1958) for the spin $S=1/2$, $3/2$ and $5/2$ two dimensional isotropic Heisenberg models. They concluded that there

was strong evidence to support the existence of a phase transition for the $S=3/2$ and $S=5/2$ models but for $S=1/2$ the series were not well enough behaved for reliable analysis.

Very shortly afterwards however Mermin and Wagner (1966) proved rigorously for a variety of models, including the general spin isotropic Heisenberg and XY models, that there can be no ferromagnetic or antiferromagnetic order for any non-zero temperature. Stanley and Kaplan (1966) then made the observation that should the pair correlation functions be only gradually attenuated, then the susceptibility may become infinite without the onset of long range order. Mathematically this means that the susceptibility constructed from the sum (2.2.6) becomes infinite without the correlation length becoming infinite. Mubayi and Lange (1969) have used Green's function techniques with a judicious choice of decoupling scheme to find results for the $S=1/2$ isotropic Heisenberg model consistent with the Stanley-Kaplan conjecture. Yamaji and Kondo (1973a) using a different decoupling scheme arrive at a totally different result and conclude that there is no Stanley-Kaplan transition.

Moore (1969) has derived and analysed series expansions for the classical XY and Heisenberg models on two dimensional lattices and concludes that there is good

evidence for a phase transition. On the other hand Yamaji and Kondo (1973b) find, from extended series for the spin- $\frac{1}{2}$ isotropic Heisenberg model, that there is no apparent divergence of the susceptibility series.

Kosterlitz and Thouless (1973) have found a possible type of ordered state for some of the two dimensional models including the spin ∞ XY model. Camp and Van Dyke (1975) derived and analysed series expansions for the spin ∞ XY and Heisenberg models. Their results seemingly support the conjecture of Kosterlitz and Thouless (1973) that the susceptibility behaves as $\exp(At^{-\nu})$ as $t \rightarrow 0$.

7.3 The Two Dimensional XY Model

In this section we review some numerical results for the two dimensional spin- $\frac{1}{2}$ XY model obtained by Betts, Elliot and Ditzian (1970). They derived the high temperature series expansion for the fluctuation in order parameter, $Y(K)$, for the triangular and square lattices and analysed these series using standard techniques and the method of conformal transformations.

For the series on the triangular lattice, the main poles of Padé approximants to $d \ln Y(K) / dK$ are at approximately $0.5 \pm 0.1 i$ and $\pm 0.6 i$. However after transforming their series via the quadratic transformation

$$K = \bar{K}/(1 - \bar{K}^2) \quad (7.3.1)$$

the poles closest to the origin are located on the real \bar{K} axis. The effect of the transformation (7.3.1) is to move the points $K = \pm i/2$ uniquely to the points $\pm i$ respectively. The series $Y(\bar{K})$ obtained after transformation is much better behaved than the original series and analysis yields the estimates $\bar{K}_c = 0.501 \pm 0.005$, with $\gamma = 1.50 \pm 0.02$. The corresponding value for K_c for the untransformed series is $K_c = 0.67 \pm 0.02$. Hence Betts et al. conclude that the XY model on the triangular lattice appears to have a Stanley-Kaplan type of phase transition.

7.4 Analysis of the Density Series

In this section we present the results of the analysis of series for the fluctuation in order parameter on the triangular lattice in terms of the magnetic site density for the quenched and annealed site XY models. Since we are concerned with obtaining evidence for or against the existence of a phase transition we will examine in detail one series only. The series we use is the fluctuation in order parameter as a series in density p , for the quenched site case at $K = 0.65 \approx K_c$. A preliminary investigation of the quenched site series for various values of K indicated by extrapolation that at $K = 0.65$, p_c would be approximately

1.0 . Scaling theory predicts that the critical behavior of this series should be the same as for the high temperature series for the pure XY model. The series we study below is

$$\begin{aligned}
 Y(p, K=0.65) = & p + 1.8841255\dots p^2 + 1.9364491\dots p^3 \\
 & + 2.2323519\dots p^4 + 2.3617032\dots p^5 \\
 & + 2.5257507\dots p^6 + 2.6158758\dots p^7 \\
 & + \dots
 \end{aligned} \tag{7.4.1}$$

The high temperature series for the free energy f and fluctuation in order parameter Y for the quenched site XY model on the triangular lattice are:

$$\begin{aligned}
 f(p, K) = & \ln 2 + \frac{3}{4} p^2 K^2 + \frac{1}{2} p^3 K^3 + \left(-\frac{1}{32} p^2 - \frac{5}{16} p^3 + \frac{3}{8} p^4\right) K^4 \\
 & + \left(-\frac{1}{4} p^3 - \frac{1}{2} p^4 + \frac{3}{8} p^5\right) K^5 + \left(\frac{1}{480} p^2 + \frac{1}{60} p^3 - \frac{31}{160} p^4 \right. \\
 & \quad \left. - \frac{5}{8} p^5 + \frac{15}{32} p^6\right) K^6 \\
 & + \left(\frac{17}{160} p^3 + \frac{23}{60} p^4 - \frac{21}{160} p^5 - \frac{13}{16} p^6 + \frac{21}{32} p^7\right) K^7 \\
 & + \dots
 \end{aligned} \tag{7.4.2}$$

and

$$\begin{aligned}
Y(p,K)/p = & 1 + 3pK + 7\frac{1}{2} p^2 K^2 + (-\frac{1}{4} p - 2\frac{1}{2} p^2 + 17\frac{1}{4} p^3)K^3 \\
& + (-4p^2 - 10\frac{1}{4} p^3 + 38\frac{5}{8} p^4)K^4 \\
& + (\frac{1}{40}p + \frac{1}{5} p^2 - 14\frac{11}{20} p^3 - 31\frac{1}{8} p^4 + 85\frac{5}{16} p^5)K^5 \\
& + (\frac{173}{80} p^2 + 7\frac{11}{60} p^3 - 44\frac{1}{480} p^4 - 85\frac{1}{16} p^5 + 186\frac{21}{32} p^6)K^6 \\
& + (-\frac{51}{20160} p + \frac{109}{160} p^2 + 14\frac{3789}{10080} p^3 + 33\frac{1851}{10080} p^4 \\
& - 122\frac{1365}{4032} p^5 - 220\frac{15}{32} p^6 + 405\frac{45937}{140000} p^7)K^7 \\
& + \dots
\end{aligned} \tag{7.4.3}$$

The series (7.4.2) and (7.4.3) are of insufficient length to analyse with confidence. The series of Betts and co-workers referred to in the previous section are several terms longer.

We present now the results of the analysis for the low density order parameter fluctuation series (7.4.1). Estimates of p_c from poles of Padé approximants to $d \ln Y(p)/dp$ are given in Table 7.1. The estimates of p_c presented in the table are not the poles closest to the origin however and consequently do not give consistent estimates of the location of the physical singularity. In each case the pole closest to the origin is on the negative real axis at about $p \approx -0.85$. In order to move this singularity outside the radius of convergence of the series

Table 7.1 Estimates of p_c and, in parentheses, $\bar{\gamma}$ from Padé approximants to the series for $d \ln Y(p)/dp$. A missing entry means that all poles of that approximant are unphysical

D	N=0	N=1	N=2	N=3
2	0.8237 (0.688)	0.9348 (1.076)	1.0153 (1.370)	1.0220 (1.406)
3	0.9945 (1.324)	-	1.0227 (1.411)	
4	1.1840 (4.756)	1.0579 (1.699)		

we make the transformation

$$p = \bar{p}/(2 - \bar{p}/0.8) \quad (7.4.4)$$

The effect of the above transformation is to leave the point $p=0.8$ invariant and to remove the point $p = -0.8$ to $\bar{p} \rightarrow -\infty$.

Table 7.2 shows, for Padé approximants to $d \ln Y(\bar{p})/d\bar{p}$, the closest poles to the origin and their residues. The low order Padé approximants are included for completeness only, but it is interesting to observe the consistency of estimates of \bar{p}_c throughout the table. We conclude that $\bar{p}_c = 0.885 \pm 0.005$ ($p=0.990 \pm 0.005$) and $\bar{\gamma} = 1.23 \pm 0.05$ by taking an average from the higher degree central Padé approximants. Our estimate of $\bar{\gamma}$ differs considerably from the estimate of γ found by Betts et al. (1970). If indeed $\gamma \neq \bar{\gamma}$, then a violation of universality is implied, just as for the three dimensional case. We can however analyse series for $Y(\bar{p})^{1/\bar{\gamma}}$ for various choices of $\bar{\gamma}$, in order to determine an optimum value for $\bar{\gamma}$ from the consistency of the poles of the Padé approximants. Unfortunately we find that the analysis of series for $Y(\bar{p})^{1/\bar{\gamma}}$ are insensitive to the choice of $\bar{\gamma}$. In Table 7.3 the poles of Padé approximants to $Y(\bar{p})^{4/5}$ are displayed. The central Padé approximants give an average of

Table 7.2 Estimates of \bar{p}_c and, in parentheses, $\bar{\gamma}$ from [N/D] Padé approximants to the transformed series $d \ln Y(\bar{p}) / d\bar{p}$

D	N=0	N=1	N=2	N=3	N=4
1	0.9503 (1.48)	0.9138 (1.51)	0.8901 (1.43)	0.8842 (1.40)	0.8845 (1.24)
2	0.9151 (1.27)	0.8583 (1.04)	0.8816 (1.22)	0.8845 (1.26)	
3	0.8935 (1.15)	0.8818 (1.22)	0.8868 (1.26)		
4	0.8861 (1.11)	0.8849 (1.24)			
5	0.8850 (1.10)				

Table 7.3 Estimates of \bar{p}_c from poles of $[N/D]$ Padé approximants to $\gamma(p)^{4/5}$

D	N=0	N=1	N=2	N=3	N=4	N=5
1	0.7977	0.8673	0.8832	0.8860	0.8859	0.8857
2	0.8747	0.8881	0.8865	0.8859	0.8860	
3	0.8864	0.8866	0.8851	0.8856		
4	0.8866	0.8864	0.8856			
5	0.8859	0.8856				
6	0.8856					

$\bar{p}_c = 0.8856 \pm 0.0006$, which corresponds to $p_c = 0.993 \pm 0.001$. The precision of this estimate for p_c is misleading though, because poles of Padé approximants to $Y(\bar{p})^{2/3}$ give almost the same estimate for p_c , with only slightly less precision.

The series for the fluctuation in order parameter $Y(n_m)$ in powers of the magnetic site density n_m on the triangular lattice for $K = 0.65$ is

$$\begin{aligned}
 Y(n_m) = & n_m + 2.0902426 \dots n_m^2 + 2.2863174 \dots n_m^3 \\
 & + 2.3523268 \dots n_m^4 + 2.4860704 \dots n_m^5 \\
 & + 2.6771002 \dots n_m^6 + 2.6898570 \dots n_m^7 \\
 & + \dots
 \end{aligned} \tag{7.4.5}$$

The results of the analysis of the series (7.4.5) are very similar to that presented above for the series (7.4.1) and need not be presented in detail.

We were unable to obtain more than a small part of the line of transition points in the temperature density plane. In the region $0.9 < t < 1.0$, where $t=K/0.65$, for the quenched site case the critical probability p_c is approximately given by

$$p_c = (t + 1)/2 \tag{7.4.6}$$

a similar formula holds for the annealed site case. The mean field result is

$$p_c = t$$

so the initial slope for the line of critical point differs greatly from the mean field result. This contrasts with the results found for the three dimensional models, where the initial slopes were very close to the mean field values.

7.5 Summary and Discussion

In the preceding section, evidence in support of a Stanley-Kaplan type phase transition for the XY model on the triangular lattice has been presented. Our results corroborate those of Betts, Elliot and Ditzian (1970) in respect to the existence of a phase transition and for the pure XY model indicate that $K_c = 0.67 \pm 0.04$. On the other hand the estimates of $\bar{\gamma}$ we obtained do not agree with the value $\gamma \approx 1.50$ found by Betts et al.

Recently, application of real space renormalisation group theory to the pure XY model has yielded confusing results. These results are reported briefly below. Rogiers and Dekeyser (1976) find, using a three spin cell on the triangular lattice, that there is a transition for the XY model at about $K_c \approx 0.8$. Betts and Plischke (1976) find however, using a five spin cell on the square lattice that

there is no fixed point (i.e. no phase transition) for $K < 2.0$. Also Rogiers and Betts (1976), using a seven spin cell on the triangular lattice, find $K_c \approx 1.1$. The results of both Rogiers and Dekeyser (1976) and Rogiers and Betts (1976) are suspect because negative values are found for the exponent δ , which is thermodynamically impossible.

In short the evidence for a Stanley-Kaplan transition for the two dimensional XY model is inconclusive.

CHAPTER VIII

SUMMARY OF RESULTS AND DISCUSSION

The quenched and annealed site diluted spin- $\frac{1}{2}$ XY models have been studied in some two and three dimensional Bravais lattices. We have used the finite cluster theorem (outlined in Chapter IV) to construct expansions about the magnetically disordered state for the free energy and the fluctuation in order parameter.

For the quenched site model, expansions have been constructed up to degree seven in both magnetic site concentration, p (with temperature as a parameter) and in inverse temperature (with p as a parameter). The natural expansion variable for the annealed site model is the magnetic site fugacity z . Expansions up to degree seven in z have been derived and these series have also been converted to series in magnetic ion concentration, n_m .

The results of the analysis of the series expansions for the quenched site model for the three dimensional lattices are given in Chapter V. In brief, we have found for each lattice, the line of critical points in the temperature-density plane fairly precisely. However, the apparent behavior of $\gamma(t)$, the susceptibility exponent, (where $t = T(1)/T(p)$) has some disconcerting properties.

Firstly $\bar{\gamma}(t=1) = 1.22 \pm 0.02$ does not agree with the value $\gamma(p=1) = 1.333 \pm 0.002$ obtained from the high temperature series approach. This result contradicts the scaling hypothesis, which asserts inter alia that $\bar{\gamma}(t=1) = \gamma(p=1)$. Also we have found that $\bar{\gamma}(t)$ apparently varies with reduced temperature t . This contradicts the universality principle which requires that $\bar{\gamma}(t)$ be independent of t . Very similar results have been found for the annealed site case.

For the quenched site case it can be argued that the concentration p is not a thermodynamic variable and hence the phenomenological theories of scaling and universality need not apply. This argument is weakened by the fact that the annealed site model shows the same behavior for $\bar{\gamma}(t)$, since the concentration n_m for the annealed site model is a thermodynamic variable.

The phase transition curves for the annealed site model are given in Chapter VI. The interpretation of the annealed site model as a model of $\text{He}^3\text{-He}^4$ mixtures is also given in Chapter VI along with our attempts to locate the tricritical point. The model does not appear to give a good quantitative description of the phase diagram for $\text{He}^3\text{-He}^4$ mixtures.

The two dimensional diluted XY models are examined in Chapter VII and our results seem to indicate the presence of a Stanley-Kaplan type phase transition.

Possibly one of the more interesting results we have found is that the nature of the phase transitions for the three dimensional lattices is uncomplicated by the introduction of impurities. However if there were, for instance, no precise critical density for a given temperature, but instead a small interval of critical densities, then analysis of expansions about the disordered state only might be unable to reveal the distribution of singularities.

The only important issue we have left unresolved is the discrepancy between our deduced behavior of $\bar{\gamma}$ and the predictions of scaling and universality. This difficulty cannot, in the foreseeable future, be resolved using series expansions because of the size of the eigenvalue problems involved in extending our series. Possibly a more useful approach would be to examine the problem from a general thermodynamic viewpoint.

The weak universality hypothesis could be tested by constructing series expansions for pair correlation functions. The ratio of the exponents $\bar{\gamma}/\bar{\nu}$ should be invariant along the line of critical points.

REFERENCES

- Algra, H.A., de Jongh, L.J., Huiskamp, W.J. and Carlin, R.L., 1976. To be published.
- Baxter, R.J., 1971. Phys. Rev. Lett. 26, 832.
- Baxter, R.J., 1972. Ann. Phys. 70, 193.
- Behringer, R.E., 1957. J. Chem. Phys. 26, 1504.
- Berlin, T.H. and Kac, M., 1952. Phys. Rev. 86, 821.
- Bethe, H.A., 1935. Proc. Roy. Soc. A216, 45.
- Betts, D.D., 1974. in: Phase Transitions and Critical Phenomena, Vol. 3, Domb, C. and Green, M.S., eds. (Academic Press, London).
- Betts, D.D., Elliot, C.J. and Lee, M.H., 1970. Can. J. Phys. 48, 1566.
- Betts, D.D., Elliot, C.J. and Ditzian, R.V., 1971. J. Can. Phys. 49, 1327.
- Betts, D.D., Guttman, A.J. and Joyce, G.S., 1971. J. Phys. C4, 1994.
- Betts, D.D. and Lothian, J.R., 1973. Can. J. Phys. 51, 2249.
- Betts, D.D. and Ritchie, D.S., 1975. Phys. Rev. Lett. 34, 788.
- Betts, D.D. and Plischke, M., 1976. Can. J. Phys., in press.
- Bishop, A.R. and Domany, E., 1975. (Private Communication).
- Blume, M., 1966. Phys. Rev. 141, 517.
- Blume, M., Emery, V.J. and Griffiths, R.B., 1971. Phys. Rev. A4, 1071.
- Bragg, W.L. and Williams, E.J., 1934. Proc. Roy. Soc. A145, 699.
- Brout, R., 1959. Phys. Rev. 115, 824.
- Camp, W.J. and Van Dyke, J.P., 1975. J. Phys. C8, 336.

- Capel, H.W., 1966. *Physica* 32, 966.
- Capel, H.W., 1967a. *Physica* 33, 295.
- Capel, H.W., 1967b. *Physica* 37, 423.
- Cheng, Y.C. and Schick, M., 1973. *Phys. Rev.*, A7, 1771.
- Cox, M.A.A., Essam, J.W. and Place, C.M., 1976. To be published.
- de Jongh, L.J., Betts, D.D. and Austen, D.J., 1974. *Solid State Comm.* 15, 1711.
- de Jongh, L.J., 1976. (Private Communication).
- de Jongh, L.J. and Miedema, A.R., 1974. *Adv. Phys.* 23, 1.
- Dekeyser, R. and Rogiers, J., 1975. *Physica* 81A, 72.
- Bitzian, R.V. and Betts, D.D., 1971. *Phys. Lett.* A32, 152.
- Domb, C., 1960. *Adv. Phys.* 9, 149.
- Domb, C., 1972. *J. Phys.* C5, 1399.
- Domb, C., 1974. in: Phase Transitions and Critical Phenomena, Vol. 3, Domb, C. and Green, M.S., eds. (Academic Press, London).
- Domb, C. and Hunter, D.L., 1965. *Proc. Phys. Soc.* 86, 1147.
- Domb, C. and Green, M.S., 1971. eds. of Phase Transitions and Critical Phenomena, (Academic Press, London).
- Domb, C. and Wood, D.W., 1965. *Proc. Phys. Soc.* 86, 1.
- Elliot, R.J., Heap, B.R., Morgan, D.J. and Rushbrooke, G.S., 1960. *Phys. Rev. Lett.* 5, 366.
- Elliot, R.J. and Saville, D., 1974. *J. Phys.* C7, 4293.
- Essam, J.W., 1967. *J. Math. Phys.* 8, 741.
- Essam, J.W., 1972. in: Phase Transitions and Critical Phenomena, Vol. 2, Domb, C. and Green, M.S., eds. (Academic Press, London).

- Essam, J.W. and Garelick, H., 1967. Proc. Phys. Soc. 92, 136.
- Fallot, M., 1936. Ann. Physik 6, 305.
- Fallot, M., 1937. Ann. Physik 7, 420.
- Ferer, M. and Wortis, M., 1972. Phys. Rev. B6, 3426.
- Fisher, M.E., 1967. Rep. Progr. Phys. 30, 615.
- Fisher, M.E., 1968. Phys. Rev. 176, 257.
- Fisher, M.E., 1974. Rev. Mod. Phys. 46, 597.
- Forestier, H., 1928. Ann. Chim. 9, 316.
- Fuchs, K., 1942. Proc. Roy. Soc. A179, 340.
- Garland, C.W. and Weiner, B.B., 1971. Phys. Rev. B3, 1634.
- Goellner, G., Berringer, R. and Meyer, H., 1973. J. Low Temp. Phys. 13, 113.
- Griffiths, R.B., 1967a. Phys. Rev. Lett. 14, 623.
- Griffiths, R.B., 1967b. J. Chem. Phys. 43, 1958.
- Griffiths, R.B., 1969. Phys. Rev. Lett. 23, 17.
- Griffiths, R.B., 1970. Phys. Rev. Lett. 24, 715.
- Griffiths, R.B., 1973. Phys. Rev. B7, 545.
- Griffiths, R.B. and Wheeler, J.C., 1970. Phys. Rev. A2, 1047.
- Hankey, A., Stanley, H.E. and Chang, T.S., 1972. Phys. Rev. Lett. 29, 278.
- Harris, A.B., 1974. J. Phys. C7, 1671.
- Harris, A.B. and Lubensky, T., 1974. Phys. Rev. Lett. 33, 1540.
- Ho, J.T. and Litster, J.D., 1969. Phys. Rev. Lett. 22, 603.
- Huang, K. 1963. Statistical Mechanics (John Wiley and Sons, New York).

- Kadanoff, L.P., 1966. *Physics* 2, 263.
- Kadanoff, L.P., 1971. in: Critical Phenomena, Proceedings of the Varenna Summer School, ed. M.S. Green, (Academic Press, New York).
- Kadanoff, L.P. and Wegner, F.J., 1971. *Phys. Rev.* B4, 3989.
- Kasteleyn, P.W. and Fortuin, C.M., 1969. *J. Phys. Soc. Japan* (supplement) 26, 11.
- Kikuchi, R., 1951. *Phys. Rev.* 81, 988.
- Kosterlitz, J.M. and Thouless, D.J., 1973. *J. Phys.* C6, 1181.
- Kouvel, J.S. and Comley, J.B., 1968. *Phys. Rev. Lett.* 20, 1237.
- Landau, D.P. and Keen, B.E., 1972. *Phys. Rev.* B5, 4472.
- Levelt Sengers, J.M.H., 1974. *Physica* 73, 73.
- Ma, S., 1973. *Rev. Mod. Phys.* 45, 589.
- Matsubara, T. and Matsuda, H., 1956. *Prog. Theor. Phys.* 16, 416.
- Mattis, D.C., 1965. The Theory of Magnetism (Harper and Row, New York).
- Mayer, J.E., 1937. *J. Chem. Phys.* 5, 67.
- McCoy, B.M. and Wu, T.T., 1968. *Phys. Rev.* 176, 631.
- Mermin, N.D. and Wagner, H., 1966. *Phys. Rev. Lett.* 17, 1133.
- Moore, M.A., 1969. *Phys. Rev. Lett.* 23, 861.
- Morgan, D.J. and Rushbrooke, G.S., 1961. *Molec. Phys.* 4, 291.
- Mubayi, V. and Lange, R.V., 1969. *Phys. Rev.* 178, 882.
- Niemeyer, Th. and Van Leeuwen, J.M.J., 1974. *Physica* 71, 17.
- Onsager, L., 1944. *Phys. Rev.* 65, 117.
- Pathria, R.K., 1972. Statistical Mechanics (Pergamon Press, Toronto).

- Plischke, M. and Betts, D.D., 1975. *Can. J. Phys.* 53, 987.
- Rapaport, D.C., 1972a. *J. Phys.* C5, 1830.
- Rapaport, D.C., 1972b. *J. Phys.* C5, 2813.
- Rauh, A., 1976. *Phys. Rev.* (in press).
- Rauh, A., 1976. To be published.
- Reeve, J.S. and Betts, D.D., 1975. *J. Phys.* C8, 2642.
- Reeve, J.S., 1976. *J. Phys.* C9 (in press).
- Riedel, E.K., 1972. *Phys. Rev. Lett.* 28, 675.
- Riedel, E.K., 1974. *AIP Conf. Proc.* 18, 834.
- Riedel, E.K. and Wegner, F.J., 1972. *Phys. Rev. Lett.* 29, 349.
- Riedel, E.K. and Wegner, F.J., 1974. *Phys. Rev.* B9, 294.
- Rogiers, J., 1974. Ph.D. Thesis, Katholieke Universiteit, Leuven, Belgium (unpublished).
- Rogiers, J., Dekeyser, R. and Quisthoudt, M., 1975. 81A, 93.
- Rogiers, J. and Dekeyser, R., 1976. *Phys. Rev.* B, June.
- Rogiers, J. and Betts, D.D., 1976. (Private Communication).
- Rushbrooke, G.S., 1964. *J. Math. Phys.* 5, 1106.
- Rushbrooke, G.S., 1965. *J. Chem. Phys.* 43, 3439.
- Rushbrooke, G.S., 1971. in: Critical Phenomena in Alloys, Magnets and Superconductors, eds., Mills, R.E., Ascher, E. and Jafee, R.J. (McGraw-Hill, New York).
- Rushbrooke, G.S., Baker, G. and Wood, P., 1974. in: Critical Phenomena and Phase Transitions, eds., Domb, C. and Green, M.S. (Academic Press, New York).
- Rushbrooke, G.S. and Morgan, D.J., 1961. *Molec. Phys.* 4, 1.
- Rushbrooke, G.S., Muse, R.A., Stephenson, R.L. and Pirnie, K., 1972. *J. Phys.* C7, 255.

- Rushbrooke, G.S. and Scions, , 1955. Proc. Roy. Soc. A230, 74.
- Rushbrooke, G.S. and Wood, P.J., 1958. Molec. Phys. 1, 257.
- Saul, D.M., Wortis, M. and Stauffer, D., 1974. Phys. Rev. B9, 4964.
- Schmidt, V.A. and Friedberg, S.A., 1970. Phys. Rev. B1, 2250.
- Stanley, H.E., 1971. Introduction to Phase Transitions and Critical Phenomena (Oxford University Press, New York).
- Stanley, H.E., 1974. in: Phase Transitions and Critical Phenomena, Vol. 3, eds., Domb, C. and Green, M.S. (Academic Press, New York).
- Stanley, H.E. and Kaplan, T., 1966. Phys. Rev. Lett. 17, 913.
- Stauffer, D., 1975. Physik B22, 161.
- Stauffer, D., 1976. To be published.
- Suzuki, M., 1974. Prog. Theor. Phys. 51, 1992.
- Suzuki, M., 1974. J. Phys. C7, 255.
- Syozi, I., 1965. Prog. Theor. Phys. 34, 189.
- Syozi, I. and Miyazima, S., 1966. Prog. Theor. Phys. 36, 1083.
- Takagi, S., 1972. Prog. Theor. Phys. 47, 22.
- Tyablikov, S.V., 1967. Methods in the Quantum Theory of Magnetism (Plenum Press, New York).
- Ursell, H.D., 1927. Proc. Camb. Phil. Soc. 23, 685.
- Van der Waals, J.D., 1873. Ph.D. Thesis, University of Leiden.
- Vicennini-Missoni M., 1972. in: Phase Transitions and Critical Phenomena, Vol. 2, eds., Domb, C. and Green, M.S. (Academic Press, New York).

- Wegner, F.J. and Riedel, E.K., 1973. Phys. Rev. B7, 248.
- Weiss, P., 1907. J. Phys. 6, 661.
- Widom, B., 1965a. J. Chem. Phys. 43, 3892.
- Widom, B., 1965b. J. Chem. Phys. 43, 3898.
- Wortis, M., 1974. Phys. Lett. 47A, 445.
- Wilson, K.G. and Kogut, J., 1974. Physics Reports 12C, 76.
- Yelon, W.B. and Birgeneau, R.J., 1972. Phys. Rev. B5, 2615.
- Yamaji, K. and Kondo, J., 1973a. Phys. Lett. 45A, 317.
- Yamaji, K. and Kondo, J., 1973b. J. Phys. Soc. Japan 35, 25.
- Zubarev, D.N., 1960. Sov. Phys.-Usp. 3, 320.

APPENDIX A

EXPECTATION VALUES FOR FINITE CLUSTERS

In order to utilise the finite cluster expansion as proposed in Section 4.5 we need the partition function and expectation values for each finite cluster.

If we already have the Hamiltonian for a cluster C , of say v vertices, in matrix form, then it is a simple matter to find the partition function of C . All that is required is to diagonalise the Hamiltonian to find the energy spectrum $\{\epsilon_\ell, \ell=1, 2, \dots, 2^v\}$. (The XY spin- $\frac{1}{2}$ model has 2 states per site and hence for a v vertex cluster there are 2^v states in all.) The partition function is then

$$Q(C) = \text{Tr} \exp(-\beta H) = \sum_{\ell=1}^{2^v} \exp(-\beta \epsilon_\ell) \quad (\text{A.1})$$

where $\beta = 1/k_B T$. The expectation value $Y(C)$ for the operator $y = \sum_{i,j=1}^v S_i^x S_j^x$ for the cluster C is given by

$$\begin{aligned} y &= \text{Tr} y \exp(-\beta H) \\ &= \sum_{\ell=1}^{2^v} y_{\ell\ell} \exp(-\beta \epsilon_\ell) \end{aligned} \quad (\text{A.2})$$

where $y_{\ell\ell}$ is the ℓ th diagonal element of the matrix for y in the representation where the Hamiltonian is diagonal.

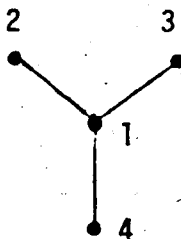
The Hamiltonian

$$H^{XY} = -J/2 \sum_{\langle ij \rangle} (\sigma_i^x \sigma_j^x + \sigma_i^y \sigma_j^y) - mH \sum_i S_i^z \quad (\text{A.3})$$

then must be constructed for each finite cluster. The most straight forward approach is to write out the Hamiltonian in the direct product representation, where for a cluster of v spins σ_i^α is given by $I \ I \ \dots \ \sigma^\alpha \ I \ \dots \ I$. Where the σ^α is the α component of the Pauli spin vector and is in the i th position in the sequence of direct products of the 2×2 identity matrix I .

By constructing the matrix for $\sum_i S_i^z$ in the direct product representation it can immediately be seen how the interaction part of H^{XY} block diagonalises into matrices corresponding to the same S^z eigenvalue. This approach is best illustrated by example.

Consider the labelled cluster



for which we have $\sum_i S_i^z = \text{diag}(4, 2, 2, 0, 2, 0, 0, -2, 2, 0, 0, -2, 0, -2, -2, -4)$ in the direct product representation, where since $\sum_i S_i^z$ has non-zero elements on the diagonal only, we write down only the diagonal elements. It is obvious then that if we exchange rows and columns 4 with 9 and 8 with 13, the

matrix $\sum_i S_i^Z$ will be in blocks of equal eigenvalues. If we also exchange the same labels in the matrix representation of $H^{INT} = \sum_{\langle i,j \rangle} (\sigma_i^x \sigma_j^x + \sigma_i^y \sigma_j^y)$, the result is the matrix

$$H^{INT} = (0) \oplus \begin{pmatrix} 0 & 1 & 1 & 1 \\ 1 & 0 & 0 & 0 \\ 1 & 0 & 0 & 0 \\ 1 & 0 & 0 & 0 \end{pmatrix} \oplus \begin{pmatrix} 0 & 1 & 1 & 0 & 0 & 0 \\ 1 & 0 & 0 & 1 & 0 & 0 \\ 1 & 0 & 0 & 0 & 1 & 0 \\ 0 & 1 & 0 & 0 & 0 & 1 \\ 0 & 0 & 1 & 0 & 0 & 1 \\ 0 & 0 & 0 & 1 & 1 & 0 \end{pmatrix} \oplus \begin{pmatrix} 0 & 1 & 1 & 1 \\ 1 & 0 & 0 & 0 \\ 1 & 0 & 0 & 0 \\ 1 & 0 & 0 & 0 \end{pmatrix} \oplus (0)$$

Thus the problem size is reduced from a 16×16 matrix to that of a 4×4 and a 6×6 matrix. These matrices are readily diagonalised to give the set of eigenvalues $0, 0, 0, \pm\sqrt{3}, \pm 1, \pm 1, \pm 2, 0, 0, \pm\sqrt{3}, 0$ and in zero field the partition function for this cluster is

$$Q = 6 + 4\cosh\sqrt{3}K + 4\cosh K + 2\cosh 2K$$

where $K = \beta J$.

The above example essentially illustrates the computational technique used to construct the partition functions of each cluster. To convert the y matrix from the direct product representation to the energy representation requires that we form the matrix

$$\bar{y} = y y^T$$

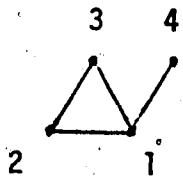
where v is the matrix of eigenvectors obtained by diagonalising the Hamiltonian. Standard routines were used to diagonalise the Hamiltonian and the entire process was computerised.

For symmetric clusters a further block diagonalisation can be achieved by writing the Hamiltonian in a symmetrised basis. However, the advantage of this refinement is offset by the relatively low symmetry of most of the graphs and the fact that the transformation to the symmetric basis is unique for each cluster.

APPENDIX B

LATTICE CONSTANTS AND PERIMETER COUNTS

The following table contains the strong lattice constants and perimeter counts for all the connected clusters of up to and including six vertices. These data are complete for the face centred cubic (FCC), the body centred cubic (BCC), the simple cubic (SCU), the triangular (TRI) and the simple quadratic (SQU) lattices. The graphs are in dictionary order and sub-headings give the number of vertices and number of bonds. Each graph is represented by an adjacency matrix A such that the matrix element A_{ij} is one if there is a bond between the i th and j th sites and zero otherwise. For example the graph



(number 7 in the list) has adjacency matrix

$$\begin{pmatrix} 0 & 1 & 1 & 1 \\ 1 & 0 & 1 & 0 \\ 1 & 1 & 0 & 0 \\ 1 & 0 & 0 & 0 \end{pmatrix}$$

Because this matrix is symmetric and all the diagonal elements are zero the graph is adequately represented by the above diagonal elements collected column by column to form the vector, $A = 1\ 1\ 1\ 1\ 0\ 0\ 0$.

An example of how these data are to be read is given below.

Consider the graph with four vertices and four bonds for which the following data are listed

	7	2	111100	
FGC:		120;	48(27)	72(28)
TRI:		12;	12(11)	

This graph is the seventh in the list and has a symmetry group of order two (i.e. symmetry number of two). The next set of numbers is the adjacency matrix in the form given above (in fact this is the graph used in the above example). The strong lattice constant for the seventh graph is 120 on the f.c.c. lattice and is embeddable 48 times with perimeter 27 and 72 times with perimeter 28. On the triangular lattice the graph can be embedded 12 times with a perimeter of 11. Note that if a graph is not strongly embeddable in a particular lattice, then no data for that lattice appear.

1 VERTICES 0 BONDS

1	1	0		
FCC:	1;		1 (12)	
BCC:	1;		1 (8)	
SCU:	1;		1 (6)	
TRI:	1;		1 (6)	
SQU:	1;		1 (4)	

2 VERTICES 1 BONDS

2	2	1		
FCC:	6;		6 (18)	
BCC:	4;		4 (14)	
SCU:	3;		3 (10)	
TRI:	3;		3 (8)	
SQU:	2;		2 (6)	

3 VERTICES 2 BONDS

3	2	110			
FCC:	42;		12 (23)	30 (24)	
BCC:	28;		12 (17)	12 (19)	4 (20)
SCU:	15;		12 (13)	3 (14)	
TRI:	9;		9 (10)		
SQU:	6;		4 (7)	2 (8)	

3 VERTICES 3 BONDS

4	6	111		
FCC:	8;		8 (22)	
TRI:	2;		2 (9)	

4 VERTICES 3 BONDS

5	6	110100				
FCC:	44;		12 (28)	24 (29)	8 (30)	
BCC:	56;		24 (20)	24 (22)	8 (23)	
SCU:	20;		8 (15)	12 (16)		
TRI:	2;		2 (12)			
SQU:	4;		4 (8)			
6	2	110010				
FCC:	282;		12 (28)	120 (29)	150 (30)	
BCC:	148;		12 (20)	48 (22)	24 (23)	36 (24) 24 (25)
			4 (26)			
SCU:	63;		36 (16)	24 (17)	3 (18)	
TRI:	27;		27 (12)			
SQU:	14;		4 (8)	8 (9)	2 (10)	

4 VERTICES 4 BONDS

7 2 111100
 FCC: 120; 48(27) 72(28)
 TRI: 12; 12(11)
 8 8 110011
 FCC: 3; 3(26)
 BCC: 12; 6(20) 6(22)
 SCU: 3; 3
 SQU: 1; 1

4 VERTICES 5 BONDS

9 4 111110
 FCC: 24; 24(28)
 TRI: 3; 3(10)

4 VERTICES 6 BONDS

10 24 111111
 FCC: 2; 2(24)

5 VERTICES 4 BONDS

11 24 1101001000
 FCC: 9; 3(32) 6(34)
 BCC: 70; 6(21) 32(23) 30(24) 2(26)
 SCU: 15; 12(17) 3(18)
 SQU: 1; 1(8)
 12 2 1101000100
 FCC: 828; 24(33) 276(34) 408(35) 120(36)
 BCC: 672; 48(23) 192(25) 96(26) 168(27) 144(28)
 SCU: 204; 48(18) 120(19) 36(20)
 TRI: 18; 18(14)
 SQU: 20; 8(9) 12(10)
 13 2 1100100010
 FCC: 1902; 36(33) 336(34) 804(35) 726(36)
 BCC: 820; 12(23) 96(25) 60(26) 192(27) 192(28)
 SCU: 267; 24(18) 84(19) 120(20) 36(31) 4(32)
 TRI: 81; 6(13) 75(14) 36(21) 3(22)
 SQU: 34; 4(9) 16(10) 12(11) 2(12)

5 VERTICES 5 BONDS

14 4 1111001000
 FCC: 96; 48(32) 48(33)

15	2	1111000100			
FCC:	576;	72(32)	288(33)	216(34)	
TRI:	24;	24(13)			
16	2	1111000001			
FCC:	792;	48(32)	384(33)	360(34)	
TRI:	36;	36(13)			
17	2	1101000110			
FCC:	48;	24(31)	24(32)		
BCC:	216;	48(23)	120(25)	24(26)	24(27)
SCU:	48;	24(18)	24(19)		
SQU:	8;	8(9)			

5 VERTICES 6 BONDS

18	2	1111101000			
FCC:	168;	120(31)	48(32)		
TRI:	6;	6(12)			
19	2	1111100010			
FCC:	240;	96(31)	144(32)		
TRI:	12;	12(12)			
20	8	1111001001			
FCC:	72;	12(30)	24(31)	36(32)	
TRI:	3;	3(12)			
21	2	1111000101			
FCC:	24;	24(30)			
22	12	1101000111			
BCC:	12;	12(23)			

5 VERTICES 7 BONDS

23	6	1111111000			
FCC:	24;	24(30)			
24	2	1111101010			
FCC:	72;	72(30)			
TRI:	6;	6(11)			

5 VERTICES 8 BONDS

25	4	1111111100			
FCC:	24;	24(28)			
26	8	1111101011			
FCC:	6;	6(29)			

6 VERTICES 5 BONDS

27	120	11010010001000			
BCC:	56;	24(24)	24(25)	8(26)	
SCU:	6;	6(18)			

28	6	110100100001000				
FCC:	204;	60 (38)	24 (39)	120 (40)		
BCC:	856;	96 (26)	48 (27)	192 (28)	368 (29)	120 (30)
		24 (31)	8 (32)			
SCU:	156;	72 (20)	72 (21)	12 (22)		
SQU:	4;	4 (10)				
29	8	110100010001000				
FCC:	540;	12 (38)	120 (39)	240 (40)	144 (41)	24 (42)
BCC:	564;	48 (26)	168 (28)	48 (29)	144 (30)	120 (31)
		36 (32)				
SCU:	126;	12 (20)	48 (21)	66 (22)		
TRI:	3;	3 (16)				
SQU:	4;	4 (10)				
30	2	110100010000100				
FCC:	5208;	60 (38)	600 (39)	1860 (40)	2112 (41)	576 (42)
BCC:	2564;	24 (26)	192 (28)	144 (29)	480 (30)	576 (31)
		504 (32)	504 (33)	216 (34)	24 (35)	
SCU:	696;	24 (20)	120 (21)	300 (22)	216 (23)	36 (24)
TRI:	54;	6 (15)	48 (16)			
SQU:	32;	4 (10)	16 (11)	12 (12)		
31	2	110100010000001				
FCC:	5628;	120 (38)	1008 (39)	2052 (40)	1896 (41)	552 (42)
BCC:	3912;	48 (26)	408 (28)	336 (29)	792 (30)	912 (31)
		672 (32)	504 (33)	216 (34)	24 (35)	
SCU:	876;	48 (20)	192 (21)	336 (22)	264 (23)	36 (24)
TRI:	54;	12 (15)	42 (16)			
SQU:	52;	8 (10)	32 (11)	12 (12)		
32	2	110010001000010				
FCC:	12654;	204 (38)	984 (39)	2940 (40)	5016 (41)	3510 (42)
BCC:	4492;	12 (26)	144 (28)	96 (29)	528 (30)	648 (31)
		768 (32)	984 (33)	612 (34)	432 (35)	216 (36)
		48 (37)	4 (38)			
SCU:	1107;	96 (21)	252 (22)	456 (23)	252 (24)	48 (25)
		3 (26)				
TRI:	237;	24 (15)	213 (16)			
SQU:	82;	4 (10)	24 (11)	36 (12)	16 (13)	2 (14)

6 VERTICES 6 BONDS

33	2	111100100001000				
FCC:	864;	144 (37)	432 (38)	288 (39)		
34	2	111100100000010				
FCC:	1152;	48 (37)	624 (38)	480 (39)		
35	6	111100010000100				
FCC:	890;	16 (37)	216 (38)	432 (39)	216 (40)	
TRI:	16;	16 (15)				
36	1	111100010000010				
FCC:	7632;	48 (36)	336 (37)	1680 (38)	3504 (39)	2064 (40)
TRI:	144;	12 (14)	132 (15)			

37	4	111100000100010				
FCC:	1128;	48 (37)	408 (38)	528 (39)	144 (40)	
TRI:	12;	12 (15)				
38	2	111100000100001				
FCC:	5352;	288 (37)	1056 (38)	2304 (39)	1704 (40)	
TRI:	108;	12 (14)	96 (15)			
39	4	110100100001100				
FCC:	24;	12 (35)	12 (37)			
BCC:	396;	24 (24)	72 (26)	132 (27)	96 (28)	72 (29)
SCU:	72;	60 (20)	12 (21)			
SQU:	4;	4 (9)				
40	2	110100011001000				
FCC:	180;	36 (36)	96 (37)	48 (38)		
BCC:	768;	72 (26)	288 (28)	144 (29)	168 (30)	96 (31)
SCU:	156;	24 (20)	96 (21)	36 (22)		
SQU:	12;	12 (10)				
41	2	110100011000010				
FCC:	312;	24 (36)	168 (37)	120 (38)		
BCC:	1032;	48 (26)	264 (28)	72 (29)	336 (30)	192 (31)
		96 (32)	24 (33)			
SCU:	168;	48 (21)	96 (22)	24 (23)		
SQU:	16;	8 (10)	8 (11)			
42	4	110100011000001				
FCC:	96;	24 (36)	48 (37)	24 (38)		
BCC:	504;	48 (26)	216 (28)	48 (29)	168 (30)	24 (32)
SCU:	96;	24 (20)	48 (21)	24 (22)		
SQU:	8;	8 (10)				
43	12	110010001000011				
FCC:	28;	24 (36)	4 (37)			
BCC:	4;	4 (32)				
SCU:	4;	4 (20)				
TRI:	1;	1 (13)				

6 VERTICES 7 BONDS

44	4	111110100010000				
FCC:	72;	24 (35)	48 (36)			
45	4	111110100001000				
FCC:	288;	144 (36)	120 (37)	24 (38)		
TRI:	3;	3 (14)				
46	1	111110100000100				
FCC:	1584;	384 (36)	912 (37)	288 (38)		
TRI:	24;	24 (14)				
47	2	111110100000001				
FCC:	1056;	120 (36)	696 (37)	240 (38)		
TRI:	18;	18 (14)				
48	4	111110001000100				
FCC:	192;	96 (36)	96 (37)			

49	4	111110001000010			
FCC:	600;	108 (36)	288 (37)	204 (38)	
TRI:	12;	12 (14)			
50	2	111110001000001			
FCC:	1584;	96 (36)	816 (37)	672 (38)	
TRI:	36;	36 (14)			
51	8	111100100110000			
FCC:	36;	36 (36)			
52	2	111100100101000			
FCC:	1344;	48 (35)	288 (36)	576 (37)	432 (38)
TRI:	24;	24 (14)			
53	1	111100100001010			
FCC:	96;	48 (35)	48 (36)		
54	4	111100100000011			
FCC:	48;	48 (35)			
55	2	111100010100100			
FCC:	120;	48 (35)	72 (36)		
56	1	111100010100010			
FCC:	192;	96 (35)	96 (36)		
57	8	111100000100011			
FCC:	552;	48 (36)	288 (37)	116 (38)	
TRI:	12;	12 (14)			
58	6	110100100001110			
BCC:	96;	72 (26)	24 (27)		
59	4	11010011101000			
BCC:	120;	48 (26)	72 (28)		
60	4	110100011001010			
FCC:	6;	6 (34)			
BCC:	96;	12 (26)	48 (28)	24 (29)	12 (30)
SCU:	18;	12 (26)	6 (22)		
SQU:	2;	2 (10)			

6 VERTICES 8 BONDS

61	4	11111100001000			
FCC:	108;	108 (36)			
62	6	11111100000001			
FCC:	168;	48 (35)	120 (36)		
63	2	111110101010000			
FCC:	120;	24 (34)	96 (35)		
64	1	11111010101000			
FCC:	480;	336 (35)	144 (36)		
TRI:	12;	12 (13)			
65	1	111110101000010			
FCC:	720;	288 (35)	432 (36)		
TRI:	24;	24 (13)			
66	4	111110100010001			
FCC:	144;	48 (34)	96 (35)		

67 4 111110100001001
 FCC: 12; 12 (34)
 68 1 11111010000101
 FCC: 96; 96 (34)
 69 4 111110001000101
 FCC: 288; 48 (34) 96 (35) 144 (36)
 TRI: 6; 6 (13)
 70 2 111100100101010
 FCC: 48; 24 (33) 24 (34)
 71 4 111100010100011
 FCC: 24; 24 (34)
 72 48 11010000001111
 FCC: 3; 3 (24)
 73 8 110100011101100
 FCC: 24; 24 (26)

6 VERTICES 9 BONDS

74 2 111111110010000
 FCC: 96; 48 (33) 48 (34)
 75 2 111111110000100
 FCC: 144; 144 (34)
 76 4 111111110000001
 FCC: 120; 48 (33) 72 (34)
 77 12 111111100010001
 FCC: 24; 24 (34)
 78 8 111110101110000
 FCC: 24; 24 (34)
 79 2 1111101001000
 FCC: 96; 72 (34) 24 (35)
 80 2 111110101010010
 FCC: 120; 24 (33) 96 (34)
 TRI: 6; 6 (12)
 81 6 111110101001100
 FCC: 32; 32 (34)
 TRI: 2; 2 (12)
 82 2 111110101001010
 FCC: 120; 120 (34)
 TRI: 6; 6 (12)

6 VERTICES 10 BONDS

83 2 111111110010100
 FCC: 72; 72 (32)
 84 2 111111110010001
 FCC: 48; 48 (32)
 85 8 111111110000110
 FCC: 24; 24 (32)

86 2 111110101101100
FCC: 24; 24(33)

6 VERTICES 11 BONDS

87 16 111111100110
FCC: 6; 6(30)
88 2 11111110010101
FCC: 24; 24(31)

6 VERTICES 12 BONDS

89 48 11111111111111
FCC: 1; 1(32)